DOI:10.15774/PPKE.ITK.2020.008

Spontaneously occurring and disinhibition-induced synchronous activities in the human neocortex, in vitro

A thesis submitted for the degree of

Doctor of Philosophy

by

Ágnes Kandrács

Scientific advisor:

Lucia Wittner, PhD

Faculty of Information Technology and Bionics

Pázmány Péter Catholic University

Budapest 2019

DOI:10.15774/PPKE.ITK.2020.008

Abstract

Understanding the role of the distinct neuron populations in the generation of synchronous activities is essential for the advancement of treatments to restrain epilepsy. Hypersynchronous events, such as epileptic seizures and interictal spikes, also called paroxysmal discharges, are associated with hyperexcitability and the bursting behaviour of pyramidal cells in the animal models of epilepsy. Human experiments revealed that both excitatory and inhibitory neurons could have a leading role in the development of epileptiform events, depending on the seizure morphology. The aim of the recent study was to investigate the distinct level of synchronies in the non-epileptic and epileptic, as well as in the disinhibition-induced processes. Furthermore, single-cell activity was analysed to uncover the role of excitatory and inhibitory mechanisms in the generation of different types of synchronies. 24-channel laminar multielectrode was used to register local field potential gradients in postoperative neocortical slices derived from patients with or without the manifestation of epilepsy in their anamnesis. Spontaneous synchronous population events were generated in physiological conditions both in epileptic and non-epileptic samples. In addition, spontaneous interictal-like discharges emerged in epileptic tissue. Both of these population activities were eliminated by the application of the $GABA_A$ receptor blocker bicuculline. In the meantime, bicuculline-induced hypersynchronous discharges, interictal spikes and seizures started to raise. These interictal-like events were simple in non-epileptic tissue, while they showed high temporal and spatial diversity in the epileptic slices. Only about one-half of the active neurons raised their firing in the presence of spontaneous activity. While the spontaneous synchronous population events were the result of a balanced activity of excitatory and inhibitory cells, spontaneous interictal spikes were led by bursting pyramidal cells. The disinhibition induced population activities recruited the vast majority of the neurons, with the prominent role of interneurons. The data presented here suggest that a dynamic balance of excitatory and inhibitory networks characterise the physiological synchronies. Whereas, a disturbance in this balance leads to the paroxysmal events in the epileptic neocortex. Furthermore, the results propose noticeable differences between human epilepsies and animal models, as well as between in vivo and pharmacologically manipulated in vitro processes.

DOI:10.15774/PPKE.ITK.2020.008

Contents

DOI:10.15774/PPKE.ITK.2020.008

DOI:10.15774/PPKE.ITK.2020.008

Abbreviations

ACSF - artificial cerebrospinal fluid

AED - antiepileptic drug

AP - action potential

BIC - bicuculline methiodide

bIIS - interictal-like spike induced by bicuculline

BIPA - bicuculline-induced population activity

bPC - bursting principal cell

CCM - cerebral cavernous malformation

CSD - current-source density

CDG - cortical dysgenesis

CDP - cortical dysplasia

Cck - cholecystokinine

CNS - central nervous system

DG - dentate gyrus

EPSP - excitatory postsynaptic potential

FS - fast-spiking

$GABA_A$ - A-type γ-aminobutyric acid

GJ - gap junction

HFO - high-frequency oscillation

HS - Hippocampal sclerosis

IB - intrinsically-bursting

IEI - interevent interval

IN - inhibitory interneuron

IPSP -inhibitory postsynaptic potential

IIS - interictal spike

LFP - local field potential

LFPg - local field potential gradient

DOI:10.15774/PPKE.ITK.2020.008

MGFP - mean global field power

MR - magnetic resonance

MUA - multi-unit activity

NeuN - neuronal nuclear protein

NoEpi - patient without clinical manifestation of epilepsy

NoMed - patient with only one seizure

PA - population activity

PC - principal cell

PDS - paroxysmal depolarizing shift

PETH - perievent time histogram

ResEpi - patient with pharmacoresistant epilepsy

RS - regular-spiking

sIID - spontaneous interictal-like discharge

SO - Slow oscillation

SPA - spontaneous population activity

SSt - somatostatin

SUA - single-unit activity

TreatEpi - patient with pharmacologically treatable epilepsy

UC - unclassified cell

VIP - vasointestinal peptide

DOI:10.15774/PPKE.ITK.2020.008

1. Introduction

Hypersynchronous discharges observed in postoperative human neocortical slices are thought to be the outcome of epileptogenic processes. It has several reasons. Both human and experimental focal epilepsies are characterised by the presence of high amplitude, fast EEG spikes followed by a slow wave, the so-called interictal spikes (IISs) [1]. At the same time, spontaneous synchronous population activities were observed on slices prepared from the human epileptic neocortex [2]–[6] or the hippocampal formation [7]–[11] during physiological conditions. These spontaneous population bursts had a waveform resembling in vivo IISs [7], [12], [13]. Since healthy human tissue was not available for obvious ethical reasons, researchers reached for animal brain preparations as a control. However, the comparison of distinct species has its pitfalls as well. No spontaneous field potentials could be detected in vitro in healthy rodent [3], [14] nor primate [15] neocortical slices. Though populational spiking was evoked by activating a single PC in neocortical slices of tumour patients [16]. Moreover, the observation of population activity arising in healthy rodents and primate hippocampal slices raised the possibility that synchronous bursts are not related to epilepsy [15], [17].

It is important to understand the cellular characteristics and firing pattern of single neurons to reveal the contribution of different circuits to the generation of synchronous events. The paroxysmal depolarisation shift and bursting behaviour were linked to the initiation of IISs in animals [1]. The leading role of bursting excitatory cells in the generation of hypersynchronous events was proposed by the observations in the Mg^{2+}-free [14], in the K^{+}-channel blocker 4-aminopyridine [18], as well as in the bicuculline [19] models of epileptiform activity in the human neocortex. The physiological conditions of the cortex are associated with the dynamic balance of excitatory and inhibitory mechanisms. In epilepsy, this balance is disturbed during seizure activity [20]. It has been shown that seizures with different onset were generated by different mechanisms. Some hypersynchronous events were initiated by interneurons [20]–[22], while others were triggered by the enhanced excitatory processes [3], [9], [21] in both human and experimental epilepsy.

DOI:10.15774/PPKE.ITK.2020.008

In the present study, postoperative human neocortical slices derived from epileptic and non-epileptic (tumour) patients were investigated. The first attempt was to show whether human neocortical circuits are able to maintain synchronous activity spontaneously, without the presence of an epileptogenic agent. What is the difference between the behaviour of epileptic and non-epileptic neuron networks? Do the same circuits contribute to the synchronous events observed in the to patient groups? The $GABA_A$ receptor-mediated transmission was eliminated to investigate further the role of different neuron populations in distinct conditions. How does the lack of GABAergic inhibition change the behaviour of the cells? How will it affect the synchronisation? Do the same neuron circuits participate in the spontaneous and induced population discharges? Is there any resemblance between human epilepsy and the disinhibition model of epilepsy? Can they be compared at all? Does it worth to investigate human samples when the animal models are available? The present study attempted to find answers to these and some related questions.

DOI:10.15774/PPKE.ITK.2020.008

2. Literature Review

2.1 The neocortex

2.1.1 Structure

The grey matter that makes up most of the cerebrum is called the cerebellar cortex. Its 2-4 mm thick layer contains billions of nerve cell bodies, dendrites, (mostly unmyelinated) axons, and neuroglia. All the higher-level psycho-physical functions such as sensory perception, object- and event-representation, planning, and decision making are thought to be the manifestations of network mechanisms of neurons in the cortex. Because the cerebral cortex has grown faster than the more profound white matter during embryonic development, its surface is covered with gyri (folds), fissures and sulci (deeper and shallower grooves). The longitudinal fissure divides the cerebrum into two cerebral hemispheres. Each hemisphere is further divided into four cortical lobes. They are identified by the bones which are being located superior to them: the so-called frontal, temporal, parietal and occipital lobes [23]–[25].

The cerebral cortex has two phylogenetically separated areas. The more primitive allocortex is located in the temporal lobe, and it consists of the piriform lobe and the hippocampus. The neocortex constitutes the remaining, vast majority of the cortex. The latter is divided into six horizontal layers considering the characteristic neuron populations, their shapes, sizes, density and specific nerve fibres: (1) the outermost layer I is the molecular layer, containing only a few (mainly inhibitory) neurons; (2) layer II is the external granular layer with small pyramidal cells and interneurons; (3) layer III is called the external pyramidal layer, which consists of almost all the cell types found in the neocortex; (4) layer IV is the internal granular layer containing small excitatory cells, such as spiny stellate cells, and also interneurons; (5) layer V is the internal pyramidal layer with its large pyramidal cells and a few interneurons; (6) finally, layer VI is called multiform layer, referring to its cellular heterogeneity, which blends gradually into the white matter [23]–[26]. Another horizontal division of the neocortex came into general use, which takes into account the functionality of the different areas. In this sense, the supragranular

DOI:10.15774/PPKE.ITK.2020.008

layers, consisting of layers I-III, is participating in both associational and commissural intracortical connections. The granular layer, which is actually layer IV, plays an essential role in thalamocortical communication. While the most prominent function of the infragranular layers, i.e. layers V and VI, is to maintain the connection between the cerebral cortex and subcortical areas [26].

The neocortex is made up of small processing units called cortical columns. Each unit is thought to be responsible for one or a few signal processing tasks. The columns are of 2.5-3 mm height extending through the entire neocortex, but appear to be only 0.2-0.3 mm in diameter forming tapering cylinders. Although the structure of these modules is dynamic. Cortical circuits are capable of 're-wire' their connections as a response to modulatory control signals, thus some neurons are able to be part of multiple functional cell assemblies. Each of the approximately 2 million such modules that constitute the neocortex contains approximately 5000 neurons. The structural complexity of the neocortex is demonstrated by the fact that each module sends axons to 50-100 other cortical columns and receives non-specific afferent fibres from the same amount of them [24], [25].

2.1.2 Cortical neurons and circuits

A non-exhaustive overview of the main neocortical neuron population can be seen on *Table 2.1* and *Figure 2.1*. This is because the variability of different cell types in the neocortex exceeds the limitations of a PhD dissertation. Moreover, discoveries are being made day by day regarding the cortical organisation [24], [25], [29], [30].

The excitatory pyramidal cells constitute the great majority (almost 70%) of the neocortical neuron population. They can be found basically in every cellular layer. The name comes from the conical shape of the somata which has a single, prominent apical dendrite oriented to the surface of the cortex. The basal dendrites are arranged in a radiating, almost horizontal pattern. The long, descending neurite also starts at the basis of the cell body with some initial collaterals. While the apical dendrite usually traverses through several layers, the basal dendrites barely leave the layer of the somata. The axon collaterals can either form local clusters or project across layers and columns all along to the white matter. Usually, the neurites of pyramidal cells in the layer III stays in the neocortex, while layer V pyramidal cells send projections to subcortical areas [24], [25], [29], [30].

The other typical excitatory cell type of the neocortex is the spiny stellate cell, which can be found mainly in layer IV. It has a spherical soma, with multiple, short, radiating dendrites, which are restricted to the same layer and column. In contrast to that, the neurite shows an

DOI:10.15774/PPKE.ITK.2020.008

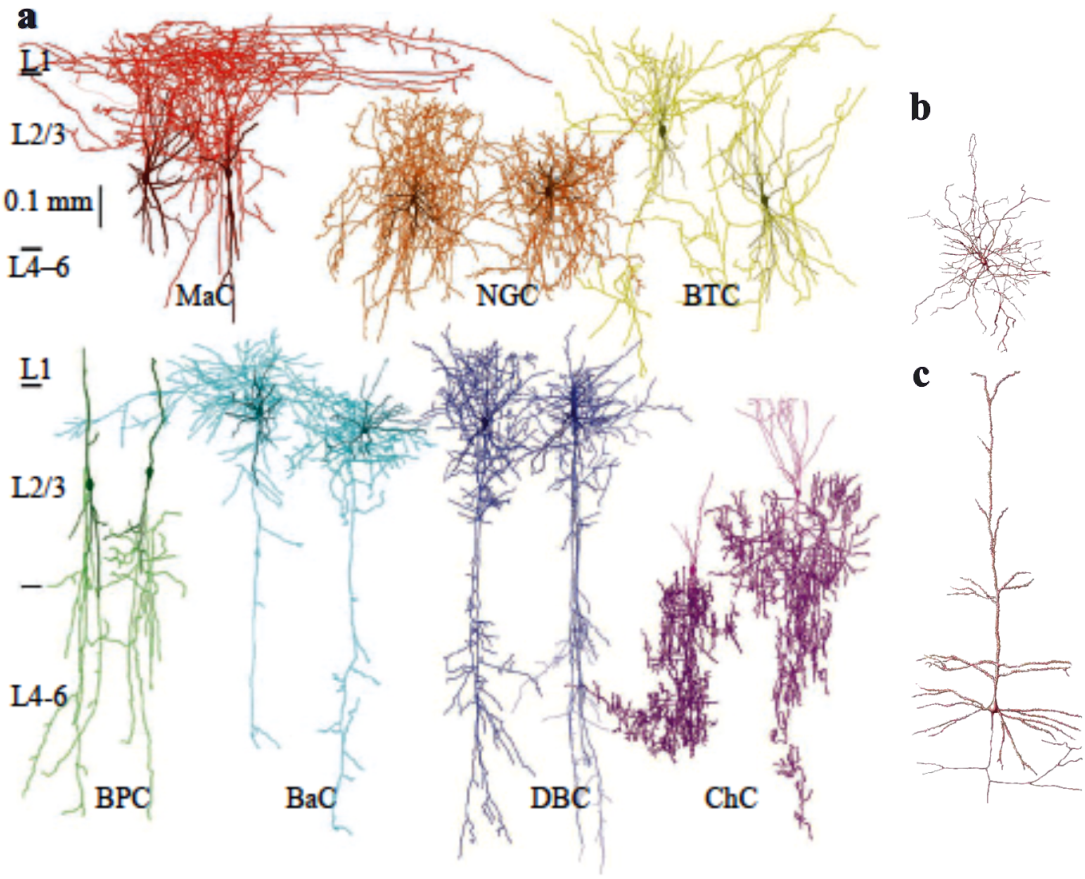

Figure 2.1. Schematic figures of different neuron types found in the neocortex. On the left (a): Martinotti cells (MaC), neurogliaform cells (NGC), bitufted cells (BTC), bipolar cells (BPC), basket cells (BaC), double bouquet cells (DBC) and chandelier cells (ChC) [27]. On the right: stellate cell (b) and pyramidal cell (c) [28]. Cortical layers from I to VI are indicated on the left. Bar = 0.1 mm.

extensive arborisation in layers II and III, moreover, some collaterals descend to layer V or VI or (according to some studies) even project to other cortical areas. A common characteristic of the excitatory neurons, both spiny stellate cells and pyramidal cells, that their dendrites are densely covered by small spines which receive synapses from other excitatory cells. While the source of their inhibitory input takes place on the somata [24], [29], [30]. Henceforth, all excitatory, spiny cell (including pyramidal cells) in the neocortex will be referred to as a principal cell (PC).

The highly heterogeneous group of inhibitory neurons constitute 20-30% of neocortical cells. Their characteristic features are the smooth dendrites with low spine densities and the lack of apical dendrites. Usually, the axon stays within the column, that is why they are called interneurons [24], [25], [29], [30]. During the development in the nomenclature (and the continuous identification) of different cell types in the cortex, the expression interneuron became misleading as it was usually used synonymously with inhibitory cells [31], [32]. Despite a series of studies de-

DOI:10.15774/PPKE.ITK.2020.008

scribing the symmetrical (inhibitory) nature if synapses created by interneurons, there exist cells with local arborisations, which can establish asymmetrical (excitatory) synapses as well [31], [33]–[35]. Notwithstanding, in the recent study, the expression interneuron (IN) refers to all GABAergic (releasing neurotransmitter gamma-aminobutyric acid, GABA) nonprincipal cell. In contrast to pyramidal cells, interneurons usually have prominent dendrites aiming towards the white matter, while the neurite, which can arise either from the soma or a primary dendrite is oriented towards the pial surface. Inhibitory neurons receive both excitatory and inhibitory synapses on their cell body [24], [25], [29], [30].

The most prominent interneuron is the basket cell. The name is derived from the nature that the axons form baskets around the somata (or proximal dendrites) of the targeted pyramidal cells. Basket cells can be found in layers II-VI with several beaded, mainly aspiny dendrites. They can have either sparse or dense local axonal cluster, with variable bouton density. While large basket cells have conspicuous collaterals elongating across multiple layers or columns, only a few small basket cells have far-reaching projections [24], [25], [29], [30].

Bitufted cells have an ovoid cell body with two dendritic tufts on the opposite sides, which are sometimes accompanied by an additional dendrite. They send inhibitory synapses to the dendrites of the targeted neurons. Their axons traverse vertically across layers, mostly staying within the column. While their somata only can be found in layers II-V, their dendrite trees are able to extend to the adjacent layers too [24], [29], [32], [36].

Just as bitufted cells, bipolar cells also prefer to send synapses to the dendrites of the targeted cells, but in this case, the effect can be either inhibitory or excitatory. Their spindle-shaped somata might be located in layers II-V. They have very simple dendritic and axonal trees. The two primary dendrites originate from the two opposite poles of the cell body and span vertically, usually through all cortical layers. Occasionally it ends in a dendritic tuft in layer I. The neurite typically emerges from one of the primary dendrites and traverses across multiple layers. The axon has a meagre number of boutons, and the population of its targeted neurons is restricted [24], [29], [32].

Double bouquet cells are characterised by elongated dendrites extending radially above and below the somata and an axon that forms a cascade of vertically oriented, mainly descending collaterals. The collaterals of the axon form narrow columnar bundles with a high density of boutons. [24], [29], [30]. Double bouquet cells can be found in layers II-V, but only the ones located in layers II and III tend to develop inhibitory synapses [24], [29], [32].

The small, round soma of neurogliaform cells might be found in layers I, III and IV sending inhibitory synapses to the dendrites of local interneurons and pyramidal cells. They are charac-

DOI:10.15774/PPKE.ITK.2020.008

terised by dense, thin, short, aspiny, finely beaded, radiating dendrites which are rarely branched around. Their axons are very thin, intricately branched with highly intertwined arborization and covered by tiny boutons. Usually, the dendritic and axonal field of neurogliaform cells is confined within the same layer and column [24], [29], [32], [37].

Martinotti cell is another interneuron which preferentially targets dendrites, located in layers II, III, IV and V. They have beaded dendritic branches with sparse spines. The local axonal cluster (primarily intralaminar and intracolumnar) is quite dense, which projects to layer I, where it spread across multiple columns [24], [29], [32].

Cajal-Retzius cells are interneurons exclusive to layer I. They mainly innervate dendritic tufts surrounding different interneuron types at the same time. They are characterised by large somata and long horizontal dendrites. The horizontally projecting neurite generates short ascending and descending axonal collaterals [24], [29].

Last but not least, chandelier cells are interneurons of layers III and V, which preferentially innervates the axon initial segment of the targeted neurons, usually pyramidal cells. The name comes from the characteristic appearance of the axon terminal, forming short vertical bouton arrays. The axonal clusters are usually restricted to the layer and column of the cell body. Dendrites are mostly aspiny and beaded, have sparse branches which might elongate through multiple layers [24], [29].

DOI:10.15774/PPKE.ITK.2020.008

Table 2.1. Main neuron types of the neocortex (modified from R. B. Wells, 2005)

Cell Type	Signalling Class	Primary Neurotransmitter	Co-localised neuropeptide	Location of Cell Body	Dendritic Location	Principal Axonal Targets
pyramidal cell	regular spiking, irregular spiking	glutamate	somatostatin, cholecystokinine	layers II-VI	all layers	white matter, dendrites.
spiny stellate cell	regular spiking	glutamate		layer IV	layer IV	dendrites in II-IV.
basket cell	fast-spiking, regular spiking, continuous bursting	GABA	neuropeptide Y, cholecystokinine, vasoactive intestinal peptide, somatostatin	layers III-V		soma and proximal dendrites with intra-laminar and intra-columnar projections and long inter-columnar projections.
bitufted cell	fast-spiking, irregular spiking, continuous bursting, regular spiking	GABA	somatostatin, cholecystokinine, vasoactive intestinal peptide	layers II-V	adjacent layers	intra-columnar over all layers.
bipolar cell	fast-spiking, continuous bursting, regular spiking	GABA	vasoactive intestinal peptide	layers II-IV	all layers	dendritic shafts over all layers but few and very restricted target cells.
double bouquet cell	fast-spiking, continuous bursting	GABA	vasoactive intestinal peptide	layers II-V	around the soma	dendrites over all layers in a column.
neurogliaform cell	fast-spiking	GABA	neuropeptide Y	layers I, III, IV	local layer	dendritic shafts in the same layer, column.
Martinotti cell	fast-spiking, continuous bursting, irregular spiking	GABA	neuropeptide Y, somatostatin, cholecystokinine, neuropeptide Y+somatostatin	layers II, III, V, VI	as the soma	dendrites with intra-laminar and intra-columnar projections and inter-columnar projections.
Cajal-Retzius cell		GABA		layer I	layer I	local dendrites.
chandelier cell	fast-spiking, continuous bursting	GABA		layers III, V	layers III, V, VI	local axons in same layer and column.

DOI:10.15774/PPKE.ITK.2020.008

2.2 Epilepsy and related diseases

2.2.1 Some words about the epilepsy

The word *epilepsy* is derived from the Greek word *epilambanein*, which means *to be seized* or *to be taken hold of*. This terminology refers to the belief that seizures were caused by the possession of supernatural forces or gods on the body, usually as a punishment. The origin of the description of the disease goes back to ancient Babylon, but it was also noticed by Chinese and Indian physicians over three millennia ago. Although Hippocrates was the first one, who insisted the neuropathological origin (in about 400 BC), the most common treatment of the 'Sacred Disease' consisted of spiritual incantation until the seventeenth century [38], [39]. Within Lumeleian Lectures in 1849, Robert Bentley Todd, an Irish physiologist explained epileptic seizures with electric discharges in the brain. This theorem started to be seminated only after 41 years by John Hughlings Jackson [39]. With his contribution, Victor Horsley was the first neurosurgeon, who performed craniotomy in order to cure epilepsy, so that he launched the development of the epilepsy surgery [40].

The definition of the *epilepsy* have been differentiated from the *seizure* long ago by the International League Against Epilepsy (ILAE). According to their report from 2005, *'an epileptic seizure is a transient occurrence of signs and/or symptoms due to abnormal excessive or synchronous neuronal activity in the brain'* [41]. In contrast to that, epilepsy is a disorder of the brain which meets at least one of the following conditions: (1) the patient suffers from at least two unprovoked seizures occurring at least 24 h apart; (2) the patient undergoes one unprovoked seizure with a high risk of another occurrence over the following ten years; (3) the patient has been diagnosed with an epilepsy syndrome [41], [42].

Seizures are classified into three groups according to their manifestation (*Figure 2.2*): (1) focal onset seizures are initiated from an area or a group of cells in one side of the brain; (2) generalized onset seizures affect both sides of the brain; (3) seizures with unknown origin or if it is not witnessed by anyone are called unknown onset seizures. Focal onset seizures can be further divided depending on whether the subject was aware of self and environment during the seizure or not. Another way of classification of focal seizures is whether it is associated with motor or non-motor symptoms [43], [44]. There is a special seizure type called 'focal to bilateral tonic-clonic', where the name refers to the propagation pattern of the seizure, and it has been categorised separately because of its significance [43]. Generalised onset seizures can be associated with tonic-clonic or other motor symptoms or with non-motor symptoms (absence seizures) [43], [44]. Finally, unknown onset seizures might be referred to as 'unclassified', or

DOI:10.15774/PPKE.ITK.2020.008

they can be assigned by other features (if it is known) such as motor, nonmotor or tonic-clonic seizures [43].

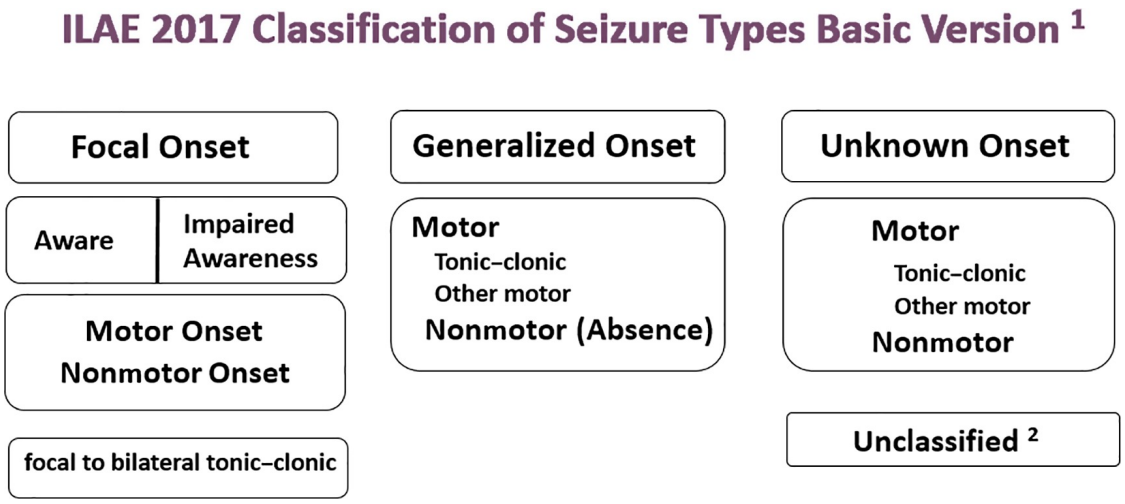

Figure 2.2. The basic ILAE 2017 operational classification of seizure types. [1] Definitions, other seizure types and descriptors are listed in the accompanying paper and glossary of terms. [2] Due to inadequate information or inability to place in other categories [43].

After the determination of the seizure type, the second step in the diagnosis is the categorisation of epilepsy. The type of epilepsy can be focal, generalised or unknown, just as it is for seizures, but it has an additional type called combined generalised and focal epilepsy. A patient with epilepsy of one type can have seizures with different onset. The third level of the diagnosis is to determine epilepsy syndrome. The epilepsy syndrome is being specified by a cluster features such as seizure types, EEG, imaging features, age at onset and remission, seizure triggers, diurnal variation, prognosis and distinctive comorbidities (e.g. intellectual and psychiatric dysfunction) which might occur together [45].

Unto this day, the most widely used treatment of epilepsies is based on antiepileptic drugs (AEDs). Though it is still not clear how anticonvulsants prevent the generation of seizures [39], [46]–[48]. Furthermore, it is remained uncertain whether drug treatments only suppress seizures or arrest epilepsy in long term [39]. The most commonly used phenobarbital was introduced in 1912, and similarly to other AEDs, it has not been much improved since then [39], [46], [47]. The development in the localisations of focal seizures and of EEG techniques fostered the evolution of epilepsy surgery [39], [40]. Despite the high successful-rate (70-80%) and the fact, that it is the only therapy that actually cures epilepsy, surgical treatment is only used after the failure of two or three adequate AEDs and after the patient was diagnosed with pharmacoresistant epilepsy [39].

Epilepsy is a disease which can occur in any mammal. The incidence is likely to increase

DOI:10.15774/PPKE.ITK.2020.008

with the development of the brain [39]. It is widely distributed around the world without racial, geographical or social class barriers. Epilepsy occurs at all ages, in both sexes [39], [49]. About 65 million peoples worldwide have epilepsy currently [50]. The estimated incidence of the disorder is 50 per 100000 population, while the prevalence approximates 700 per 100000 in the developed countries [50], [51]. These rates are higher in low-income areas [50].

Several comorbid conditions can be associated with epilepsy, including psychiatric disorders, infectious diseases or accidents. These conditions can appear as a consequence of epilepsy or epilepsy treatment, or they might share a common aetiology with the disorder [50]. The mortality rate of patients with epilepsy is 2-3 times higher than that of the general population. This might be caused by the aftereffect of the seizure (e.g. an accident), the adverse reaction of the treatment or a fatal outcome of an underlying disease (e.g. tumour) among others [52]. Epilepsy disorder is associated with stigma and psychological, social, cognitive, and economic repercussions [41]. After decades of research of epilepsy, the understanding of the mechanisms underlying the disease still has gaps. Finding more information about these phenomena may lead to new ways to tackle seizures and developing new treatments.

2.2.2 Tumour-associated epilepsy

The incidence of tumours in patients diagnosed with epilepsy is about 5% [53], [54]. While the chances that epilepsy will be developed in patients with a brain tumour is at least 30%, but this value is highly proportional to the type of tumour and other factors [54], [55]. Grade, location, and morphology, as well as the changes in the microenvironment and genetic factors, contribute to the emergence of seizures [54]–[56].

Low-grade tumours have the highest epileptogenicity. A possible reason is that these kinds of tumours have longer time to grow aberrants pathways so it can deafferentate normal brain tissue. Which, by that, will be isolated from normal regulation. The incidence of seizures in the presence of dysembryoplastic neuroepithelial tumours is almost 100%, while it is 60-85% in low-grade astrocytomas or oligodendrogliomas [54]–[56]. Developmental tumours are often associated with cortical dysplasia or other structural abnormalities which tend to participate in the generation of seizures. In case of rapidly growing tumours, the epilepsy is known to be caused by the abrupt ways of tissue damage such as necrosis [54], [55].

Superficial and cortical tumours are associated with the development of seizures, unlike non-cortical, deeper lesions, or any lesion in the white matter, which are rarely epileptogenic [54]. Within cortical lesions, the ones in the temporal, frontal and parietal lobes tend to generate more seizures than those in the occipital regions [54]–[56].

DOI:10.15774/PPKE.ITK.2020.008

Peritumoural morphology has an effect on the epileptogenesis too. (1) Neurons with aberrant migration to the white matter, (2) enhanced excitation caused by peritumoural pyramidal cells which have less inhibitory and more excitatory synapses or (3) the affected regions with abnormal physiology can increase epileptic activity [54], [55]. As the consequence of tumour, synaptic vesicles go through changes, and the enhanced expression of gap junctions (GJs) causes intensified intercellular communication [55]. Further, an imbalance between inhibition and excitation was discovered as a result of the modification in the GABA and glutamate concentrations [55], [57], [58]. Moreover, alteration in the angiogenesis around the tumour tissue causes hypoxia, which changes the pH of the interstitial fluid in the adjacent regions. These events drive cells to swell and damage glial cells, which lead to enhanced neuronal excitability and thus, epileptogenicity [54], [55].

Treatment of patients with tumour-associated epilepsy might include the combination of AEDs, surgery, radiation therapy or chemotherapy. A significant amount of epilepsies related to brain tumour shows refractoriness to AEDs as the result of the loss of receptor sensitivity or as the effect of multidrug-resistance proteins. Newer AEDs are preferable over conventional treatments because they have fewer side-effects and limited interactions with other drugs. In case of the failure of monotherapy, the application of the combination of drugs is indicated. In addition, control of tumour growth might help in the suppression of seizures, especially when the attempt of medical cure fails, which consists of neurosurgery, chemotherapy and radiotherapy. It raises further problems that antitumour treatment can cause epileptic seizures itself. Moreover, interactions between AEDs and chemotherapy might reduce effectiveness and intensify the side effects of both therapies. [54]–[56], [59].

2.2.3 Other linked disorders

Hippocampal sclerosis (HS) is typically the anatomical basis of mesial temporal lobe epilepsy, but it can be associated with other epilepsy syndromes as well. In the case of pharmacoresistant epilepsies, HS is one of the major pathologies. HS is a disorder of the hippocampal nerve tissue, characterised by histological and functional changes. Usually, selective loss and degeneration of CA1 and CA3 pyramidal cells can be observed with an extensive proliferation of interneurons and pathological glia reaction [60], [61]. HS is linked with granule cell dispersion (GCD), where these cells (instead of forming a dense, compact block) are being scattered, reaching out to the stratum moleculare, while the intermediate space is widening [61], [62]. GCD often alternates with granule cell loss and is thought to be the consequence of seizures instead of being a pre-existing abnormality [61]. Another accompanying symptom of HS is the sprouting of mossy

DOI:10.15774/PPKE.ITK.2020.008

fibres in the dentate gyrus. The recurrent axons of granule cells grow more extensive branches through their normal projection region and in addition to that, they innervate granule cells and interneurons in the stratum moleculare [61], [62]. These local 'short-circuits' synchronise the adjacent neurons, and together with the increased excitatory inputs, establish the generation of excessive epileptogenicity [60]–[62].

Cortical dysgenesis (CDG) is a disorder which emerges during the development of the cerebral cortex. It is the second most common cause of epilepsy (24% of cases) after HS, according to studies at the National Hospital in London. The aetiology can be a genetic disorder or some form of external insult (toxins, infections, drugs, etc.) [63]–[65]. The neurons which constitute the cortex, originate from neuroblasts located in the ventricular zone close to the midline of the developing brain. These cells continually proliferate, differentiate and migrate throughout the prenatal (and to some extent, throughout the postnatal) life. More than 25% of these primitive neurons suffer programmed cell death. CDG is the result of an aberration which might occur at any time during neural development, but most often between the 7th and 16th gestational weeks. The pathological characteristics of the disease depend rather on the timing than on the origin of the distortion [63], [65]. Subcortical and subependymal heterotopias are common causes of epilepsy. The formation of inappropriate cell groups may derive from the abnormal termination of the migration process, excessive migration, or the lack of fetal programmed cell death. The dysembryoplastic neuroepithelial tumour, a neoplastic dysgenesis, is also involved in the development of epileptic seizures. It is usually benign, heterogeneous, dysplastic and proliferative, and has a well-defined intracortical lesion which usually affects the temporal lobe [65].

Although most studies use the terms local cortical dysplasia (CDP) and CDG synonymously, there are differences between them concerning their extent, localisation, or their underlying pathogenesis [66]. In the case of CDP, the overlying neocortex is usually macroscopically normal. It only shows histological abnormalities with irregular lamination and bizarre neurones [65], [67]. Both genetic and acquired factors might be involved in the genesis of CDP. It can occur not only during childhood but also in adults. It can be restricted to the temporal lobe or extend to other areas. Sometimes CDP is associated with other principal lesions such as HS, tumour or vascular malformations [68], [69]. For a seizure-free life, the resection of the epileptogenic zone is essential [69].

Epilepsy is a prevalent manifestation of cerebral cavernous malformations (CCMs), and what is more, it is often diagnosed only after the first occurrence of a seizure. CCMs 'are clusters of dilated sinusoids filled with blood and lined with endothelium without intervening parenchyma' [70]. It is the outcome of vascular cavern proliferation caused by repetitive lesional haemor-

DOI:10.15774/PPKE.ITK.2020.008

rhages. With the development of neuroimaging techniques, several seizures previously classified as cryptogenic (i.e. with unknown origin) appeared to be the consequence of cavernous malformation. The incidence of epilepsy is highly proportional to the type of the lesion [70]. CCMs are malformed blood vessels and usually do not affect the grey matter directly. They induce seizures by changing the conditions of the adjacent brain regions [70], [71]. Sometimes epilepsy can be cured simply by the resection of the critical area. Other times changes caused in the brain tissue result in a permanent epileptogenic focus, which becomes independent of the original lesion [70]. CCMs can induce alteration in relatively distant brain regions, affecting present or even creating new epileptogenic foci [70], [72]. The treatment of CCMs induced epilepsy consists of medication, lesionectomy, the resection of the epileptogenic region or new-line therapies, such as vagus nerve stimulation [70].

2.3 Electrophysiological and molecular background of cell firing

2.3.1 The generation of action potentials

Electrophysiological phenomena are based on the ionic composition and its alteration formed on both sides of the cell membrane. While the extracellular space contains higher concentrations of positively charged sodium ions and negatively charged chloride ions, the intracellular space contains mainly positively charged potassium ions and negatively charged proteins. As proteins are not able to traverse through the membrane, the migration of ions through ion channels or transport proteins is responsible for the establishment of the membrane potential. The Hodgkin-Katz-Goldman equation determines the resting membrane potential of a typical neuron:

$$U = \frac{RT}{F} ln \frac{P_K [K]_{out} + P_{Na} [Na]_{out} + P_{Cl} [Cl]_{in}}{P_K [K]_{in} + P_{Na} [Na]_{in} + P_{Cl} [Cl]_{out}}, \tag{2.1}$$

where R is the gas constant [8.413 J / (mol * K)], T is the absolute temperature (310 K), F is the Faraday's constant (9.649 * 104 C / mol), P_{ion} is the relative permeability for the corresponding ions, while $[ion]_{in}$ and $[ion]_{out}$ are the ionic concentration inside and outside the cell, respectively. For a typical neuron U = -65 mV. If the membrane potential is moved in a negative direction, the cell is hyperpolarised, and if it is more positive, the cell is depolarised. When the degree of depolarisation reaches a given threshold, action potentials (APs) are generated [24], [28], [73], [74].

The propagation of action potential on the axon was described by Alan Lloyd Hodgkin, Andrew Huxley and Bernard Katz in 1952 in a 5-part series of articles. Their model draws a parallel between a neuron and a simple electrical circuit. The membrane offers resistance to the flow of

DOI:10.15774/PPKE.ITK.2020.008

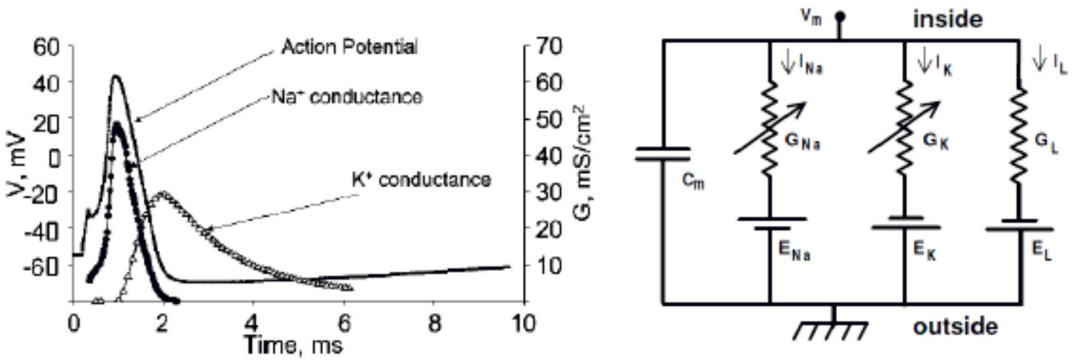

Figure 2.3. The role of conductances. Left: the change in channel conductances during the generation of an action potential (time (in ms) on the abscissa, membrane potential (in mV) on the ordinate, and the conductance (in mS / cm^2) on the right); Right: electrical circuit corresponding to an axon (G = conductance, I = ion current, E = reverse potential, L = leakage, c = capacitance) [75], [76].

charged ions and thus exhibits membrane resistance. The current, i.e. the ions, pass through ion channels, which are represented by parallel conductances. Just as a real capacitor the membrane is bordered by two conductors (i.e. cytoplasm and extracellular fluid), thus it is able to store electrical charge. In case of a capacitor, the gathering of ions on one side of the insulator will push away the ions of the same charge on the other side, while attracting the opposite charges. Thus capacitors are conducting electricity without changing the ion concentration between the two sides of the membrane. In contrast to that, in case of a resistance/conductance, the actual ion flow through the membrane causes a change in the membrane potential [77], [78].

The depolarisation of the membrane by stimuli enhances the conductance of Na^+ channels, triggering an inward flow of Na^+ ions into the intracellular space. This further increases the membrane potential, which opens additional Na^+ channels. When the depolarisation reaches a certain threshold, an action potential is generated. The inactivation of Na^+ channels and the activation of K^+ channels cause the repolarisation of the cell membrane. The latter means an outward flow of positive ions to the extracellular space and results in after-hyperpolarisation of the cell [24], [75]–[78].

APs can be generated at any part of the neuron. Usually, it initiates on the axon initial segment, as the threshold of the generation of APs is the lowest here. This is because a high density of Na^+ channels can be found here with a low activation threshold. Once an AP is generated, it travels orthodromically down to the axon terminals, where it causes neurotransmitter release. The AP propagates antidromically back as well through the soma and dendrites and causes changes in the intracellular processes [24], [29], [75], [77].

DOI:10.15774/PPKE.ITK.2020.008

2.3.2 Chemical synapses

The basis of the signalling between neurons is the synapse. The presynaptic neuron sends an axon to the dendrites, the soma or even to the axon of the postsynaptic neuron and forms a synapse. The two main synaptic types of the neocortex are chemical and electrical synapses (gap-junctions) [24], [29], [77].

In case of a chemical synapse, when an impulse reaches the axon terminal of the presynaptic neuron, Ca^{2+} channels open and Ca^{2+} ions flow into the synaptic end bulb. This sign triggers the exocytosis of the vesicles and neurotransmitters are being released into the synaptic cleft. The neurotransmitters diffuse across the cleft and bind to receptors which are connected with ion channels and cause a change in the conductance of the postsynaptic membrane (either on the dendrite, soma or axon). Excitatory neurotransmitters, like glutamate, allows inward Na^{+} flow, causing excitatory postsynaptic potential (EPSP), and having a depolarising effect. In contrast to that, the inhibitory neurotransmitters, such as GABA, let inward Cl^{-} flow or outward K^{+} flow, which results in inhibitory postsynaptic potential (IPSP) and hyperpolarises the postsynaptic membrane. The superposition of all incoming EPSPs and IPSPs will determine, whether an AP will be initiated on the axon initial segment or not [23], [24], [29], [77]. Together with neurotransmitters, other neuroactive substances, so-called neuromodulators are participating in the communication between cells of the central nervous system (CNS). Neurotransmitters induce postsynaptic responses with quick in onset (< 1 ms) and short in duration (less than tens of milliseconds). These fast postsynaptic potentials usually affect local circuits, allowing the neurons to perform an enormous number of computations in a short period of time. In contrast, neuromodulators are characterised by delayed onset and prolonged duration. They might vary in shape, size and the effect on the functional features of neurons or networks. The slow synaptic potential caused by neuromodulators has rather a modulatory impact on the excitability of the neurons. When the receptor binding site is being the part of the macromolecule which forms the ionic channel, it is called ionotropic. When the receptor is acting indirectly on the channel via a second messenger, it is usually called metabotropic [30].

2.3.3 GABAergic transmission

GABA is the primary inhibitory neurotransmitter of the mammalian CNS. It is synthesised from glutamate by an enzyme called glutamic acid decarboxylase in the cytoplasm of the axon terminals of GABAergic neurons. It is being released to the synaptic cleft via exocytosis as a consequence of the depolarisation of the presynaptic neuron and diffuses to the targeted receptors. The reuptake of GABA molecules from the cleft is executed by either the presynaptic nerve terminals

DOI:10.15774/PPKE.ITK.2020.008

or by the surrounding glial cells. The former way, GABA might be reutilised. Whereas, in glial cells, GABA is being converted to glutamine, which is transferred back to the GABAerg neuron and being converted back to glutamate (*Figure 2.4*) [30], [79], [80]. GABA have three major receptor types, the ionotropic $GABA_A$ and $GABA_C$, and the metabotropic $GABA_B$ receptors [30], [81], [82].

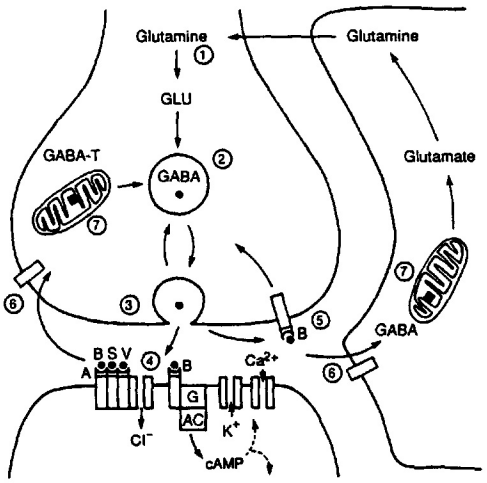

Figure 2.4. Molecular mechanisms of a GABAergic synapse. (1) synthesis of GABA from glutamine; (2) transport and storage of GABA; (3) release of GABA via exocytosis; (4) binding to a $GABA_A$ receptor that can be blocked by bicuculline (B), picrotoxin, or strychnine (S) and can also be modified by benzodiazepines, such as valium (V); $GABA_B$ receptors, are linked via a G-protein to the opening of K^+, or the reduction in Ca^{2+}, channels; (5) release of GABA is under the control of presynaptic GABA receptors; GABA is removed from the synaptic cleft by uptake into terminals or glia (6); and (7) processing of GABA back to glutamine. (From [30], [83], [84])

$GABA_A$ receptors can be found on the postsynaptic membrane [30], [85]. There are 16 known $GABA_A$ receptor subunits which constitute various combinations of pentamers resulting in ligand-gated ion-channels permeable to Cl^- ions [30], [85], [86]. The influx of Cl^- ions hyperpolarises the postsynaptic membrane and thus inhibits the generation of an action potential [30], [85]. $GABA_A$ receptors can bind benzodiazepine and barbiturate on different binding sites as well [30], [85], [87]. While benzodiazepines increase the opening frequency, barbiturates prolong the opening duration of the ion channels, thus might suppress seizure activity with varying degrees of success [30], [85], [88]. The competitive $GABA_A$ receptor antagonist bicuculline widely used in the description of animal models of epilepsy. The sensitivity of the receptor might be reduced by the increased level of intracellular free Ca^{2+} [30], [89]. According to certain studies GABA might have an excitatory effect as well in immature neurons [90] or in specialised neuronal populations [91]–[93] due to the raised intracellular Cl^- concentration [94].

$GABA_B$ receptors cause slow postsynaptic inhibition by opening inwardly rectifying K^+ channels [94], [95]. They are also suspected

DOI:10.15774/PPKE.ITK.2020.008

to reduce dendritic excitability by inhibiting voltage-gated Ca^{2+} channel sensitivity [94], [96]. $GABA_B$ receptors can be found presynaptically as well inhibiting the release of either excitatory or inhibitory neurotransmitters depending on the nature of the synapse [30], [94]. Certain $GABA_B$ agonists, such as baclofen, have been reported to induce hyperexcitability [85].

$GABA_C$ receptors are ligand-gated Cl^- channels just as $GABA_A$ receptors, composed of GABA ρ subunits [97]–[99]. They are found most prominently in the retina [98], [99]. Responses related to $GABA_C$ receptors are characterised by even slower onset and offset kinetics than the ones sustained by the metabotropic $GABA_B$ receptors [97], [99]. $GABA_C$ receptors are blocked by neither $GABA_A$ nor $GABA_B$ receptor antagonists, as they are not modulated by their agonists as well. In contrast, it has shown sensitivity to picrotoxin, a Cl^- channel blocker [98], [99].

According to a widespread hypothesis, epileptic hyperexcitability is the result of the decreased inhibition in the neocortex. This idea was supported by the fact that GABA receptor agonists suppress epileptic activity, while GABA receptor antagonists, as well as drugs that inhibit GABA synthesis, induce seizures [14], [100]. Furthermore, several studies demonstrated the reduced number or function of $GABA_A$ subunits in patients with mesial temporal lobe epilepsy [14], [101], [102]. Although, whether these malfunctions are associated with the pathophysiology of seizures (such as HS) has not been clarified [14], [101]. But, it is not only the lack of GABAergic transmission, that might lead to aberrant excitability in the neocortical networks. According to recent studies, the increased level of intracellular Cl^- ions in epilepsy converts GABA-mediated responses into EPSP, which might contribute to the developing hyperexcitability at the pathogenic areas [103].

2.3.4 Gap-junctions

The gap-junction is the other main type of synapses together with the chemical synapse. It forms a physical connection between neighbouring neurons, extending through the membrane of both cells. Gap-junctions consist of a class of proteins called connexins [30], [32], [104]. Cells can express different types of connexins, but usually, there is one type which predominates. Six connexins form the hemichannel of the water-filled pore of a gap-junction [32], [104]. Gap-junctions have been observed in the retina, between olfactory granule cells, and in some brainstem nuclei, as well as in the thalamus and neocortex of mammals [30], [105]–[107].

Gap-junctions are forming symmetrical bidirectional synapses between particular GABAergic neurons (mainly among the same class) [30], [32], [107]. Whether PCs are able to sustain electrical connections is yet a matter of debate. Though there were some attempts to prove the

DOI:10.15774/PPKE.ITK.2020.008

presence of gap junctions between excitatory cells [108]. Despite the uncertainty, it can be stated that INs have a considerably higher affinity to form electrical coupling. Gap junctions allow a direct exchange of ions or intracellular messengers (cAMP, IP_3, small peptides) between cells [32], [104]. They are able to deliver both depolarising and hyperpolarising signals, thus inducing both excitatory and inhibitory PSPs. Usually, gap-junctions allow current flow in one direction much better than in the other, having a rectifying effect on the signalling [32]. They are also known to act as low-pass filters, which transmit slow membrane potentials but attenuate fast changes, such as APs [30], [32], [107]. It has been shown that electrical coupling between cortical INs can result in jointly firing neuronal networks, which might have an unclarified role in epileptiform hypersynchrony [14], [30], [32], [109], [110].

2.3.5 Neuropeptides

Neuropeptides are small protein-like molecules which are responsible for the communication between neurons in both central and peripheral nervous systems [23]. They differ from neurotransmitters (such as GABA or glutamate) concerning their size, signalling function, synthesis and storage. Neurotransmitters are synthesised in nerve terminals, stored in small synaptic vesicles, thus they can act very fast, but have only a short-term response which is restricted to the synaptic specialisation [98], [111]. In contrast to that, neuropeptides are synthesised in the cell body, kept and transferred to the terminals by large dense-core vesicles. They have a slower but prolonged action since they do not undergo reuptake such as classical neurotransmitters do. They have an affinity to be released at higher firing rates, especially during burst-firing patterns [32], [98].

Neuropeptides are not confined to the synaptic cleft. They might diffuse some distance to activate receptors further from the release site [98], [111]. This mechanism is called volume transmission. Thus, neuropeptides are able to affect a large number of neurons at the same time. They are released to the synaptic cleft with other, classical neurotransmitters (coexistence), which might affect their actions on the targeted neurons [98]. They exert their influence through metabotropic receptors having either excitatory or inhibitory effect [23], [98], [111]. These targeted receptors might be located on the presynaptic or postsynaptic cell, as well as on adjacent or relatively distant neurons [79].

GABAergic INs of the neocortex produce various neuropeptides, such as somatostatin (SSt), cholecystokinine (Cck), neuropeptide Y, vasointestinal peptide (VIP), and substance P [30], [112], [113]. The role of these peptides though remained ambiguous [30]. SSt and its receptors influence GABA and acetylcholine release and thus modulate neuronal excitability. It might

DOI:10.15774/PPKE.ITK.2020.008

inhibit neuronal Ca^{2+} currents, modulate inwardly rectifying K^{+} currents, and depress glutamatergic EPSPs, which leads to reduced neuronal firing [30], [98]. Cck and neuropeptide Y are thought to reduce glutamate and GABA release from the presynaptic terminals as well [111], [114].

2.3.6 Firing patterns

After the investigation of repetitive discharge properties of neocortical cells, McCormick et al. (1985) have distinguished three characteristic firing patterns: regular-spiking (RS), intrinsically-bursting (IB), and fast-spiking (FS) (*Figure 2.5*). The signalling type was determined by observing the neuronal response when it is injected with a constant excitatory current [24], [115]. In the case of RS cells, the initially high firing rate, which is contingent upon the injected current, slows down, and the neuron establishes a steady discharging pattern. This phenomenon is called spike train adaptation or accommodation [24], [29], [30], [115]. The density of the high voltage-gated Ca^{2+}-channels and the affected Ca^{2+}-dependent K^{+}-channels thought to be responsible for the degree of the adaptation [24], [115], [116]. The vast majority of PCs are RS cells [24], [29], [30], [115]. Their AP duration is 0.6-1.0 ms at one-half amplitude, they have a prominent afterhyperpolarisation, and their activity has been captured in layers II-VI of the neocortex [115].

IB discharges are characterised by three to five APs superimposed on a slow depolarising envelope. During the course of the burst, the amplitude of the spikes, as well as the rate of the rise show a decline, while the duration of the spikes increases. It is terminated by an afterhyperpolarisation period and followed by either a single discharge or another burst [24], [29], [115]. The individual spikes resemble those generated by RS cells, but they are accompanied by a prominent afterdepolarisation, which might form a slow, low-amplitude depolarising wave during a burst [117]. Bursts are thought to be the outcome of transient low-threshold Ca^{2+} current generated by low-voltage-gated Ca^{2+} channels [24], [115], [118]. IB neurons are observed to be PCs of the layers IV and V [24], [29], [115].

The classical FS pattern is characterised by the series of APs with short interspike interval [119]. The spikes are brief compared to those of RS or IB cells, and they are followed by a short but prominent afterhyperpolarisation phase [24], [30], [115], [117], [119]. The individual spikes are usually faster than 0.5 ms and can be unambiguously separated from the other two firing patterns [115], [117]. Smooth or sparsely spiny, GABAergic, nonpyramidal cells are thought to be the sources of FS discharges. Their firing frequency does not change when they are injected with an excitatory current, thus they are often called non-accommodating cells as well [24], [30], [115]. The fast upstroke of the AP might be related to sodium-dependent mechanisms. The rapid

DOI:10.15774/PPKE.ITK.2020.008

repolarisation can be the result of the large-scale sodium channel inactivation. Although, the prominent postspike undershoot is thought to be related to a rapidly activating and inactivating potassium conductances. Finally, the absence of adaptation could be explained by the lack of prolonged potassium conductances [115]. Mechanisms underlying the electrogenesis of FS is yet obscure.

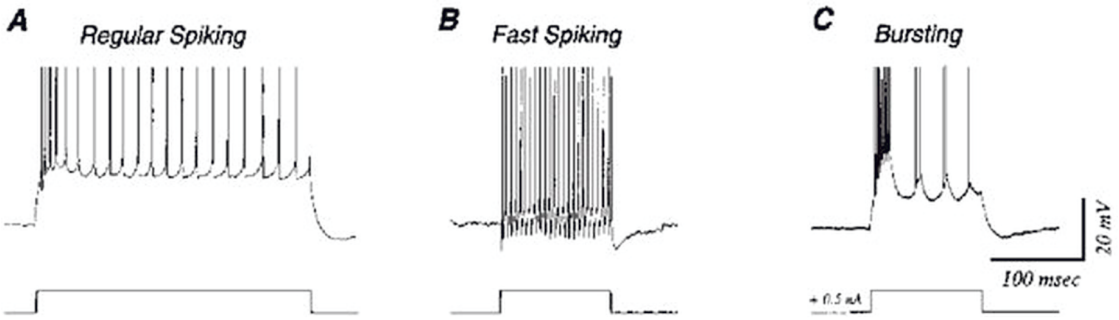

Figure 2.5. Characteristic response of neurons in the CNS to constant current pulses. PCs show regular spiking (A) or intrinsically bursting (C) firing behaviour. The most prominent discharge pattern of INs is fast-spiking (B) [120].

INs seem to be more variable concerning their characteristic firing patterns. There have been attempts to classify the electrical properties of them in more detail. Five main categories have been identified: (1) Nonaccomodating cells are the most frequently observed among INs, firing repetitively, with no or minimal change in the interspike interval. They have relatively fast AP with deep afterhyperpolarisation phase. (2) The second most frequently encountered INs have accommodating, repetitive firing pattern with a decrease in discharge frequency. Though, accommodating cells have higher firing frequency and slower accommodating capability than RS cells. (3) Stuttering cells have high-frequency clusters of APs with little or no accommodation, interrupted by silent periods with unpredictable length. (4) Irregular spiking INs produce random discharges which do not form a certain cluster of APs. (5) Bursting behaviour has been observed among INs as well. The initial high-frequency clusters with their strong afterhyperpolarisation periods can be followed by other bursts, they can appear as a single phenomenon, or they might be an initial segment for an accommodating firing pattern [24], [29], [30].

2.4 Brain oscillations and synchronous events

2.4.1 The sources of oscillations in the CNS

Two main mechanisms behind rhythmic generation have been proposed in the CNS: intrinsic membrane properties and synaptic circuits [30]. The former relies on the idea of autorhythmic

DOI:10.15774/PPKE.ITK.2020.008

neurons in the CNS. Pacemaker neurons are capable of possessing organised ionic conductances, which endow them to respond to inputs with oscillations at different frequencies. In addition to that, many neurons act like resonators, which means that they prefer to accommodate specific frequencies [30], [121]. Low-threshold Ca^{2+} conductance might have an essential role in the maintenance of rhythmic behaviour, which was most commonly observed in neurons with oscillatory properties. It is being inactivated at the resting membrane potential and being deinactivated with hyperpolarisation. The study of the low-threshold Ca^{2+} conductance led to the conclusion that even subthreshold depolarisation might result in AP generation if it is superimposed on either depolarising or hyperpolarising modification in the membrane potential [121]. Another influential component is the nonactivating or persistent Na^{+} conductance, which is able to maintain prolonged, low amplitude membrane potential changes, the so-called plateau potentials. As such, it does not generate an AP, but instead, it regulates excitability by triggering the initiation of spiking [121], [122]. Other, ligand-activated voltage-dependent and voltage-independent conductances are participating in the neuronal integration and oscillation as well. In these cells, the ionic conductances are organised in such a manner that the membrane potential rebound, which follows the afterhyperpolarisation phase, can generate a new AP. The second AP is triggering a sequence of firing which lasts until the rebound is not able to reach the threshold anymore and the oscillation ceases [121].

GABAergic mechanisms have a key role in the rhythmic generation based on synaptic interactions. Networks consisting of both excitatory and inhibitory elements are capable of self-organisation and generating complex properties [123]. The communication between INs and PCs are reciprocal. They are very well connected, INs might inhibit more than 60% of PCs located within 100μm and also receive input from a significant amount of them [94], [124]–[128]. Thus, not only the level of local network connectivity, that determines the volume of active INs but INs influence it through their inhibitory responses as well. This is called feedback inhibition (*Figure 2.6*) [94], [124], [127], [129]. Stabilisation maintained by negative feedback results in various forms of oscillations [123].

Both excitatory and inhibitory cortical cells receive long-range excitatory afferent inputs too from subcortical areas or other cortical regions, forming a feedforward inhibition (*Figure 2.6*) [94], [124], [129]. The same afferent has a more substantial effect on INs than on PCs so that a slight change in the network excitability induces inhibition on the circuit [94], [130]. This simple coupling of PCs and INs increases the precision of spike timing substantially. Any diversion from these simple circuits unavoidably increases the complexity of the firing patterns of participating neurons. Lateral inhibition is an extended version of feedback inhibition (*Figure 2.6*). In this

DOI:10.15774/PPKE.ITK.2020.008

case, an IN is activated by a PC and suppressing the neighbouring PCs of it. The achievement of increased autonomy by competition is called 'winner takes all' mechanisms and is intended to disable the spread of APs [123]. Feedback and feedforward inhibitory circuits together ensure the simultaneous occurrence of excitation and inhibition in the neocortex [94]. They do not just increase or decrease together but are having highly disruptive interference. Any alteration in the balance of excitation or inhibition proceeds to compensatory effects [94], [131].

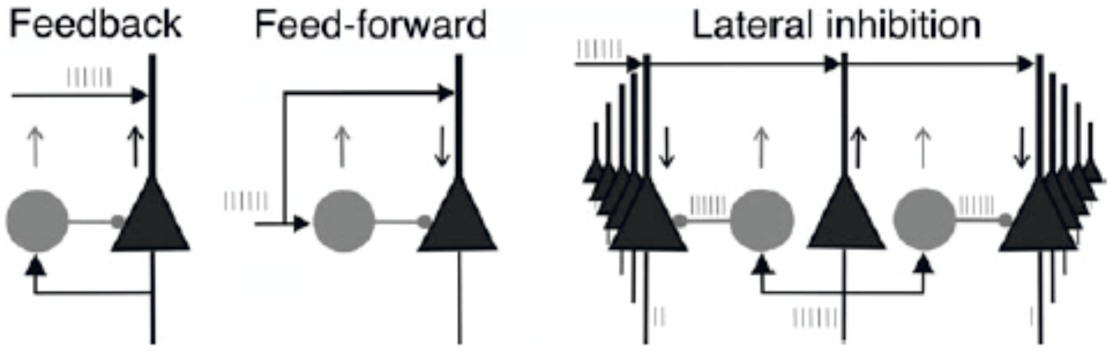

Figure 2.6. Different roles of INs in neuronal networks. Grey circles and black triangles indicate INs and PCs, respectively. Arrows show the direction of information flow. Feedback inhibition creates stability in the system, feed-forward inhibition acts as a filter of signalling, while lateral inhibition maintains the autonomy of certain neurons of the network [123].

Besides excitatory connections, INs receive inhibitory inputs from each other as well [94], [132], [133]. In a chain of INs, the first neuron suppresses the second neuron. As a consequence, the third IN will be less affected by the second. Thus the third neuron is capable of restraining its own target, and so on. This is called disinhibition. However, of course, to construct the simplest oscillatory network, an external force is needed to maintain spiking activity. The initial random spiking of INs is disturbed by some co-occurrence of discharges. These small groups will express more potent inhibition, causing more neuron suppression and then release at the same time, once the inhibition fades away. In an appropriate network, by the end of the process, most of the neurons will fire synchronously. Adding a PC to the system, we expect the outcome to be the same. Since, during the synchronous discharges of INs, all neurons are suppressed rhythmically. This scenario can be observed during an epileptic seizure. Nevertheless, these oscillatory networks are easily disturbed because even a slight perturbation in timing can have an immense deteriorating effect on the synchronisation, which is very likely to happen under physiological conditions. [123].

Gap-junctions between INs are thought to have a crucial role in the generation of synchronous activity [94]. A subthreshold change in the membrane potential of one or a few cells

DOI:10.15774/PPKE.ITK.2020.008

can be transmitted to the electrically coupled neurons [107]. On the other hand, a presynaptic AP might result in a postsynaptic spikelet within a very short period of time, thus leading to the coherent behaviour of INs on the submillisecond level. This simultaneous occurrence is not reduced by the blockade of excitatory of chemical synapses. Thus it is thought to be mediated by gap-junctions. However, only 30% of the synchronised APs were elicited from those spikelets [107], [134]. Therefore, subthreshold signalling and transmission of spikes through electrical synapses assist to the coordination of network mechanisms [107].

2.4.2 Slow oscillation as a default activity of cortical networks

Slow oscillation (SO) is implied to be a default activity emerging in cortical networks [135]. It consists of slowly alternating active and silent periods. During an Up state, neurons prefer to stay at a depolarised, subthreshold membrane potential, at which they tend to be more active with a higher probability of firing. While, in the case of a Down state, neurons tend to maintain a hyperpolarised membrane potential and stay in silence [135], [136].

SO is a collective phenomenon determined by the neuronal, synaptic and connectivity features of the cortex. It is originated from the coexistence of certain dynamical elements such as bistability, activity-dependent adaptation, and endogenous noise [135]. Bistable neurons are simultaneously attracted into both Up and Down states. Furthermore, the strong synaptic coupling leads to a reverberating network activity. An alteration between the two periods is required to maintain the populational dynamics. Activity-dependent adaptation refers to the mechanisms which allow the transition from Up to Down states [135], [136]. During the active phase, neuronal excitability gradually decreases due to the reduction of the net input current received by the neurons. This leads to the destabilisation of synaptic reverberation pushing the network toward the Down state. Through the silent period, the adaptation strength relaxes and the system is approaching toward a higher excitability [135]. Mechanisms underlying this adaptation might include ion channel-mediated currents, short-term synaptic depression and GABAergic activation. The periodic re-entry into the Up state is triggered by the so-called endogenous noise, which is the consequence of local cell firing rates and fluctuations in the inputs [135], [136].

Both excitatory and inhibitory elements are participating in the increased neuronal firing rate during an Up state [135]–[137]. The balance of excitation and inhibition is crucial for shaping the emergence of the pattern. Though, there are compensatory effects, designed to preserve the physiological activity [135]. When, for example, the fast inhibition is blocked, the multiunit firing rate during Up states increases, which leads to more efficient recruitment of activity-dependent K-channels. This shortens the duration of excitement and elongates Down

DOI:10.15774/PPKE.ITK.2020.008

states. The higher the level of firing rates during Up states, the more efficient the muting of the network. When a critical level of fast inhibition blockade is attained, the compensating mechanism fails and epileptiform discharges might occur [135], [138].

2.4.3 Spontaneous synchronous discharges in the human cortex

It has long been the subject of debate whether cortical tissue resected from human patients is able to generate spontaneous synchronous activities in vitro [3], [139]. It seems to be proved that synchronous discharges resemble those obtained by scalp or intracranial EEG, can emerge in slices prepared from the epileptic human neocortex [2]–[6]. The activity develops in a physiological perfusion solution. It does not need any artificial manipulation, neither the change of the ion concentration nor the application of pharmacons nor the movement of the tissue [3]. It appears regardless of the age or gender of the patient, but it has not yet been clarified, whether these sharp field potentials are the results of pathological mechanisms or they emerge spontaneously in the healthy tissue as well. The verification of this issue face some complication as synchronous discharges have not been found in non-primate species, and healthy human tissue is not available for obvious ethical reasons [3], [6].

Spontaneous synchronous discharges have similar characteristics to interictal spikes (IIS) experienced on in vivo recordings of epileptic patients, which might lead to the misconception of the phenomenon [6], [7]. These simultaneous population bursts consist of rhythmically recurring extracellular local field potential (LFP) deflections. Applying a band-pass filter on the extracellular recording between 1 and 100 Hz highlights the waveform resembles IISs [12], [13]. After the application of wide-band filtering, a superimposed increase of neuronal firing, and high-frequency oscillations (HFOs) have been observed concurrently with the sharp field potentials [5], [6], [140]. The populational discharge of neurons builds up gradually before the beginning, and decline after the end of the event [140]. On the intracellular level, it is associated with large, complex postsynaptic potentials, which might be accompanied by synchronous cell firing [6], [140]. Both excitatory and inhibitory chemical signalling, as well as electrical coupling, are thought to be involved in the coordination of the network [3], [5]. It has been shown that non-NMDA glutamate receptors and $GABA_A$ receptors both have a role in the generation of spontaneous potentials, while it is not reliant on NMDA receptors nor $GABA_B$ receptors [3].

2.4.4 Development of seizures

The presence of two concurrent events is essential for the initiation of a seizure: the high-frequency bursts of APs and the excessive hypersynchronisation of the neuron population. In-

DOI:10.15774/PPKE.ITK.2020.008

tracellularly, the emergence of these outbursts is the result of an epilepsy-related phenomenon called paroxysmal depolarizing shift (PDS) [85], [141], [142]. The PDS is triggered by an enormous network-level EPSP caused by AMPA receptor-mediated fast neurotransmission. A sustained depolarising plateau is mediated by currents of L-type voltage-gated calcium channels and NMDA receptor channels. The influx of extracellular Ca^{2+} leads to the activation of voltage-dependent sodium channels, and thus to the generation of repetitive cell firing. The cessation of bursting and the decline of depolarisation amplitude are thought to be the consequence of the progressive inactivation of the channels. The PDS is terminated by a rapid repolarisation followed by hyperpolarisation, which might be mediated by Ca^{2+}-dependent K^+ channels, $GABA_A$ or $GABA_B$, depending on the type of the neuron [85], [141], [142].

In healthy tissue, the propagation of hypersynchronous discharges is prevented by the hyperpolarisation of the neurons and the surrounding inhibition induced by the recruited IN populations. In contrast to that, the epileptic neocortex maintains repetitive discharges, which lead to an increased extracellular K^+ level. It thus decreases the amount of outward K^+ currents, preventing the hyperpolarisation of the neighbouring neurons. The extent of Ca^{2+} accumulates in the synaptic terminals, which boosts the release of neurotransmitters. Furthermore, the NMDA receptors enhance the Ca^{2+} influx due to the depolarisation-induced activation. These mechanisms lead to the process by which seizure activity is able to propagate into contiguous areas or to relatively distant areas as well [85].

2.4.5 Interictal activity

Interictal discharge (IIS) is observed on human EEG between seizures in focal epilepsies [1], [7], [142], [143]. It appears spontaneously [1], [7], [142], though experiments showed that it could be induced by pro-convulsive drugs too [1], [139], [144]. It is characterised by a fast ($<$ 200 ms), high-amplitude ($>50\,\mu$V) LFP transient followed by a slower wave of few hundreds of milliseconds [1], [7], [38], [142]. These events recur periodically [1], [38], [143] and are associated with a PDS with a superimposed sequence of fast APs at 200-500 Hz similar to those observed during seizures [1], [142]. Most recent studies suggest using the term PDS for only in the case of IISs while applying distinguishing terminology for burst discharges related to other epileptic mechanisms [142]. Only specific subpopulations of cortical neurons are able to generate bursting activity during normal conditions, such as those located in the CA1 and CA3 of the hippocampus [1], [145], [146], in the layer V of the neocortex [1], [147] or in the deeper structures of the piriform cortex [1], [148], [149]. Others, like those, found in the CA1 of the hippocampus [1], [146], in the superficial layers of the piriform cortex [1], [148], or in the deeper layers of

DOI:10.15774/PPKE.ITK.2020.008

the entorhinal cortex [1], [150], need ineffective inhibition and enhanced excitation to induce high-frequency discharges. The conductances responsible for bursting behaviour diverse in the case of different neuron types (R-type calcium current or sodium conductances) [1]. Along with chemical signal transmission, gap-junctions have been proposed to have a role in the generation of interictal events as well [1], [151].

IIS has been observed during seizure-free periods of epileptic patients. It has long been a subject of debate, whether this activity preludes ictal discharges or it is intended to prevent the hypersynchronous bursting behaviour [1], [142]. Some assumed that seizures could be considered as a consequence of the melting of the PDS, which thus can serve as a hallmark of pathological discharges [142], [152]. On the other hand, PDS has a resemblance to giant depolarising potentials observed in neonatal rats, which are thought the play a crucial role in cell growth and differentiation [142], [153]. A possibility raises that PDS contributes to the neurodevelopment in matured neuronal networks [142], [154]. Changes in the circuits of the cortex might lead to epileptic hyperexcitability [142]. This hypothesis is supported by the fact that IIS is observable early, right after the injury triggering the epileptic processes. In contrast to that, the emergence of the seizure activity needs a relatively long latency period to set the stage for the hypersynchronous discharges [142], [155].

The anti-epileptic nature of IISs is confirmed by the inverse relation between the occurrence of IISs and seizures. The frequency of interictal events decreases or remain stable before the seizure, and being enhanced after it ended [1], [142], [143]. Furthermore, the suspension of anticonvulsants reduces the IIS frequency prior to the emergence of ictal discharges [142], [156]. Another evidence is the refractoriness caused by IISs, which inhibits cell discharges and the development of seizures [142], [157], [158]. These observations might imply that IISs actually prevent the formation of ictal activity rather than contributing to it.

2.4.6 High-frequency oscillations

High-frequency oscillations (HFOs) are field potentials which reflect a short-term synchronisation of cellular activity in the cortex [159]. Two main types of fast network oscillations have been investigated here, ripples and fast-ripples. Ripples are brief, sinusoid-like waves, between 130 and 250 Hz. They were observed in the entorhinal cortex and hippocampus of several mammalian species and humans [46], [159]. Ripples chiefly show up during immobility or episodes of slow-wave sleep. They are thought to have a role in memory consolidation. In contrast to that, fast-ripples used to be referred to as the pathological counterpart of ripples [46]. Its peculiar frequency range is between 300 and 700 Hz. Fast-ripples were observed in the areas of epileptic

DOI:10.15774/PPKE.ITK.2020.008

seizure generation and the adjacent areas [46], [159]. That is why it has been hypothesised to indicate the substrate of epileptogenicity.

A multi-unit activity rise has been observed during HFOs. However, the degree of the increase is half as much during ripples as those measured during fast-ripples. Presumed PCs showed to reach a maximal firing rate coinciding with the peak of the ripple. While, putative INs had a firing rate maximum too, but it arose prior to the oscillation. Thus, INs could inhibit firing activity before the field potential and release during the synchronous discharge. Phase analysis showed that PCs like to fire during the negative phase of the ripple cycle, whereas INs have a lag of 0.5 ms. The rhythmic inhibitory post-synaptic potential might have a robust regulatory effect on PC discharges and contribute to the synchronisation, which leads to ripple field potentials. In the case of fast-ripples, PCs tend to fire during the negative phase of the oscillation too [46]. Although the role of INs has not yet been revealed in the maintenance of pathological HFOs, cells are not likely to have a firing rate over 400 Hz [46], [160]. This supports the hypothesis that fast-ripples might recruit a large number of cells with synchronous discharges, but they appear to be out of phase with each other. Thus, they emerge a field potential oscillation with higher frequencies [160].

Subsequent studies suggested that along with chemical synapses, gap junctions have a crucial role in the mechanisms underlying synchronisation [46], [107], [159], [160]. Electrical coupling might help to sharpen the tuning of oscillatory activity by supporting the simultaneous interneuronal firing when the IPSP decreases [107], [160], [161]. Draguhn and colleagues found that HFO persists during the suppression of chemical synaptic transmission. While, it is being enhanced or reduced by the increase or decrease of gap junction efficacy [46], [159]. Some also suggested that the role of electrical coupling in the synchronisation might approve the theory of gap junctions between PCs as well [46], [159].

2.5 Bicuculline

The convulsant alkaloid bicuculline is widely used to induce hypersynchronous discharges in mammalian epilepsy models and human samples as well [2], [3], [14], [19], [90], [140], [162]–[166]. It exerts its influence by being a competitive antagonist of $GABA_A$ receptors [167]–[169]. Although certain studies attempted to prove that bicuculline is rather being an allosteric inhibitor [168], [170]. A common matter between the followers of the two theory is that the bicuculline weakens GABA activated conductances by decreasing the channel opening time [168], [170], [171]. Bicuculline is difficult to use because it is unstable in certain conditions: at physiological pH and 37 $^\circ$ it is hydrolysed to bicucine which is a relatively inactive GABA antagonist.

DOI:10.15774/PPKE.ITK.2020.008

Furthermore, it is not properly dissolvable in aqueous solutions. Thus, quaternary salts (such as bicuculline methiodide or methochloride) was synthesised, which are stable between pH 2 and 8 and are much more soluble in water [167]–[169]. A non-GABA receptor-mediated function of the bicuculline salts has been uncovered. It is very likely that these agents block Ca^{2+}-dependent K^{+} currents. Which thus reduce the period of afterhyperpolarisation and permits the membrane to maintain an optimal level of depolarisation for burst-firing [168], [169], [172].

DOI:10.15774/PPKE.ITK.2020.008

3. Methods

3.1 Description of patients

We received written consent from all patients. Our protocol was approved by the Hungarian Ministry of Health and by the Regional and Institutional Committee of Science and Research Ethics of Scientific Council of Health (ETT TUKEB 20680-4/2012/EKU) and performed in accordance with the Declaration of Helsinki.

3.1.1 Epileptic patients

Neocortical tissue samples were obtained from 60 epileptic patients (*Table 3.1*). According to the diagnosis of epilepsy and the appearance of seizures, subjects have been divided into three groups. Most of the patients suffered from pharmacoresistant epilepsy (ResEpi, n = 42). In their case epilepsy was not curable by any single or combined drug treatment, therefore the resection of the epileptogenic zone was indicated. The rest of the epileptic patients were either pharmacologically treatable (TreatEpi, n = 10) or suffered from only one seizure in their life without the need for medical intervention (NoMed, n = 8). These two former groups were operated in order to resect their brain tumour. Those who suffered from seizures were diagnosed with epilepsy in an average of 14 ± 13 years (min.: 2 weeks, max.: 50 years) before their surgery. Thirteen epileptic patients were diagnosed with cortical dysplasia, 2 of them with additional hippocampal sclerosis. Six patients suffered from gliosis and/or dysgenesis, two of them with hippocampal sclerosis. Twenty patients were diagnosed with tumour of glial origin, three of them with necrosis and one of them with hippocampal sclerosis. Five patients had carcinoma metastasis, and two patients had other tumours. The rest of the patients were diagnosed with hippocampal sclerosis (n = 8), cavernoma (n = 5) or encephalitis (n = 1). In addition to the clinical histology results, histopathological changes (signs of tumour infiltration or dysgenesis) of the obtained tissue have been verified with Nissl staining, the neuronal marker NeuN, the glial fibrillary acidic protein and a specific interneuron marker parvalbumin immunostaining. 31 male

DOI:10.15774/PPKE.ITK.2020.008

and 29 female subjects constituted the epileptic group within the age range of 18 and 72 years (mean ± st.dev.: 39 ± 15 years).

3.1.2 Non-epileptic patients

Forty-four subjects suffering from brain tumour without epilepsy were used as a control group (NoEpi, *Table 3.1*). These patients - as it is stated in their anamnesis - did not show clinical manifestation of epileptic seizure before the date of their brain surgery. Preoperative clinical EEG recordings confirmed in eight of these patients that no electrographic signs of epileptic activity were present on their scalp EEG. The majority of non-epileptic patients suffered from tumour of glial origin (n = 21). Eighteen of them had glioblastoma, one together with astrocytoma and one with oligodendroglioma, while the remaining three patients with glial tumour had only astrocytoma. Those who were not diagnosed with glial tumour had carcinoma metastaticum (n = 16), melanoma metastaticum (n = 2), meningioma (n = 2), cavernoma with haematoma (n = 1), haematoma (n = 1) or neurocytoma (n = 1). The distance of the obtained neocortical tissue from the tumour had been assessed by the neurosurgeon, based on magnetic resonance (MR) images, intraoperative pictures and occasionally defined by a navigational system. Signs of dysgenesis or tumour infiltration have been verified by immunohistochemical procedures described in *section 3.1.1*. 22 male and 22 female subjects participated in the study within the age range of 31 and 82 years (mean ± st.dev.: 61 ± 12 years).

3.2 Tissue preparation

The obtained neocortical samples were originated from all four cortical lobes: 18 epileptic and 14 non-epileptic tissue from the frontal lobe, 31 epileptic and 12 non-epileptic tissue from the temporal lobe, six epileptic and 12 non-epileptic tissue from the parietal lobe and five epileptic and six non-epileptic tissue from the occipital lobe have been examined. After resection, neocortical tissue samples were placed in an ice-cold, oxygenated solution containing (in mM) 248 D-sucrose, 26 $NaHCO_3$, 1 KCl, 1 $CaCl_2$, 10 $MgCl_2$, 10 D-glucose and 1 phenol red, equilibrated with 5% CO_2 in 95% O_2 while it was transported to the experimental lab and prepared for electrophysiological recordings. The pia mater and larger blood vessels were removed, and slices of 500 μm thickness containing all the neocortical layers were made by Leica VT1000S vibratome. Slices were transferred then to an interface chamber where they were kept for an hour to restore before the recordings. They were maintained at 35-37°C, perfused with a standard physiological solution containing (in mM) 124 NaCl, 26 $NaHCO_3$, 3.5 KCl, 1 $MgCl_2$, 1 $CaCl_2$, and 10 D-glucose, equilibrated with 5% CO_2 in 95% O_2.

DOI:10.15774/PPKE.ITK.2020.008

Table 3.1. Patient data. Stage of epilepsy: ResEpi: pharmacoresistant epilepsy, TreatEpi: treatable epilepsy, NoMed: no need for medication, NoEpi: no epilepsy. Gender: F: female, M: male. Distance from the tumour: close is <3 cm, distant is >3 cm, but in most cases >5 cm. N/A: not available.

Stage of epilepsy	Patient ID	Gender	Age	Diagnosis	Lobe	Duration of epilepsy	Distance from tumour	Anatomy
ResEpi	E1	F	22	encephalitis	parietal	1 month		normal/cell loss
ResEpi	E2	F	21	focal cortical dysplasia with glioneural heterotopia	frontal	2 years		dysgenetic
ResEpi	E3	F	18	bilateral frontal polymicrogyria	frontal	5 years		dysgenetic
ResEpi	E4	M	24	ganglioglioma grade I	temporal	4 years	distant	normal
ResEpi	E5	F	18	focal cortical dysplasia II B	temporal	5 years		dysgenetic
ResEpi	E6	M	51	hippocampal sclerosis	temporal	50 years		normal
ResEpi	E8	F	33	focalis corticalis dysplasia II B	occipital	31 years		normal+dysgenetic
ResEpi	E10	M	21	hippocampal sclerosis	temporal	21 years		normal
ResEpi	E11	M	29	cavernous malformation	temporal	3 years		N/A
ResEpi	E12	M	40	hippocampal sclerosis	temporal	35 years		normal
ResEpi	E13	F	53	hippocampal sclerosis	temporal	40 years		normal
ResEpi	E14	M	53	ganglioglioma grade I	parietal	18 years	close	normal
ResEpi	E15	M	35	focal cortical dysplasia + hippocampal sclerosis	temporal	34 years		normal
ResEpi	E16	M	26	subependymal gliosis (dysgenesis) + hippocampal sclerosis	temporal	24 years		normal
ResEpi	E17	F	38	focal cortical dysplasia + hippocampal sclerosis	frontal	31 years		normal
ResEpi	E18	F	35	focal cortical dysplasia II B (with balloon cells)	frontal	30 years		normal
ResEpi	E21	M	56	haemangioma cavernosum	temporal	26 years		N/A
ResEpi	E23	F	33	haemangioma cavernosum	temporal	5 years		normal
ResEpi	E25	M	53	hippocampal sclerosis	temporal	24 years		normal
ResEpi	E27	M	27	hippocampal sclerosis	temporal	2 years		normal
ResEpi	E29	M	18	focal cortical dysplasia	parietal	5 years		dysgenetic
ResEpi	E30	M	30	microdysgenesis + hippocampal sclerosis	temporal	17 years		dysgenetic
ResEpi	E31	M	31	complex dysembrioplastic neuroepithelial tumour	temporal	10 years	distant	N/A
ResEpi	E32	F	31	focal cortical dysplasia II B (with balloon cells)	parietal	18 years		dysgenetic
ResEpi	E34	F	18	hippocampal sclerosis	temporal	4 years		N/A
ResEpi	E35	F	37	cavernous malformation	temporal	6 years		N/A

DOI:10.15774/PPKE.ITK.2020.008

Table 3.1 continued from previous page

Stg. of epi.	Patient ID	Gender	Age	Diagnosis	Lobe	Duration of epilepsy	Dist. from tu.	Anatomy
ResEpi	E39	F	36	hippocampal sclerosis	temporal	30 years		N/A
ResEpi	E40	M	32	anaplastic oligoastrocytoma grade III	frontal	4 years	distant	N/A
ResEpi	E41	F	26	radionecrosis (2 years earlier: pylocytic astrocytoma)	temporal	13 years	close	N/A
ResEpi	E42	M	44	subpialis gliosis (dysgenesis)	frontal	22 years		N/A
ResEpi	E45	M	48	focal cortical dysplasia II B	frontal	39 years		N/A
ResEpi	E46	F	38	ganglioglioma grade I	temporal	10 years	close	N/A
ResEpi	E51	M	29	cortical dysplasia	temporal	14 years		dysgenetic
ResEpi	E57	F	19	focal cortical dysplasia II B (with balloon cells)	frontal	15 years		dysgenetic
ResEpi	E58	F	35	haemangioma cavernosum	temporal	5 years		normal
ResEpi	E59	M	30	focal cortical dysplasia II B (with balloon cells)	parietal	27 years		normal
ResEpi	E63	M	34	diffuse low-grade glioneural tumor + hippocampal sclerosis	temporal	20 years	close	infiltrated
ResEpi	E64	M	32	focal cortical dysplasia II B (with balloon cells and dysmorph neurons)	parietal	23 years		normal
ResEpi	E65	F	31	ganglioglioma grade I	temporal	1 year	close	normal
ResEpi	E66	F	41	hippocampal and temporal gliosis	temporal	9 years		normal
ResEpi	HP1	M	36	temporal gliosis	temporal	7 years		normal
ResEpi	O42	M	72	glioblastoma multiforme	frontal	9 months (1 seizure)	distant	normal
TreatEpi	E24	M	71	glioblastoma grade IV	frontal	1 week (1 seizure)	close	normal
TreatEpi	E28	F	60	anaplastic oligodendroglioma grade III, recidiva	frontal	10 years	close	N/A
TreatEpi	T1	F	54	oligodendroglioma grade II	frontal	2 weeks (1 seizure)	distant	N/A
TreatEpi	T3	F	18	anaplastic ependymoma grade III	frontal	1 month	distant	normal
TreatEpi	T5	F	35	oligodendroglioma grade III	occipital	1 month (1 seizure)	close	infiltrated
TreatEpi	T9	F	48	lung small cell carcinoma metastaticum	occipital	2 weeks (1 status epilepticus)	close	infiltrated
TreatEpi	T10	M	44	glioblastoma multiforme, astrocytoma grade IV	temporal	3 weeks	distant	normal
TreatEpi	T13	M	53	radionecrosis (6 years earlier: anaplastic oligoastrocytoma grade III)	frontal	6 years (1 seizure)	distant	N/A
TreatEpi	T31	M	64	lung carcinoma metastaticum	temporal	3 months (1 seizure)	distant	normal
TreatEpi	T46	F	68	glioblastoma grade IV	temporal	2 weeks	close	N/A
noMed	E19	F	72	radionecrosis (1 year earlier: astrocytoma grade II)	frontal	2 years	close	normal
noMed	E20	F	33	glioblastoma grade IV	frontal	3 month	distant	N/A
noMed	E26	M	44	anaplastic ganglioglioma grade III	temporal	3 months (1 seizure)	distant	N/A
noMed	E33	M	63	lung adenocarcinoma metastaticum	occipital	2 weeks (1 seizure)	close	N/A
noMed	E44	F	32	anaplastic astrocytoma grade III	frontal	N/A (1 seizure)	distant	N/A

DOI:10.15774/PPKE.ITK.2020.008

Table 3.1 continued from previous page

Stg. of epi.	Patient ID	Gender	Age	Diagnosis	Lobe	Duration of epilepsy	Dist. from tu.	Anatomy
noMed	T22	M	65	epidermoid carcinoma metastaticum	occipital	13 months (1 seizure)	distant	normal
noMed	E56	M	58	lung adenocarcinoma metastaticum	temporal	10 months (1 seizure)	close	infiltrated
noMed	E60	F	36	anaplastic astrocytoma grade III	frontal	N/A (1 seizure)	close	infiltrated
noEpi	T2	M	59	glioblastoma multiforme sarcomatosum	temporal		close	N/A
noEpi	T4	F	69	glioblastoma multiforme	temporal		distant	normal
noEpi	T6	M	31	cavernoma, haematoma intracerebralis acuta	frontal		distant	normal
noEpi	T7	F	58	glioblastoma multiforme, meningitis	temporal		close	infiltrated
noEpi	T8	F	78	glioblastoma multiforme, astrocytoma grade IV	temporal		distant	normal
noEpi	T11	F	57	glioblastoma multiforme grade IV	occipital		distant	normal
noEpi	T12	M	59	glioblastoma, with oligodendroglioma fragments grade IV	frontal		close	normal
noEpi	T14	M	67	lung anaplastic carcinoma metastaticum	temporal		close	N/A
noEpi	T15	F	67	meningioma grade I	frontal		distant	N/A
noEpi	T16	F	69	gastrointestinal adenocarcinoma metastaticum	occipital		close	N/A
noEpi	T17	F	74	glioblastoma multiforme grade IV	parietal		distant	normal
noEpi	T18	M	68	melanoma malignum metastaticum	parietal		distant	normal
noEpi	T19	M	69	lung adenocarcinoma metastaticum	parietal		close	N/A
noEpi	T20	F	59	breast carcinoma metastaticum	frontal		close	infiltrated
noEpi	T21	F	69	kidney carcinoma metastaticum	parietal		distant	normal
noEpi	T23	F	81	meningioma grade I	frontal		distant	normal
noEpi	T24	M	55	lung adenocarcinoma metastaticum	temporal		distant	N/A
noEpi	T25	F	55	glioblastoma multiforme	parietal		distant	N/A
noEpi	T26	F	63	glioblastoma multiforme grade IV	parietal		close	N/A
noEpi	T27	F	61	lung carcinoma metastaticum	frontal		distant	N/A
noEpi	T28	M	49	kidney carcinoma metastaticum	occipital		close	N/A
noEpi	T29	F	62	lung adenocarcinoma metastaticum	parietal		close	N/A
noEpi	T32	M	79	glioblastoma multiforme grade III	temporal		close	N/A
noEpi	T33	M	45	anaplastic astrocytoma	frontal		close	N/A
noEpi	T34	F	64	haematoma	frontal		distant	N/A
noEpi	T35	M	60	glioblastoma grade IV	temporal		distant	N/A
noEpi	T36	M	58	lung adenocarcinoma metastaticum	frontal		close	N/A
noEpi	T38	M	82	stomach anaplastic carcinoma metastaticum	temporal		close	N/A

DOI:10.15774/PPKE.ITK.2020.008

Table 3.1 continued from previous page

Stg. of epi.	Patient ID	Gender	Age	Diagnosis	Lobe	Duration of epilepsy	Dist. from tu.	Anatomy
noEpi	T39	M	37	centralis neurocytoma grade II	frontal		distant	N/A
noEpi	T40	M	45	anaplastic astrocytoma grade III	temporal		close	N/A
noEpi	T42	F	59	breast carcinoma metastaticum	frontal		close	N/A
noEpi	T43	M	73	melanoma malignum metastaticum	temporal		distant	N/A
noEpi	T44	F	58	breast carcinoma metastaticum	occipital		distant	N/A
noEpi	T45	F	56	glioblastoma grade IV	occipital		distant	N/A
noEpi	T56	M	64	glioblastoma multiforme grade IV	parietal		close	normal
noEpi	T57	F	73	glioblastoma multiforme grade IV	frontal		close	infiltrated
noEpi	T58	M	42	glioblastoma multiforme grade IV	frontal		close	normal
noEpi	T61	F	40	anaplastic astrocytoma grade III	parietal		distant	normal
noEpi	T64	M	63	glioblastoma multiforme grade IV	parietal		close	normal
noEpi	T67	F	57	glioblastoma multiforme grade IV	parietal		close	normal
noEpi	T68	F	72	neuroendocrine carcinoma metastaticum, grade III	parietal		distant	normal
noEpi	T69	M	49	anaplastic astrocytoma grade III	frontal		distant	N/A
noEpi	HP3	M	55	epithelial lung carcinoma metastaticum	temporal		distant	Normal
noEpi	HP4	M	69	planocellular keratoid carcinoma metastaticum	occipital		close	N/A

DOI:10.15774/PPKE.ITK.2020.008

3.3 Recordings

3.3.1 Extracellular recordings

Extracellular recordings were obtained in an interface chamber while standard, oxygenated physiological solution was perfused, as it was described in section *Tissue preparation*. Local field potential gradient was captured by a laminar microelectrode with 24 contact points and 150 μm of inter-contact spacing [10], [12], [13], [173], [174]. The multielectrode was placed on the brain slices perpendicular to the pial surface so that it covered all the neocortical layers (*Figure 3.1*). Depending on the thickness of the grey matter, usually, channels 1-12 captured signals from the supragranular layers (layers I-III), channels 13-15 captured signals from the granular layer (layer IV), and channels 16-23 captured signals from the infragranular layers (layers V-VI). The 23 channels are derived from the gradient of the 24 contact points. Slices were scanned from one end to the other at every 300-400 μm. For the recordings, a custom-made voltage gradient amplifier of pass-band 0.01 Hz to 10 kHz was used. Signals were digitized with a 32 channel, 16-bit resolution analogue-to-digital converter (National Instruments, Austin TX, USA) at 20 kHz sampling rate, recorded with a home written routine in LabView 8.6 (National Instruments, Austin TX, USA).

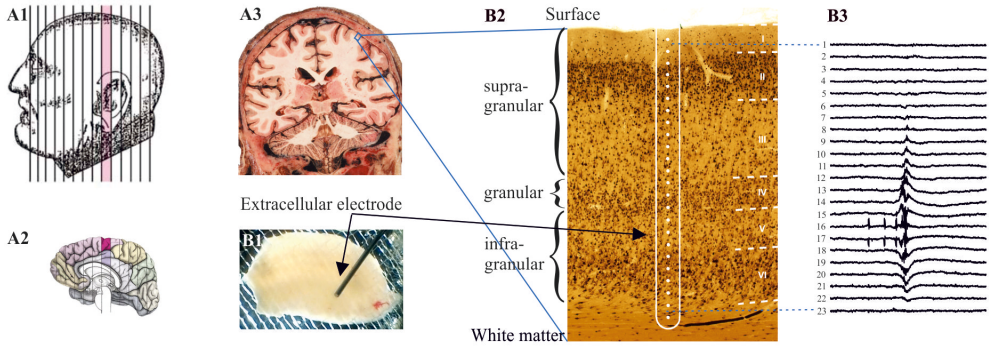

Figure 3.1. LFPg recordings were captured by a 24-channel laminar electrode. It was placed on the brain slice perpendicular to the brain surface so that the contact points of the electrode covered all the cortical layers. A1-A3 illustrates a section of the human brain in the coronal plane [175]. B1-B3 shows the electrode positioning on the neocortical slices with the corresponding gradient recordings.

DOI:10.15774/PPKE.ITK.2020.008

3.4 Drugs

Bicuculline methiodide (BIC, 20 μM or 50 μM), an A-type γ-aminobutyric acid ($GABA_A$) receptor antagonist was applied to suppress receptor-mediated signalling. The drug was obtained from Tocris Bioscience (Izinta Kft., Hungary). A solution of 100 ml containing bicuculline was washed into the interface chamber during most of the experiments. Epochs of 10-minutes length were recorded continuously during the whole experiment (control - BIC application - washout). The washout period endured until the reappearance of the spontaneous population activity (SPA). In the absence of an SPA, the washout persisted for an hour.

3.5 Data analysis

Data processing was performed by Neuroscan Edit 4.5 program (Compumedics Neuroscan, Charlotte, NC, USA), Klusters [176], and home written C++ and Matlab (The MathWorks, Natick, MA, USA) routines.

3.5.1 Analysis of the synchronous spontaneous population activities and interictal-like discharges

The presence or absence of population activities and single units were noted for all the records of every slice. Usually, a 5-10 minutes long capture containing detectable synchronous spontaneous population activities (SPAs) and spontaneous interictal-like discharges (sIIDs, *Figure 3.2*) were chosen for further analysis. If necessary, artefacts and noises disturbing the detection were removed and replaced by a baseline signal.

Population activity detection was performed on LFPg records after Hamming linear derivation and bandpass filtering between 3 and 30 Hz (zero phase shift, 12 dB/octave). Events larger than 2x standard deviation of the signal were detected and included in the analysis. The highest amplitude time point of this peak was selected as time zero for further synchronous event-related investigations.

LFPg, current-source density (CSD) and multi-unit activity (MUA) analyses were performed using standard techniques [10], [173], [174]. Briefly, the detected SPAs were cut into time windows from -300 ms to 300 ms related to the maxima of each peak - applied as timepoint zero - as it was described in the previous paragraph. These epochs were averaged across the whole recording. In the end, they were baseline corrected using a time window between -300 ms and -100 ms before the peak as reference. The length of events was obtained from these averaged recordings on the channel displaying the largest LFPg amplitude, at 50% of that amplitude. The

DOI:10.15774/PPKE.ITK.2020.008

recurrence frequency of the SPAs and sIIDs was calculated by dividing the number of events by the length of the detection period (those time intervals where the events were detected). This value was provided in Hz. The location of SPAs and sIIDs was visually evaluated.

Current source density, an estimate of population trans-membrane currents is the second spatial derivative of the LFP. As spatial potential gradient recordings were obtained originally, only one additional derivation was performed on the raw LFPg [173]. These derivated recordings were processed the same way as it was described in the previous paragraph: they were cut into epochs of ±300 ms related to the peak of the detected events, they were averaged across the recording, and they were baseline-corrected for more appropriate estimation. For visual evaluation, heatmaps of averaged CSDs were made for all SPAs and sIIDs, where current sources and current sinks were indicated by cool and warm colours, respectively.

Multiple unit activity, together with the action potentials of single neurons provides information about the local cellular response to the field potential (*Figure 3.2*). To gain these low-amplitude, high-frequency signals, high-pass filtering above 500 Hz (zero phase shift, 24 dB/octave) and full-wave rectification were performed on the raw LFPg recordings. After it was cut into epochs of ±300 ms, the waveform was smoothed in order to improve visualisation. Last, epochs were averaged, and baseline corrected just as it was described at the LFPg and CSD analysis. Heatmaps for the averaged MUAs were drawn, where an increase in the cellular activity was represented by warm colours. The amplitudes were measured on the channels with the largest peak.

3.5.2 Analysis of the bicuculline-induced population activities

The algorithm analysing bicuculline-induced population activities (BIPAs) was similar to the one which was described in the analysis of SPAs in the previous subsection. Although some changes in the subtasks were necessary due to the various characteristics and behaviour of the waves (*Figure 3.2*).

Visual evaluation, artefact removal, and peak detection were performed using standard techniques (for details, see subsection *Analysis of the synchronous spontaneous population activities*). For LFPg, CSD and MUA analyses epochs were cut from -500 ms to 1500 ms related to the peak of the particular event in the cases of both bicuculline-induced interictal-like spikes (bIISs) and bicuculline-induced seizures. High-pass filter, linear derivation and averaging were made as it was described, but in the case of BIPAs, the reference interval for baseline correction contained the time window from -500 ms to -300 ms before the peak. The amplitudes were calculated from the channels of the largest peak on the LFPg.

DOI:10.15774/PPKE.ITK.2020.008

Measuring the length at the half-max of the amplitude was not applicable in the case of BIPAs since the length of the LFPg deflections were not equal on the different channels. Moreover, the peak of the deflection was at considerably different time point on the different channels. Therefore, the length of bIISs was calculated using the mean global field power (MGFP) from the channels where the event was present. The MGFP corresponds to the spatial standard deviation of field potential amplitude values obtained with multiple channel recording [177], [178]. The average length was determined at 5% of the maximal MGFP amplitude. In the case of temporally complex bIISs, the length of the first component was calculated. The MGFP method could not be applied in case of SPAs because the LFPg amplitude of these events is low, and therefore the 5% height of the maximal values dropped below the noise level and provided an imprecise measurement. The duration of BIC-induced seizure-like activities was defined by manual estimation applying the butterfly plot of all channels. A butterfly plot was generated from the averaged LFPg in the case of recurring seizures, to include all seizure events.

The initiation site, as well as the direction and the speed of the propagation of BIPAs were determined across channels (i.e. across cortical layers). The phenomenon usually consists of large LFPg deflections superimposed by increased cellular activity. However, in some cases, the LFPg peak is almost invisible, so we have to rely on the increased MUA itself. To solve this problem, after applying a 0.5 Hz high-pass filter, we calculated the power of the LFPg records. For the detection, a two-step thresholding process was used, where threshold 1 indicated presumable peaks, while threshold 2 determined the initiation points of these peaks on all channels. In case of complex events, only the first peak was taken into account.

The spreading speed of the BIPA events across the channels was defined by dividing the delay between the starting points of the events by the distance between the two electrode contacts in question. This speed value was determined for every channel pair, up to 5 contacts apart. For each event, the speed was determined by taking the median of these pairwise speed values.

3.5.3 Analysis of high-frequency oscillations

High-frequency oscillations were analysed in the frequency range of 130-700 Hz during SPAs, sIIDs and BIPAs. The raw recordings captured with 20 kHz sampling rate were low-pass filtered under 700 Hz, then downsampled to 2 kHz. Epochs from -1000 ms to 1047.5 ms compared to the SPA and sIID peak, epochs from -500 ms to 1547.5 ms compared to the bIIS peak and epochs from -500 ms to 15883.5 ms compared to the seizure peak were used only on the channels where the population activities were present. Different time windows were chosen considering the wave properties. Wavelet analysis was performed, then the results were baseline corrected

DOI:10.15774/PPKE.ITK.2020.008

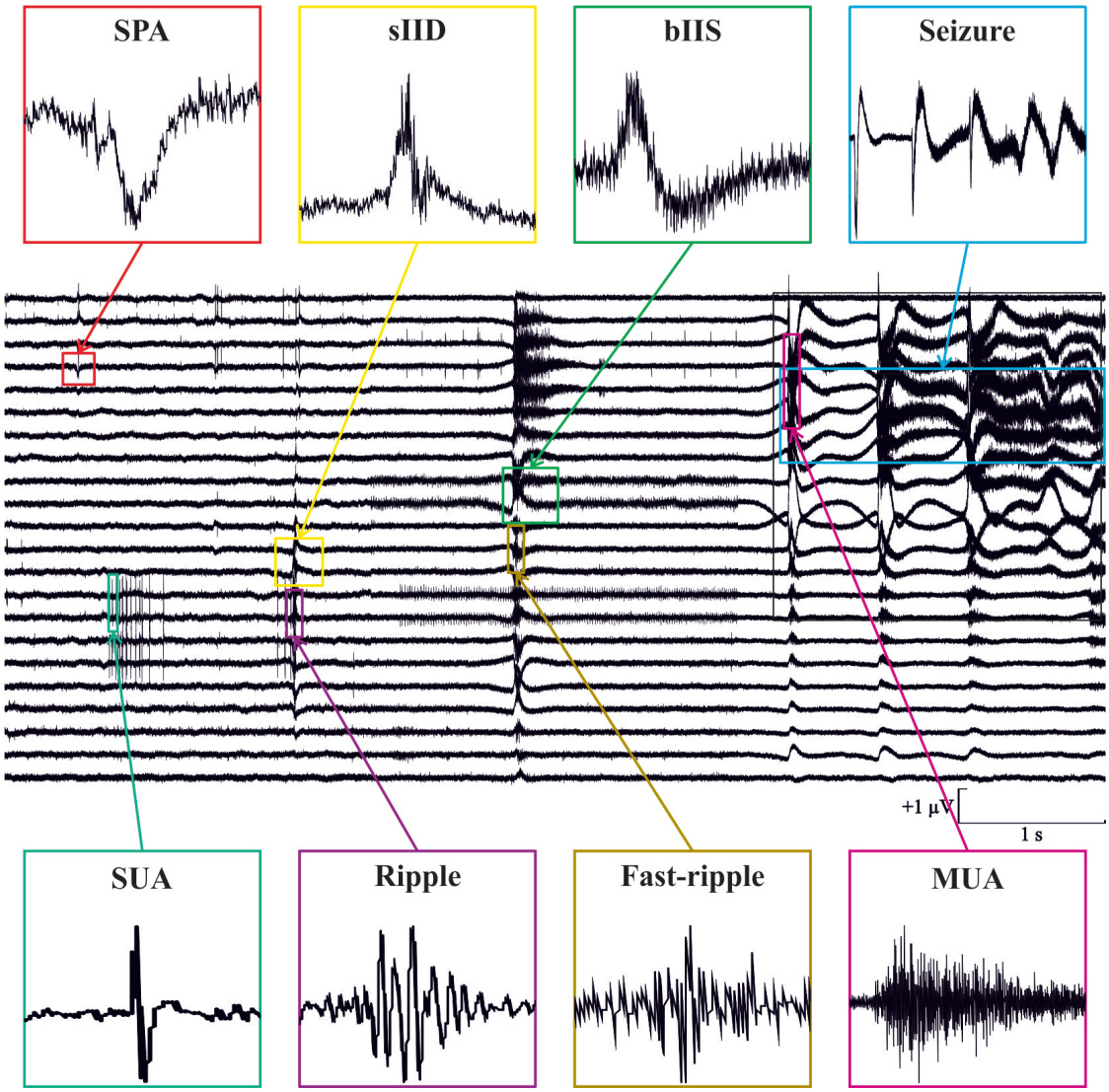

Figure 3.2. Different kind of activities on the LFPg recordings: (1) SPA and (2) sIID appear during physiological conditions. While sIID has been detected only in epileptic tissue, SPA emerged in all patient groups. After the application of bicuculline, in certain cases, (3) bIIS and (4) seizure developed replacing physiological activities. (5) SUA (single-unit activity) refers to the action potentials of the individual neurons. During population activities, high-frequency oscillations were detected in both (6) ripple (130-250 Hz) and (7) fast-ripple (300-700 Hz) frequency ranges. (8) MUA indicates the increased cellular activity during the events.

DOI:10.15774/PPKE.ITK.2020.008

using an interval between -300 ms and -100 ms before the certain peak as a reference. The power increase in the ripple (130-250 Hz) and the fast-ripple (300-700 Hz) frequency ranges was determined on each channel (*Figure 3.2*). Frequencies with the maximal power increase were noted as well. Both the ripple and the fast ripple power, as well as the frequencies, were averaged across the channels, to receive one ripple and one fast ripple power and frequency parameter for each recording.

3.5.4 Analysis of single cells

Action potentials (APs) of single neurons were visually checked channel by channel on the 5-10 mins long recordings (*Figure 3.2*). Artefacts were removed if it was necessary. High pass filter was applied above 80 Hz and 500 Hz, in case of physiological conditions and during bicuculline bath, respectively. Neurons with a clear refractory period of 1.5 ms were detected separately in the control and in the BIC group.

Although the electrode was kept in the same position during the application of physiological ACSF and BIC bath, it was almost impossible to find identical neurons between the two phases due to multiple reasons. First of all, the firing pattern of neurons changed considerably after the administration of BIC. The action potentials of spontaneously active cells disappeared while others started to discharge. Furthermore, the alteration of the AP shape during epileptic discharges [179] caused by bicuculline complicated the process of clustering. In the case of these recordings, only cells with relatively high amplitude and recognisable AP were clustered, whereas small (and noisy) clusters were excluded. During the high-frequency oscillatory phases of the seizures, cluster detection might be imprecise [179]. Due to these reasons we did not attempt to follow the same neuron in control - BIC - washout recordings.

The detected APs of each cell were averaged throughout the whole recording. The separated neurons were classified into three groups: principal cells (PC), interneurons (IN) and unclassified cells (UC). Two criteria were taken into account for the classification. First, the width at the half-max amplitude was calculated on the averaged APs of each neuron. The width of the APs belonging to principal cells is considerably higher than that of the interneurons [180], [181]. Thus, neurons with an AP longer than 0.4 ms were considered to be PCs, and INs, if it was shorter than 0.2 ms (*Figure 3.3*). The residual cells remained unclassified.

The second criterium of the classification was the firing pattern of the neurons [182], [183]. As the presence of bursting PCs (bPCs) was related to epilepsy and epileptiform discharges [184], we investigated the activity of this special neuron type separately. Intrinsically bursting PCs have a peak at 3-10 ms on the autocorrelogram followed by a sharp, exponential decay.

DOI:10.15774/PPKE.ITK.2020.008

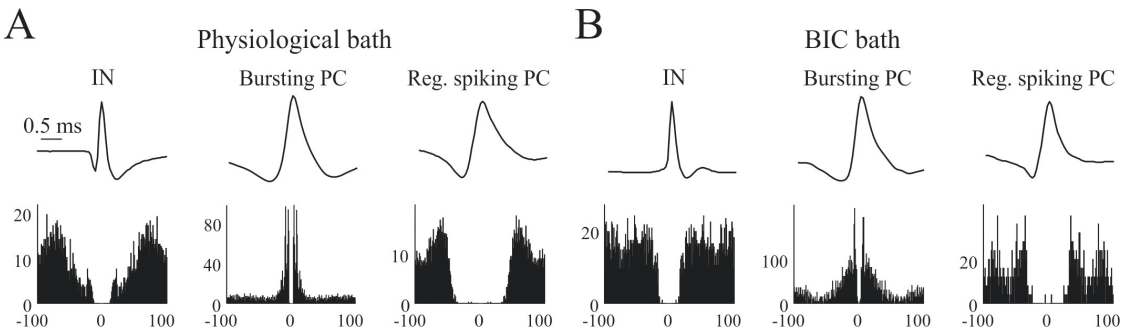

Figure 3.3. Characteristic action potentials and peri-event time-histograms of interneurons, bursting principal cells and regular spiking principal cells in physiological solution (A) and bicuculline bath (B).

Regular spiking PCs have either a steady, sustained firing without a peak or show a moderate hump with at least 10 ms of duration on the autocorrelogram. PCs without the described patterns or with too few action potentials were classified as PCs with unclear firing. A gradual rise followed by a gradual decay on the autocorrelogram is indicating the characteristic discharge dynamics of INs (*Figure 3.3*).

For each neuron, the location was determined, as well as the average firing frequency, the interevent interval (IEI, event = AP), and a measure for burstiness (percentage of APs within bursts) were calculated. Bursts were determined as a set of (at least) three APs within 20 ms. Bursts consist of more than three APs could be longer than 20 ms, but each group of three consecutive APs had to be within a 20 ms time period. Furthermore, the first AP of the burst had to be preceded, and the last AP had to be followed by a 20 ms silent period (modified from [185]).

3.5.5 Comparison of single neurons and synchronous events

This part of the analysis was performed on recordings containing SPAs and BIPAs (sIIDs were excluded) from the ResEpi (n = 15 SPA, n = 14 bIIS, n = 6 seizures) and the NoEpi (n = 14 SPA, n = 13 bIIS, n = 3 seizures) groups.

First, we aimed to find cells participating in the generation of population activities. Thus, we were searching for neurons enhancing their firing during these events. Perievent time histograms (PETHs) were calculated for each cell/SPA pair with a time window from -150 ms to 50 ms and for each cell/bIIS and cell/seizure pair with a time window from -400 ms to 200 ms with a bin size of 5 ms. The average firing frequency of the cells was calculated using these PETHS, during the time course of the events and the baseline period in between. In case of SPAs, the baseline was chosen from -150 ms to -50 ms before the peak, while the rest of the window was considered

DOI:10.15774/PPKE.ITK.2020.008

to be the 'event period'. In the case of BIPAs, the baseline and the event were chosen to be from -400 ms to -100 ms and from -100 ms to 200 ms compared to the peak, respectively. Due to the modified cellular behaviour during BIC (i.e. most of the cells fired during the population events and remained silent in between), the normalised firing change between the two period was calculated by the formula of $A \div (A + B)$. In this expression, A represents the average firing frequency during the events, while B is equal to the average firing frequency during the baseline period. Thus, all values fell between 0 and 1, so we do not have to deal with infinite or extremely huge numbers. If the firing change value exceeded 0.6, the neuron was considered to have an increased firing (which equals to an increase to 150% of its baseline firing rate).

We wished to examine how excitatory and inhibitory cell types participate in the initiation of SPA and BIPA events. Combined PETH of all PCs, INs and UCs were calculated relating to the corresponding population activity peaks. Time windows from -100 ms to 200 ms and from -200 ms to 1000 ms were used compared to the SPA and BIPA peak, respectively. With the aid of the combined PETHs, we determined on each recording which cell type starts firing during the population events. Finally, we calculated the area under the curve of the PC/IN/UC firing of the PETH relative to the total firing during the interval of -50 ms to 50 ms around the LFPg peak of SPAs, and -100 ms to 200 ms around the LFPg peak of BIPAs.

3.6 Statistical analysis

Statistica, v13 (Tibco Software Inc. Palo Alto, CA, USA, RRID: SCR 014213) was used to determine statistical significance. Distribution was verified with Kolmogorov-Smirnov and Lilliefors tests. In case of a normal distribution, a t-test was used to compare two groups, while one-way ANOVA (with Tukey's honest different significance post hoc test) was applied to compare multiple groups. If the normality test failed, the Mann-Whitney U test was performed to check two groups and Kruskal-Wallis ANOVA was performed to check multiple groups. In the main text, the mean ± SD was used for the clarification. Whereas in the tables both the median (first and third quartiles) and the mean ± SD were reported. The website http://vassarstats.net was used to test for contingency tables. Fisher's exact probability test was used for 2×3 contingency tables if the total size of the data set was lower than 300. Chi-squared test was performed if it was greater than 300.

DOI:10.15774/PPKE.ITK.2020.008

4. Results

4.1 Results related to the comparison of the different types of population synchronies in the human neocortex

4.1.1 The occurrence of population activities in the human neocortex

During the study, four kinds of population activities (PAs) have been investigated (*Figure 4.1*). These activities were emerging in postoperative neocortical tissue in vitro, resected from patients with or without epilepsy. They were manifested as LFPg deflections on the extracellular recordings during physiological conditions or bicuculline bath. In contrast to earlier studies, they appeared without the application of electrical stimulation [15], [19].

The first PA, the synchronous population activity (SPA) was spontaneously generated in the presence of physiological ACSF in slices from both epileptic and non-epileptic patients. It consists of rhythmically recurring extracellular LFP deflections associated with high-frequency oscillations and an increased neuronal firing as it was observed earlier [3], [186]. The second type of PAs, the spontaneous interictal-like discharges (sIIDs) appeared too in the presence of physiological solution, but only in slices derived from epileptic patients. This activity resembles those epileptiform population bursts which were observed during the application of 4-aminopyridine [187]. After the administration of bicuculline, these spontaneous activities disappeared, and in many cases, two other types of synchronies (bicuculline-induced population activities, BIPAs) emerged both in epileptic and non-epileptic tissue. The third PA, the bicuculline-induced interictal-like spike (bIIS) has higher amplitude and burstiness than the physiological sIID. It can further be distributed into simple and complex events (see later) considering its temporal and spatial behaviour. At last, the fourth type of synchronous event is the bicuculline-induced seizure-like activity which consists of temporally complex recurring interictal-like spikes, always invading the entire width of the neocortex. Bicuculline-induced seizures have a considerably longer duration than complex bIISs.

DOI:10.15774/PPKE.ITK.2020.008

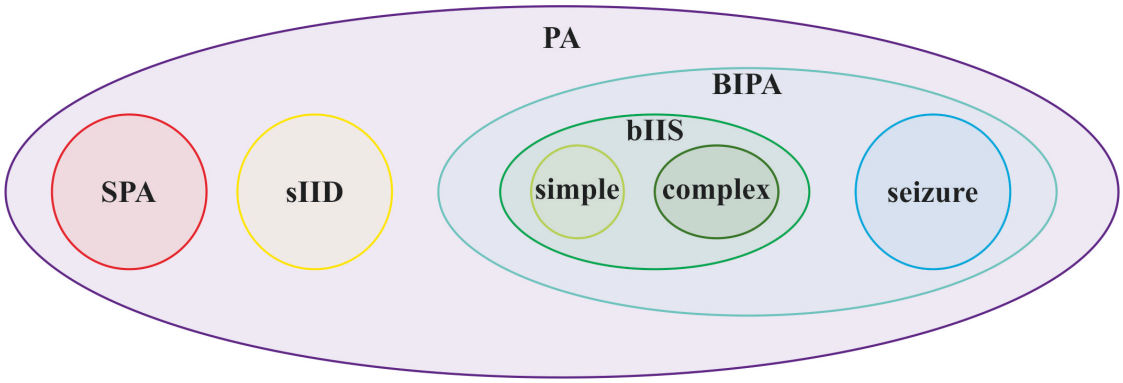

Figure 4.1. Classification of the population activities (PAs) developing in the postoperative neocortical human tissue. The spontaneous population activity (SPA) and the spontaneous interictal-like discharge (sIID) are generated during physiological conditions. After the application of bicuculline bath, these discharges disappear, and bicuculline-induced population activities (BIPAs) show up in certain cases: interictal-like spikes (bIIS) and seizure-like activity. The former can be further distributed into simple and complex events.

The emergence of synchronous activity in a physiological solution

Altogether 592 neocortical slices have been investigated, 236 slices from 42 ResEpi patients, 66 slices from 10 TreatEpi patients, 43 slices from 8 NoMed patients and 247 slices from 44 NoEpi patients (*Table 4.1*). Slices were considered to be dead if we could detect neither populational nor single-unit activity. SPAs emerged in 126/195 living slices (64.6%, 38/42 patients) from the ResEpi group, in 22/56 living slices (39.3%, 9/10 patients) from the TreatEpi group, in 6/29 living slices (20.7%, 4/8 patients) from the NoMed group and in 87/199 living slices (43.7%, 33/44 patients) from the NoEpi group (*Table 4.1*). Only a few samples were able to generate sIIDs, exclusively the ones derived from patients with epilepsy in their anamnesis (8 slices from the ResEpi and one slice from the TreatEpi groups). SPAs and sIIDs were separated by considering all network properties we investigated throughout the analyses: the layer of emergence, the recurrence frequency, as well as the LFPg, CSD and MUA amplitudes. Even though every feature showed a slight overlap, the combination of all parameters gave an apparent distinction between SPAs and sIIDs (*Figure 4.2*). Please, note, that when we refer to any population activities (SPA, sIID, bIIS or seizure), we mean all the recurring synchronous events in a certain recording. The total number of events per recording varied from 1 to 1814. Single population events will be referred to as 'population activity event'.

There was no difference between the contribution of the different lobes to the generation of SPA (*Table 4.1*). Significantly more slices generated SPA in the ResEpi slices compared to those of NoEpi ($p < 0.0001$), TreatEpi ($p < 0.01$) and NoMed ($p < 0.0001$) patients. Furthermore,

DOI:10.15774/PPKE.ITK.2020.008

more SPAs emerged in neocortical slices derived from epileptic patients (56.5%) than the ones originated from the NoEpi group (43.7%, *Table 4.2*). Furthermore, samples of epileptic patients diagnosed with a tumour generated SPAs with a lower rate (glial tumour: 47.9%, a tumour of another origin: 31.3%) than the ones with dysplasia (65.7%) or hippocampal sclerosis (83.7%) (*Table 4.2*). Significant differences in the number of slices generating SPA by aetiology in the ResEpi, TreatEpi and NoMed groups: dysplasia > glial tumour ($p < 0.05$); dysplasia > other tumour ($p < 0.01$); hippocampal sclerosis > glial tumour ($p < 0.01$); hippocampal sclerosis > other tumour ($p < 0.0001$); dysgenesis > other tumour ($p < 0.05$).

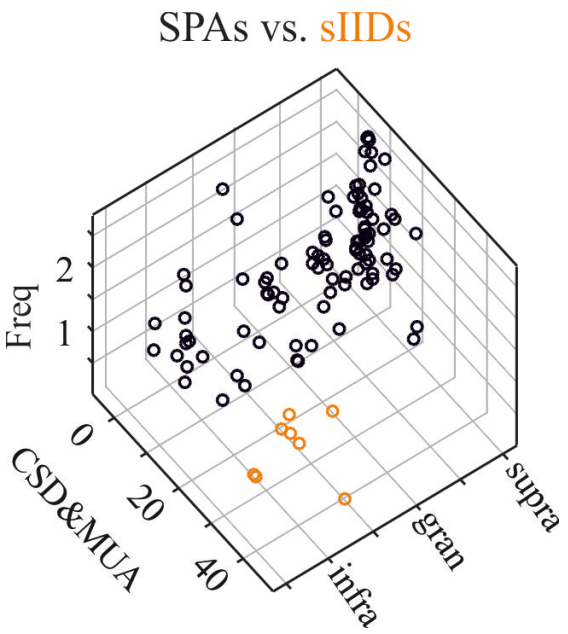

Figure 4.2. Three-dimensional plot of the examined population activity features to separate SPAs and sIIDs. The values of requrrence frequency (Freq), the average of combined CSD and MUA (CSD&MUA) and the intracortical location of all SPAs (black circles) and IIDs (orange circles) are shown.

There were differences in the emergence of SPAs in NoEpi slices, relative to their type of tumour (*Table 4.2*). Slices derived from tumour patients diagnosed with carcinoma metastasis generated SPAs with a lower rate (27.5%) than the ones with a glial tumour (54.3%, *Table 4.2*). A significant difference in the number of slices generating SPA by aetiology in the NoEpi group appeared only between glial tumour and carcinoma metastasis ($p < 0.001$). NoEpi samples have been separated according to the distance between the resected tissue and the area affected by the tumour. In brain slices relatively far from the tumour ($d > 30$ mm) the emergence of SPA was more probable (50.8%) than in the ones closer than 30 mm (33.3%).

DOI:10.15774/PPKE.ITK.2020.008

Table 4.1. SPA incidence in neocortical slices deriving from different lobes of the brain. The ratio of all slices generating SPA and all living slices have been calculated. Slices with detectable single units and/or PAs were considered to be living slices. The ratios of slices with SPA and living slices have been determined by patients as well. Mean ± std is listed.

	ResEpi			TreatEpi			NoMed			NoEpi		
	Living slices (All slices)	Ratio of slices generating SPA (%. sum of slices with SPA/sum of living slices)	Ratio of slices generating SPA (%. by patient. mean±SD)	Living slices (All slices)	Ratio of slices generating SPA (%. sum of slices with SPA/sum of living slices)	Ratio of slices generating SPA (%. by patient. mean±SD)	Living slices (All slices)	Ratio of slices generating SPA (%. sum of slices with SPA/sum of living slices)	Ratio of slices generating SPA (%. by patient. mean±SD)	Living slices (All slices)	Ratio of slices generating SPA (%. sum of slices with SPA/sum of living slices)	Ratio of slices generating SPA (%. by patient. mean±SD)
Frontal Lobe	50 (57)	70.0	52.8±30.3	26 (33)	38.5	33.9±22.7	15 (24)	13.3	10.0±20.0	59 (65)	40.7	44.5±35.2
Temporal Lobe	117 (148)	65.0	70.2±30.5	20 (22)	40.0	39.5±10.7	9 (13)	33.3	33.3±0.0	48 (73)	39.6	34.7±32.5
Parietal Lobe	28 (31)	53.6	57.1±21.4	-	-	-	-	-	-	61 (70)	52.5	57.8±34.4
Occipital Lobe	5 (6)	80.0	80.0±0.0	10 (11)	40.0	40.0±14.1	5 (6)	20.0	25.0±35.4	31 (39)	38.7	30.2±33.8
Total	195 (236)	64.6	64.7±29.4	56 (66)	41.1	38.8±17.8	29 (43)	20.7	19.6±7.9	199 (247)	43.7	43.5±34.4

DOI:10.15774/PPKE.ITK.2020.008

Table 4.2. Relationship of SPA occurrence and aetiology: The ratio of all slices generating SPA and all living slices have been calculated. Slices with detectable single units and/or PAs were considered to be living slices. The ratios of slices with SPA and living slices have been determined by patients as well. Mean ± std is listed.

Patient group	Aetiology	Number of patients	Ratio of slices generating SPA (%. sum of slices with SPA/sum of living slices)	Ratio of slices generating SPA (%. by patient. mean±SD)
ResEpi, TreatEpi, NoMed	Dysplasia	13	65.7	70.9±25.7
	Hippocampal sclerosis	13	73.2	83.7±26.0
	Dysgenesis/gliosis	6	55.2	64.8±26.9
	Glial tumour	20	47.9	54.4±33.3
	Other tumour	7	31.3	26.4±17.8
	Other	6	65.0	66.7±38.6
	Total	65	56.5	54.2±31.4
NoEpi	Glial tumour	21	54.3	58.2±34.3
	Carcinoma metastasis	16	27.5	22.0±27.9
	Other tumour	7	47.4	48.6±24.5
	Total	44	43.7	43.5±34.4

The effect of bicuculline on synchronies in the human neocortex

After previous recordings and visual evaluation, bicuculline bath has been applied on 69 slices with either SPAs or clear, extensive SUA (*Table 4.3*). In the presence of the $GABA_A$ receptor antagonist, SPAs disappeared in all cases. BIPAs developed in slices from any lobe of the neocortex spontaneously, in contrast to preceding studies, where the emergence of interictal-like activity induced by bicuculline could only be achieved by electrical stimulation [15], [19]. Significantly more slices derived from epileptic (27/43 slices) patients generated BIPAs than slices from non-epileptic (15/46 slices) patients ($p < 0.01$) (*Table 4.3*). Samples of epileptic patients diagnosed with or without tumour developed BIPAs with a comparable rate (12/21 slices with tumour and 15/22 slices without tumour). Within the NoEpi group, more synchronies could be detected but with a lower overall ratio in neocortical tissue derived from patients with tumour of glial origin than the ones with other symptoms (8/18 and 7/8 slices, respectively, not significant). The distance from the tumour had no effect on the generation of BIPAs (data not shown).

4.1.2 Characterisation of synchronous population activities

The nature of SPAs and sIIDs

DOI:10.15774/PPKE.ITK.2020.008

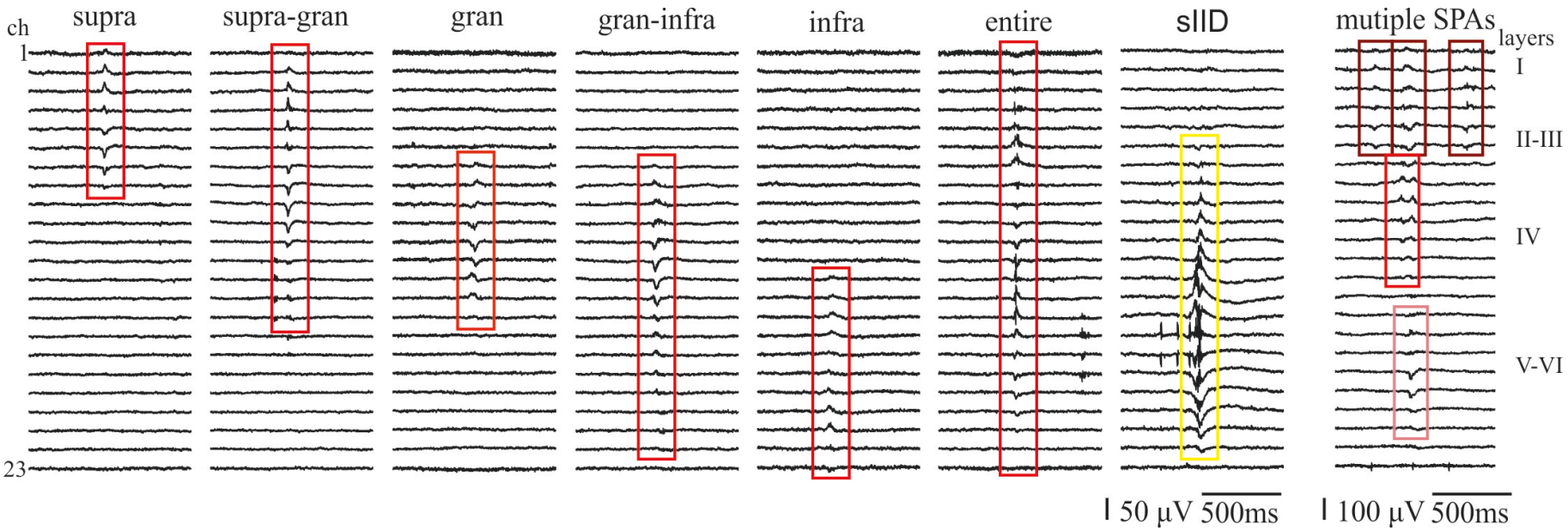

Figure 4.3. Different types of synchronous population activities in physiological bath: Six kinds of SPAs (red rectangles) have been separated according to their interlaminar spread, those emerged in the supragranular (supra), supragranular-granular (supra-gran), granular (gran), granular-infragranular (gran-infra), infragranular (infra) layers and the entire neocortex (entire). An example of an sIID was shown (yellow rectangle) to indicate the difference between the physiological and putatively pathological activities. The last subfigure illustrates multiple SPAs detected on one recording. Different shades of red express the different types of population events.

DOI:10.15774/PPKE.ITK.2020.008

Table 4.3. Changes in the population synchronies after the application of bicuculline. The number of slices with both SPA and BIPA, with BIPA but without SPA, with SPA but without BIPA, and without any kind of event have been counted.

Slices	AllEpi	ResEpi	TreatEpi	NoMed	NoEpi
SPA - BIPA (n)	19 (44.2%)	16 (55.2%)	3 (33.3%)	0 (0.0%)	12 (46.2%)
no SPA - BIPA (n)	8 (18.6%)	5 (17.2%)	1 (11.1%)	2 (40.0%)	3 (11.5%)
SPA - no BIPA (n)	7 (16.3%)	3 (10.4%)	3 (33.3%)	1 (20.0%)	8 (30.8%)
no SPA - no BIPA (n)	9 (20.9%)	5 (17.2%)	2 (22.2%)	2 (40.0%)	3 (11.5%)
Total slices (n)	43	29	9	5	26

Six kinds of SPAs have been separated by their interlaminar location in the neocortex. Multiple SPAs could be observed within the same slice as well. In some cases, multiple SPAs or SPA + sIID combos appeared simultaneously on the same recording site, while in other cases different SPAs emerged on the same slice but on different recording spots. See *Figure 4.3* and *Table 4.4* for summary. Most frequently they were generated in the supragranular layers (supra, 48% in the ResEpi, 51.6% in the TreatEpi, 57.1% in the NoMed and 55.1% in the NoEpi groups), 185 in total [3]. Less regularly they invaded the supragranular-granular (supra-gran = 64 in total, 17.2% of ResEpi, 19.4% of TreatEpi, 14.3% of NoMed and 18.1% of NoEpi SPAs), the granular (gran = 39 in total, 9.6% of ResEpi, 12.9% of TreatEpi, 14.3% of NoMed and 11.8% of NoEpi SPAs) or the infragranular (infra = 37 in total, 10.6% of ResEpi, 12.9% of TreatEpi, 14.3% of NoMed and 8.7% of NoEpi SPAs) layers. In a few cases, they appeared either in the granular-infragranular layers (gran-infra = 15 in total, 5.6% of ResEpi and 3.1% of NoEpi SPAs) or overspread the entire neocortex (entire = 23 in total, 9.1% of ResEpi, 3.2% of TreatEpi and 3.1% of NoEpi SPAs).

Interictal-like events seemed to be less variable according to their location, and they tended to be limited to the deeper structures (*Figure 4.3, Table 4.4*). Ten sIIDs could be detected in slices derived from ResEpi patients. One activity appeared in the granular layer, seven in the granular-infragranular layers and two in the infragranular layers. The only one sIID, which was generated by a sample of a TreatEpi patient, emerged in the granular layer. These putatively pathological activities could also develop alone or together with SPAs or other sIIDs at a different location in the same slice.

DOI:10.15774/PPKE.ITK.2020.008

Table 4.4. SPA and sIID distribution across neocortical layers. Population activities have been distributed by their laminar location in the neocortex. SPAs appeared either as single SPAs (a series of one kind of event within one recording) or as multiple phenomena with other SPAs (series of two or more kinds of events within one recording). They might appear even together with sIIDs. Most of the SPAs emerged from the supragranular layers. Less frequently they invaded the supragranular-granular, granular or infragranular layers. SPAs covered the granular-infragranular layers or the entire cortex scarcely. sIIDs tend to be limited to the deeper structures, namely the granular, granular-infragranular and infragranular layers.

SPAs and sIIDs in neocortical layers	ResEpi				TreatEpi				NoMed			NoEpi		
	Single SPA	Multiple SPA	Total SPA (%)	sIID	Single SPA	Multiple SPA	Total SPA (%)	sIID	Single SPA	Multiple SPA	Total SPA (%)	Single SPA	Multiple SPA	Total SPA (%)
Supra	41	54	95 (48.0%)	-	11	5	16 (51.6%)	-	1	3	4 (57.1%)	46	24	70 (55.1%)
Supra-gran	16	18	34 (17.2%)	-	3	3	6 (19.4%)	-	1	-	1 (14.3%)	10	13	23 (18.1%)
Gran	6	13	19 (9.6%)	1 (10.0%)	1	3	4 (12.9%)	1 (100.0%)	1	-	1 (14.3%)	4	11	15 (11.8%)
Gran-Infra	-	11	11 (5.6%)	7 (70.0%)	-	-	-	-	-	-	-	1	3	4 (3.1%)
Infra	4	17	21 (10.6%)	2 (20.0%)	1	3	4 (12.9%)	-	-	1	1 (14.3%)	3	8	11 (8.7%)
Entire	8	10	18 (9.1%)	-	-	1	1 (3.2%)	-	-	-	-	2	2	4 (3.1%)
Total number of SPAs or sIIDs	75	123	198	10	16	15	31	1	3	4	7	66	61	127

DOI:10.15774/PPKE.ITK.2020.008

The nature of bIISs and seizures

Interictal-like discharges induced by the blockade of the GABAergic inhibition were higher LFPg amplitude events by nature (*Figure 4.4*). Three kinds of activities have been separated according to their location, those limited to the supragranular-granular or granular-infragranular layers, or invaded the entire neocortex. bIISs appeared to be either temporally simple or complex events. Temporally simple bIISs had only one periodically recurring LFPg deflection, while temporally complex events consisted of multiple, jointly occurring waves. This second type of activity could be further separated into spatially simple or complex events. Spatially simple bIIS involved waves originated from the same cortical layers, while spatially complex events united those from separate locations. In case of the spatially complex events, the first spike usually invaded the entire width of the cortex, while during the following spikes of the bIISs the supragranular and infragranular layers were differently involved from event to event (*Figure 4.5*). Following these rules, three kinds of bIIS have been distinguished: simple-simple, complex-simple and complex-complex, where the components indicate temporal and spatial complexity, respectively.

Sixteen bIISs have been detected in slices derived from ResEpi patients. Ten of them overspread the entire neocortex (n = 7 simple-simple, n = 1 complex-simple, n = 2 complex-complex), four of them could be observed in the supragranular-granular layers (n = 2 simple-simple, n = 2 complex-simple) while two of them developed in the granular-infragranular layers (n = 2 simple-simple). Only entire bIISs emerged in samples from the TreatEpi (n = 3 simple-simple, n = 1 complex-simple), NoMed (n = 1 simple-simple) and NoEpi (n = 13 simple-simple) groups. See *Figure 4.4* and *Table 4.5* for summary.

Seizures were 15 to 28 sec long, temporally complex epileptiform events, consisting of recurring interictal-like spikes, always invading the entire width of the neocortex (*Figure 4.4*). Two spatially simple and five complex seizures have been detected in samples from the ResEpi group, while two spatially simple and one complex event developed in the NoEpi tissue. Only one simple event emerged in slices derived from both TreatEpi and NoMed patients. See *Table 4.5*.

Comparison of the different kind of synchronies

To shed light on attributes related to epileptic mechanisms, we compared slices derived from patients in the ResEpi and NoEpi groups.

During the application of bicuculline, we have detected single and recurrent bIISs and seizures. A single event means only one wave could be detected during the whole recording period, while

DOI:10.15774/PPKE.ITK.2020.008

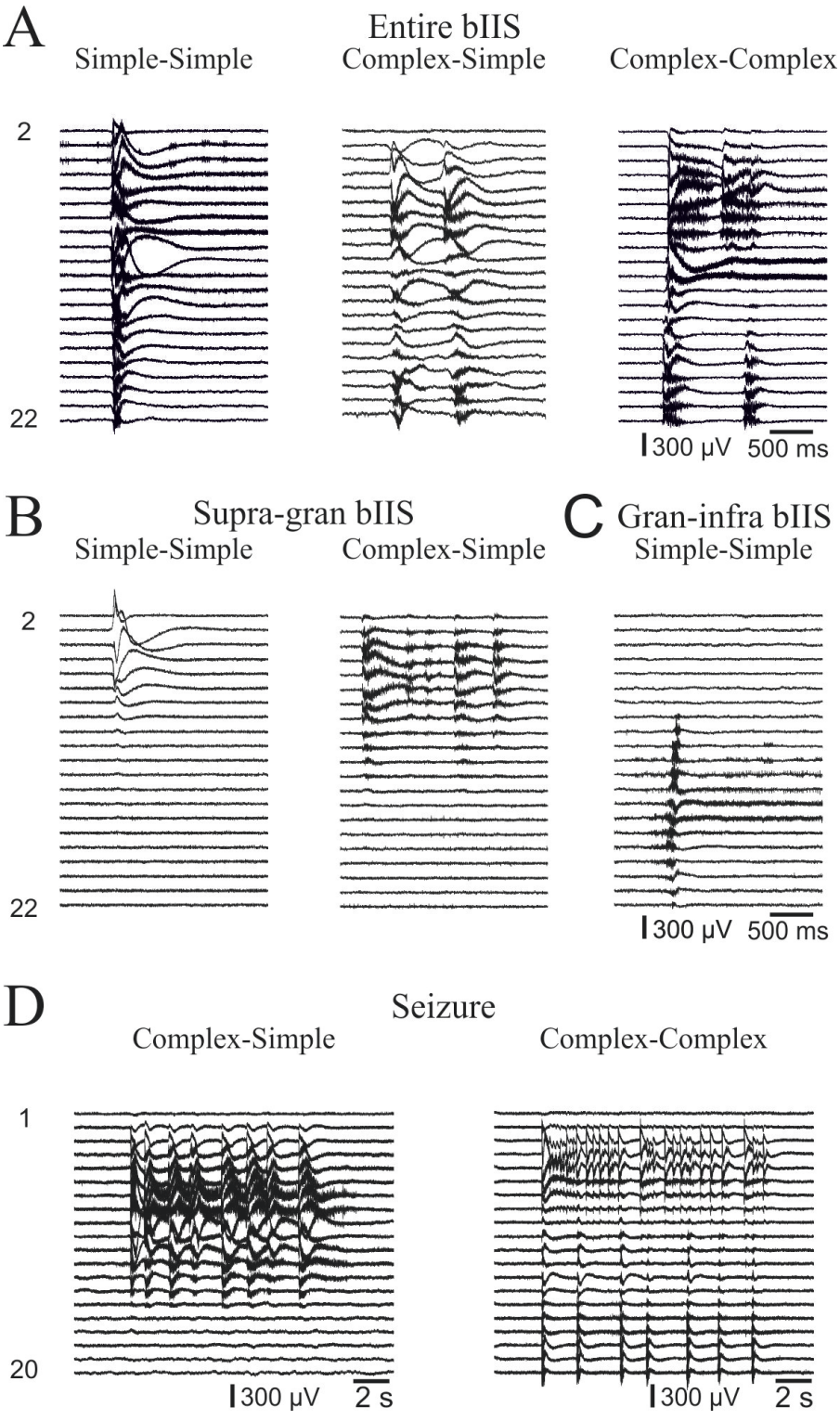

Figure 4.4. Examples of BIPA types: A) Entire bIISs with simple-simple, complex-simple and complex-complex temporal and spatial complexity, respectively. B) Simple-simple and complex-simple bIISs in the supragranular-granular layers. C) Simple-simple bIIS in the granular-infragranular layers. D) Complex-simple and simple-simple examples for a seizure.

DOI:10.15774/PPKE.ITK.2020.008

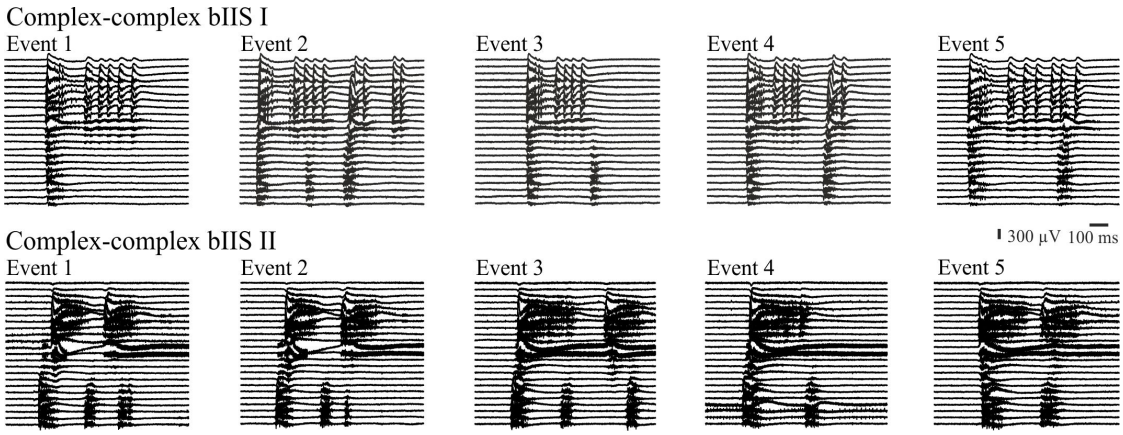

Figure 4.5. Variability of complex-complex bIISs during the timecourse of the bicuculline bath. After the first spike, the supragranular and infragranular layers were differently involved in the generation of the population activity from event to event.

Table 4.5. Distribution of bicuculline-induced epileptiform activities across different patient groups. bIISs usually invaded the entire neocortex, and in a few cases they were located in the supragranular-granular layers or granular-infragranular layers. Temporally simple events had one periodically recurring LFPg deflection. Temporally complex events consisted of multiple, jointly occurring waves. In case of spatially simple events, the waves of the temporally complex activity emerged in the same layers. Spatially complex events consisted of those from different locations. Seizures were solely entire, temporally complex events.

	Temporal complexity	Spatial complexity	ResEpi Activities n(%)	TreatEpi Activities n(%)	NoMed Activities n(%)	NoEpi Activities n(%)
bIIS (entire)	simple	simple	7 (22.6%)	3 (30.0%)	1 (16.7%)	13 (48.2%)
	complex	simple	1 (3.2%)	1 (10.0%)	-	-
	complex	complex	2 (6.5%)	-	-	-
bIIS (supra-gran)	simple	simple	2 (6.5%)	-	-	-
	complex	simple	2 (6.5%)	-	-	-
bIIS (gran-infra)	simple	simple	2 (6.5%)	-	-	-
Seizure	complex	simple	2 (6.5%)	1 (10.0%)	1 (16.7%)	2 (7.4%)
	complex	complex	5 (16.1%)	-	-	1 (3.7%)
No BIPA			8 (25.7%)	5 (50.0%)	4 (66.6%)	11 (40.7%)
Total (n)			31	10	6	27

DOI:10.15774/PPKE.ITK.2020.008

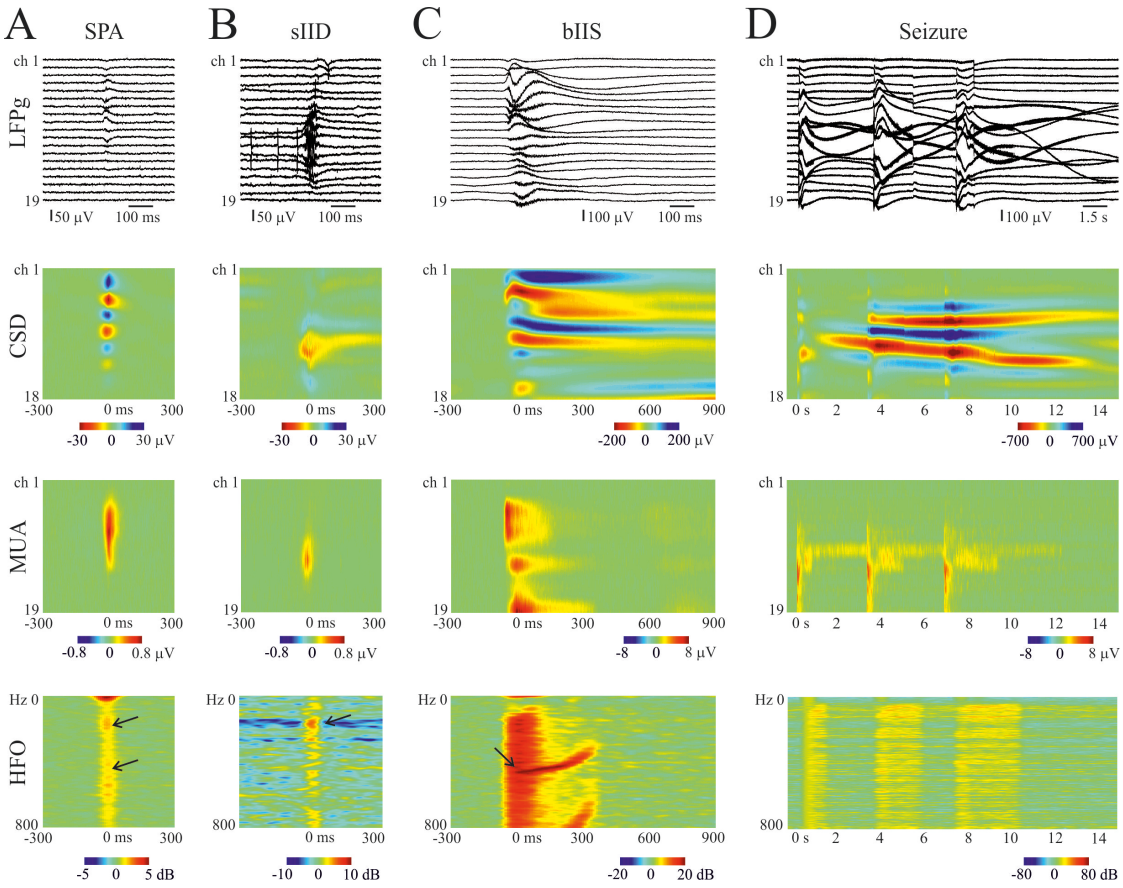

Figure 4.6. Different population activities in the human neocortex, in vitro. The LFPg shows the morphology of the distinct events on the local field potential gradient recordings. The CSD (current-source density) analysis revealed that these activities are the outcome of local mechanisms. Current sources and current sinks are indicated by cool and warm colours, respectively. The MUA (multiple-unit activity) analysis showed increased cellular firing during the LFP deflections (warm colours). As a result of the time-frequency analysis, HFOs (high-frequency oscillations) were observed. Arrows indicate local peaks in the power of HFOs at ripple and fast-ripple frequencies. In the presence of bIISs, a noticeable power increase was detected in all frequency bands. Nevertheless, the ripple and fast-ripple peak remained prominent. In the case of seizures, these local maximas were smashed away. Note the different LFPg amplitude, colour and time scales.

DOI:10.15774/PPKE.ITK.2020.008

a recurrent activity refers to periodically returning LFPg deflections. Four and seven single bIISs, while eleven and six recurrent bIISs occurred in slices resected from ResEpi and NoEpi patients. As for the seizures, only one single and six recurrent events were generated by slices in the ResEpi group, meanwhile, always single seizures arose in the NoEpi group. SPAs and sIIDs only appeared as recurrent events.

The recurrence frequency of SPAs were 1.15 ± 0.72 Hz and 1.19 ± 0.6 Hz in slices derived from ResEpi and NoEpi patients, respectively (no significant difference). While the recurrence frequency of sIID was 0.12 ± 0.12 Hz, which is significantly different from those, calculated for both ResEpi and NoEpi SPAs ($p < 0.01$, two-tailed Mann-Whitney U test). The average recurrence frequency of bIISs appeared to be 0.09 ± 0.15 Hz (5.23 ± 9.03 min^{-1}) and 0.01 ± 0.02 Hz (0.88 ± 1.09 min^{-1}) in ResEpi and NoEpi slices, respectively. These values are significantly different between patient groups ($p < 0.00001$, two-tailed Mann-Whitney U test), and also, they happen to be significantly lower compared to those calculated for SPAs ($p < 0.00001$, two-tailed Mann-Whitney U test). The recurrence frequency of seizures were 0.007 ± 0.007 Hz (0.42 ± 0.42 min^{-1}) in ResEpi slices, and 0.002 ± 0.001 Hz (0.14 ± 0.05 min^{-1}) in NoEpi slices, which were significantly different ($p < 0.05$, two-tailed Mann-Whitney U test). Seizures were not different from bIISs or sIIDs, but consistently, they were significantly different from SPAs ($p < 0.05$, two-tailed Mann-Whitney U test). All values are shown in *Table 4.6*. For a more detailed insight, the median (with the 1st and third quartiles) is also provided together with the mean ± standard deviation quantities.

In contrast to the recurrence frequency, there was a significant difference between the patient groups considering the duration of SPAs at the half-max amplitude of the peak ($p < 0.05$, two-tailed Mann-Whitney U test), which was 32.7 ± 18.76 ms for Resepi, and 23.37 ± 10.74 ms for NoEpi patients. The duration of sIID was apparently longer: 42.94 ± 21.65 ms, but not significantly longer than ResEpi SPAs. As the calculation of the length of BIPAs were different from the one used for SPAs (for details, see the *Methods* section), the comparison of these values could be misleading. Even though the difference between these activities are pretty obvious (*Figure 4.6*). The average duration of the bIISs was 0.36 ± 0.23 s in the ResEpi group and 0.44 ± 0.16 s in the NoEpi group, which were significantly not different. The seizures were 21.75 ± 4.44 s and 24.19 ± 3.48 s in slices derived from patients of the ResEpi and NoEpi groups, respectively (significantly not different), also not comparable to SPAs, sIIDs or bIISs. See *Table 4.6* and *Figure 4.7* for comparison of the mean and median of each PA lengths.

The amplitude of LFPg and MUA have been compared between patients groups as well as between the different kind of activities (*Table 4.6*, *Figure 4.6*, *Figure 4.7*). There was no signif-

DOI:10.15774/PPKE.ITK.2020.008

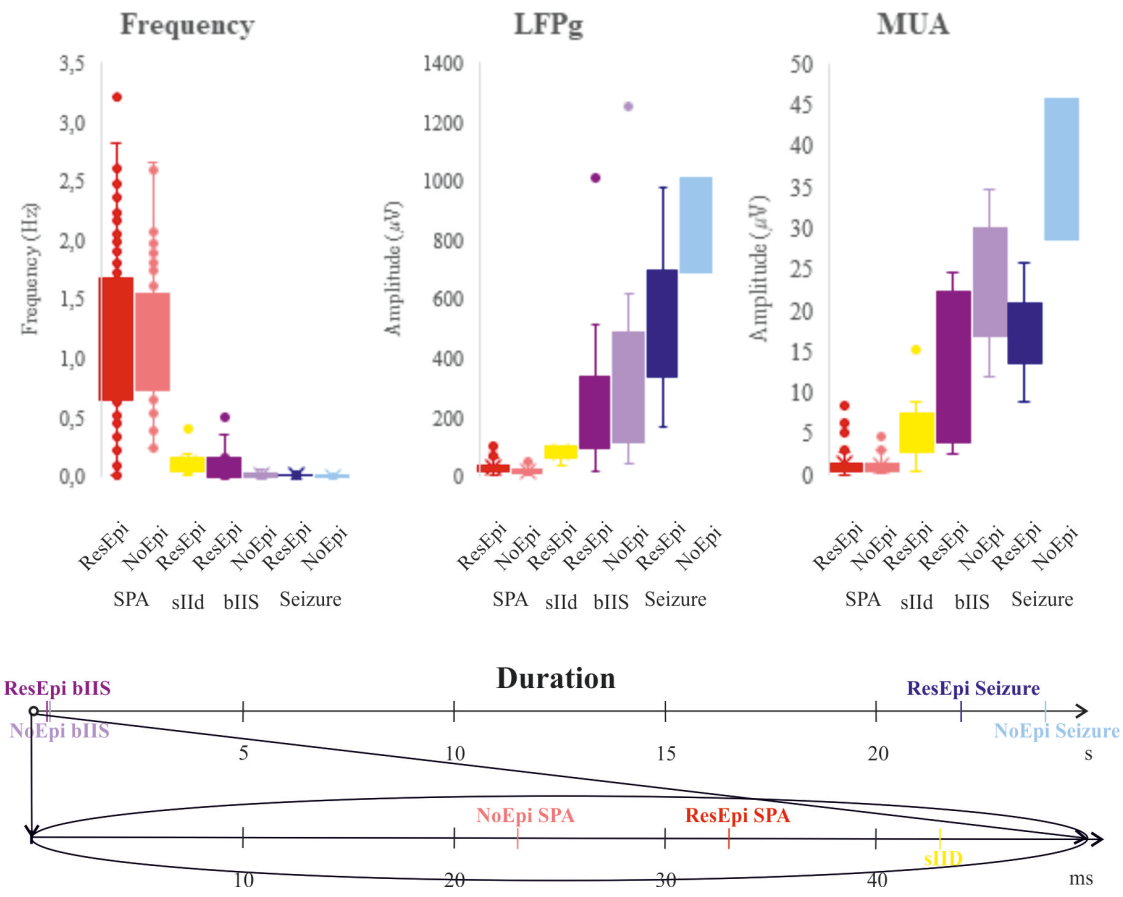

Figure 4.7. Summary of *Table 4.6*

DOI:10.15774/PPKE.ITK.2020.008

Table 4.6. Characteristics of SPAs, sIIDs, bIISs and seizures. All data are provided in **median [1st and 3rd quartile]** and in mean ± standard deviation.

Patient group	Population activity	n	Recurrence frequency (Hz; min^{-1})	Duration (ms; s)	Maximal LFPg amplitude (μV)	Maximal MUA amplitude (μV)
ResEpi	SPA	78	**1.011 [0.658 1.644] Hz** 1.151±0.722 Hz	**27.15 [22.44 37.39] ms** 32.7±18.76 ms	**24.33 [17.68 35.52]** 28.87±17.16	**0.90 [0.44 1.36]** 1.32±1.48
	sIID	9	**0.049 [0.039 0.136] Hz** 0.116±0.123 Hz	**37.35 [34.45 52.55] ms** 42.94±21.65 ms	**83.72 [66.05 100.34]** 79.80±22.72	**5.41 [3.99 5.81]** 5.80±4.29
	bIIS	15	**0.013 [0.003 0.102] Hz** 0.087±0.150 Hz **0.754 [0.186 6.114]** min^{-1} 5.236±9.027 min^{-1}	**0.30 [0.17 0.50] s** 0.36±0.23 s	**200.60 [133.66 295.71]** 262.98±241.37	**9.87 [5.64 20.23]** 12.79±8.27
	seizure	7	**0.003 [0.003 0.008] Hz** 0.007±0.007 Hz **0.201 [0.180 0.460]** min^{-1} 0.424±0.422 min^{-1}	**23.88 [18.05 25.27] s** 21.75±4.44 s	**485.87 [399.86 624.18]** 526.24±259.06	**14.96 [13.73 18.60]** 16.35±5.47
NoEpi	SPA	65	**1.087 [0.758 1.489] Hz** 1.191±0.604 HZ	**21.95 [17.35 27.55] ms** 23.37±10.74 ms	**16.11 [10.63 25.20]** 20.71±14.21	**0.85 [0.47 1.35]** 1.25±1.14
	bIIS	13	**0.003 [0.002 0.031] Hz** 0.015±0.018 HZ **0.205 [0.102 1.890]** min^{-1} 0.876±1.094 min^{-1}	**0.48 [0.32 0.58] s** 0.44±0.16 s	**296.84 [124.85 463.91]** 348.32±322.49	**20.18 [19.56 27.73]** 22.38±7.49
	seizure	3	**0.002 [0.002 0.003] Hz** 0.002±0.001 Hz **0.116 [0.109 0.158]** min^{-1} 0.139±0.052min^{-1}	**22.50 [22.19 25.35] s** 24.19±3.48 s	**839.97 [764.64 925.98]** 847.09±161.46	**36.59 [32.61 41.19]** 37.01±8.59
Significant differences			ResEpi bIIS>NoEpi bIIS (p<0.00001) ResEpi seizure>NoEpi seizure (p<0.05)	ResEpi SPA>NoEpi SPA (p<0.05)	ResEpi SPA<ResEpi sIID (p<0.05) ResEpi SPA<ResEpi bIIS (p<0.0001)	ResEpi SPA<ResEpi sIID (p<0.05) ResEpi SPA<ResEpi bIIS (p<0.00001)

DOI:10.15774/PPKE.ITK.2020.008

Table 4.6 continued from previous page

Patient group	Population activity	n	Recurrence frequency (Hz; min^{-1})	Duration (ms; s)	Maximal LFPg amplitude (μV)	Maximal MUA amplitude (μV)
			ResEpi SPA>ResEpi sIID (p<0.01)		ResEpi SPA<ResEpi seizure (p<0.001)	ResEpi SPA<ResEpi seizure (p<0.001)
			ResEpi SPA>ResEpi bIIS (p<0.00001)		ResEpi sIID>NoEpi SPA (p<0.001)	ResEpi sIID>NoEpi SPA (p<0.05)
			ResEpi SPA>ResEpi seizure (p<0.001)		NoEpi SPA<NoEpi bIIS (p<0.00001)	NoEpi SPA<NoEpi bIIS (p<0.00001)
			ResEpi sIID<NoEpi SPA (p<0.01)		NoEpi SPA<NoEpi seizure (p<0.01)	NoEpi SPA<NoEpi seizure (p<0.01)
			NoEpi SPA>NoEpi bIIS (p<0.00001)			
			NoEpi SPA>NoEpi seizure (p<0.05)			

DOI:10.15774/PPKE.ITK.2020.008

icant difference between the LFPg amplitudes of ResEpi and NoEpi SPAs: 28.87 ± 17.16 μV and 20.71 ± 14.21 μV, respectively. The amplitude of sIIDs was significantly higher, 79.80 ± 22.72μV ($p < 0.05$, two-tailed Mann-Whitney U test).The LFPg amplitude of bIISs was about one magnitude higher than that of SPAs: it was 262.98 ± 240.92 μV in ResEpi and 348.32 ± 322.49 μV in NoEpi slices (significantly different, two-tailed Mann-Whitney U test, $p < 0.0001$). bIISs were not significantly higher than sIIDs. The LFPg amplitude of bicuculline-induced seizures was significantly higher than that of SPAs ($p < 0.01$, two-tailed Mann-Whitney U test), but not significantly higher than sIIDs or bIISs: 526.24 ± 259.06 μV and 847.09 ± 161.46 μV in ResEpi and NoEpi, respectively. Similarly, MUA amplitudes during the different kind of activities have been calculated: ResEpi SPA: 1.32 ± 1.48 μV; NoEpi SPA: 1.25 ± 1.14 μV; sIID: 5.80 ± 4.29 μV; ResEpi bIIS 12.79 ± 8.27 μV; NoEpi bIIS: 22.38 ± 7.49 μV; ResEpi seizure: 16.35 ± 5.47 μV; NoEpi seizure: 37.01 ± 8.59 μV. bIISs and seizures had significantly higher MUA amplitudes than SPAs in both patient groups. sIIDs had significantly higher MUA amplitude than SPAs but did not differ significantly from bIISs or seizures. While there has been no significant difference between the same activities in the two patient groups.

The CSD analysis showed that the currents responsible for the generation of these population synchronies are local and restricted to the layers where the LFPg deflection was present (*Figure 4.6*). In the case of SPAs, most of the times, a sink-source pair or a source-sink-source triplet appeared together without any time-delay [164]. In contrast to that, during sIIDs or in the presence of bicuculline, usually, there was an initial sink or source which was followed by other sinks and sources spreading across the entire neocortex (or in the layers, where the event was present). There were no favoured type or layer in the induction of the event current. We could not find any relation between the CSD pattern and the simple or complex nature of the BIPAs.

Initiation and propagation of BIC-induced activities across cortical layers

Our goal was to observe how the different cortical layers contribute to the generation of epileptic events. We have already stated that most of bIISs and seizures covered the entire neocortex or sometimes invaded only the supragranular-granular or the granular-infragranular layers. In the case of complex events, different cortical layers were often involved separately. Earlier (in vivo) studies [12] showed that different kind of layers participate in the generation of interictal events originated from other brain areas than of the ones developed locally. In our in vitro experiments, this issue cannot be evaluated for obvious reasons, the question arises yet whether certain layers are more likely to induce synchronous events while others follow, or whether BIC-induced events appear synchronously throughout the entire width of the neocortex.

DOI:10.15774/PPKE.ITK.2020.008

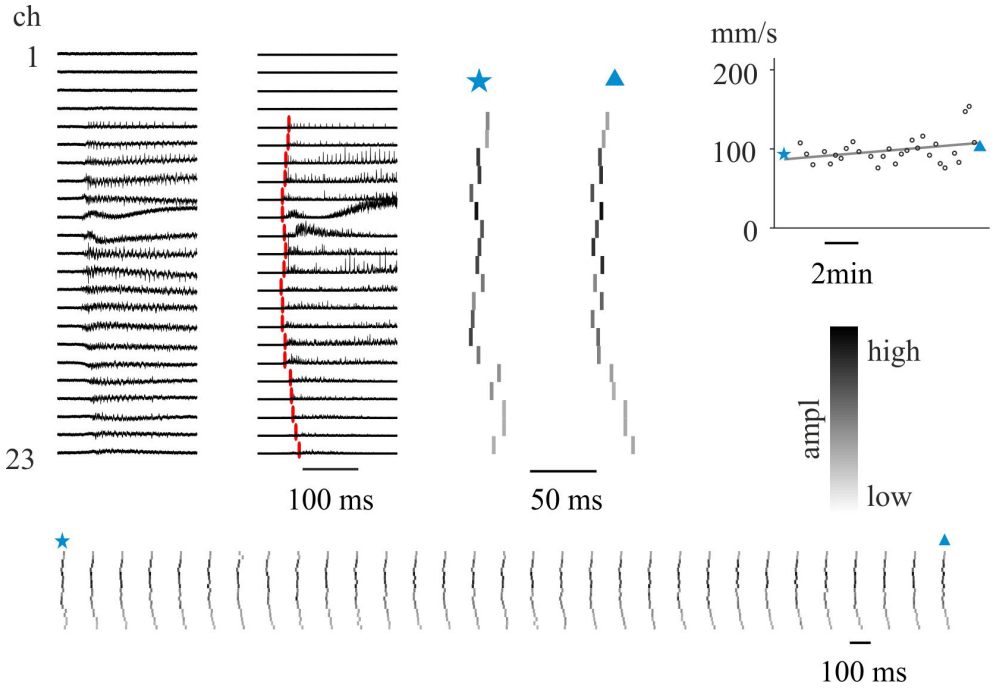

(a) No change in the propagation speed.

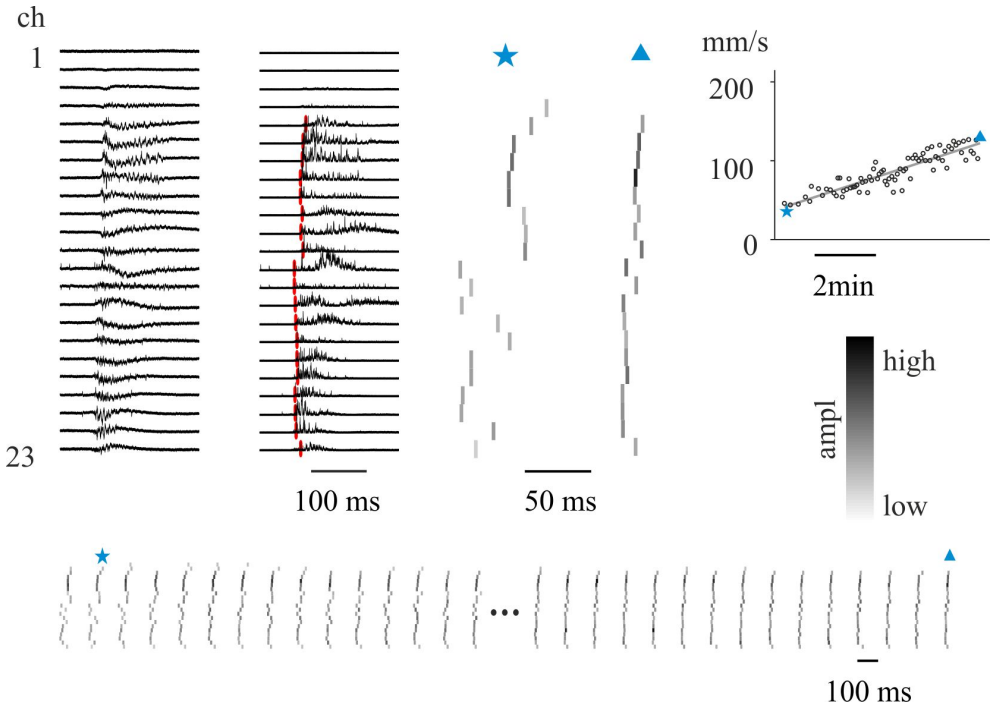

(b) Increasing propagation speed.

Figure 4.8. Continued on the following page.

DOI:10.15774/PPKE.ITK.2020.008

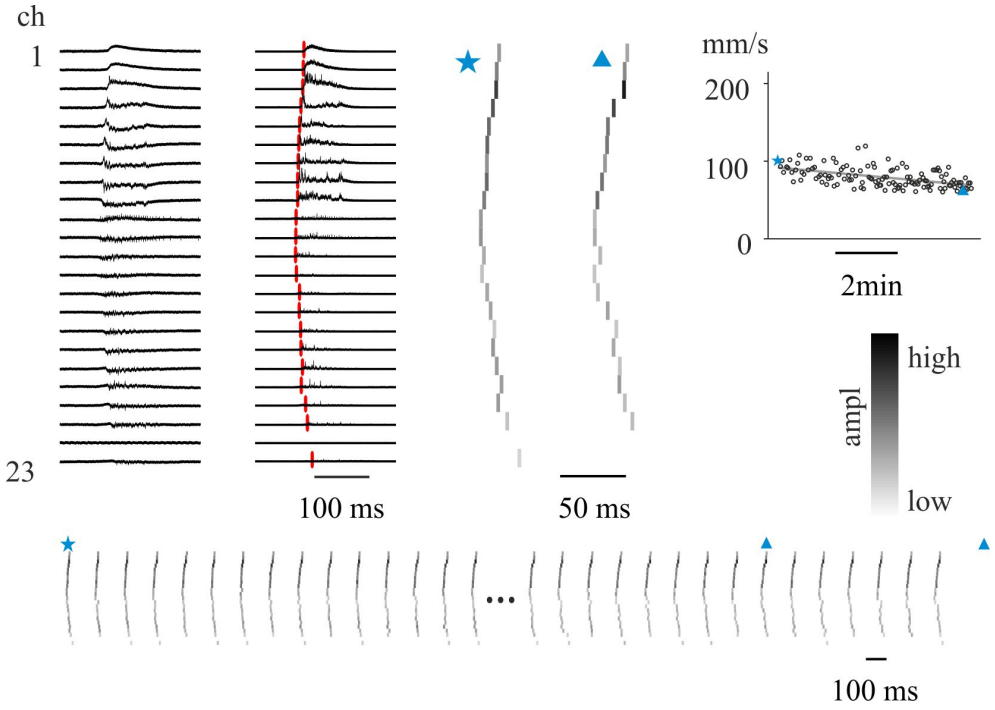

(c) Decreasing propagation speed.

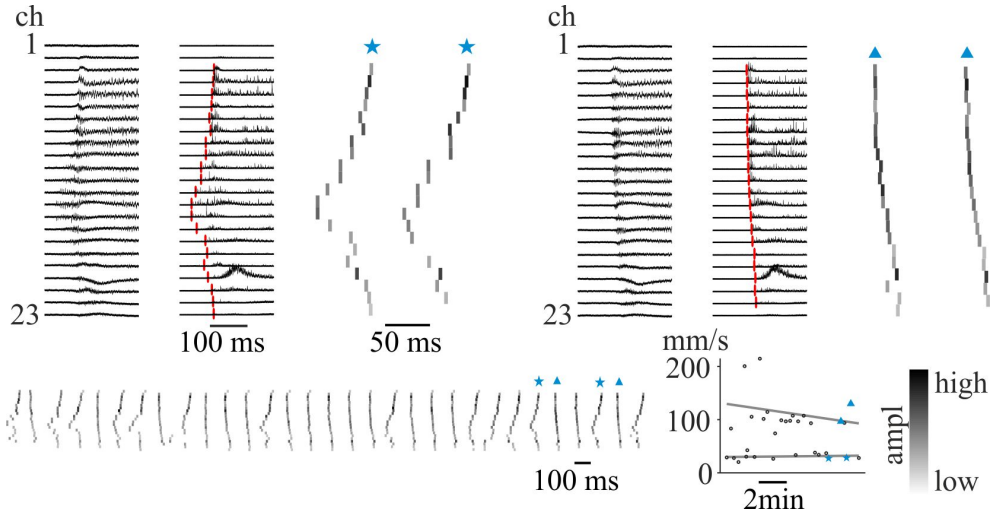

(d) Two types of propagation patterns on one recording.

Figure 4.8. The initiation and propagation of bIISs. A-D, from the left: original LFPg recording of bIISs is shown followed by a subfigure indicating the starting points of the events on each channel (red). Raster plots of the consecutive bIIS events are drawn on the bottom. Marked events (blue star and triangle) are magnified in the middle (D: middle and right). The colour intensity of grey represents the amplitude of the LFPg deflection. The propagation speed (in mm/s) of all events is plotted on the right top (A-C) or right bottom (D). In most of the cases, the propagation speed did not change significantly during the timecourse of the recording (A). Although event sequences with increasing (B) and decreasing (C) propagation speed were observed as well. On two recordings, two types of bIISs were detected with distinct propagation patterns simultaneously (D). Modified from Katharina T. Hofer.

DOI:10.15774/PPKE.ITK.2020.008

Our observation shows that simple bIISs can be initiated in any cortical layer in both patient groups: 12 ResEpi bIISs and 9 NoEpi bIISs started to develop in the supragranular layers, 4 ResEpi bIISs and 2 NoEpi bIISs were originated from the granular layer, and 6 ResEpi bIISs and 2 NoEpi bIISs were generated in the infragranular layers. The initiation site was stable across the whole recording with two exceptions. In one slice from the ResEpi group and one slice from the NoEpi group 2 events with different spreading pattern were alternating during the experiments. One complex event was generated in the granular layer and one in the infragranular layers, and they were not constant during the whole recording neither (*Figure 4.5*).

The initiation time point and the spreading direction and speed were calculated for 12 recurrent bIISs (9 from the ResEpi, one from the TreatEpi and two from the NoEpi groups) and for three recurrent seizures (all from the ResEpi group). The reason for the cutback is that only bIISs with more than six events and seizures with at least three events were used to avoid the large bias coming from the eventuality of single epileptiform events. In most of the cases, the channel of the starting point, as well as the activation sequence of the channels were changing over time, although the spreading direction usually remained constant.

The interlaminar propagation speed of bIISs was usually constant in time with a few exceptions, when it either increased (n = 3) or decreased (n = 1, *Figure 4.8*). When the propagation speed increased over time, it could reach up to a threefold increase. The average propagation speed of bIISs was varying between 19.7 mm/s and 98.7 mm/s, with a mean of 51.8 ± 23.7 mm/s in ResEpi and 74.3 ± 39.0 mm/s in NoEpi slices. We observed bIISs with low (<3 0 mm/s) and high (> 75 mm/s) propagation speed in both ResEpi and NoEpi slices. Interestingly, in the two slices, where two bIISs appeared with a different spreading pattern, one of the bIISs was slow, and the other one was fast in both cases. Seizures in ResEpi tissue propagated with a speed of 41.2 ± 12.6 mm/s. Neither the location nor the aetiology was related to the propagation speed.

4.1.3 High-frequency oscillations during population activities

HFOs have been observed during SPAs, sIIDs and bIISs in both ripple and fast-ripple frequency ranges with increased power. In case of seizures, continuous power-increase has been noted in all analysed frequencies, thus no detectable peaks were found. *Table 4.7* and *Figure 4.9* show a summary of the characteristic frequencies and powers of HFOs during the different kind of PAs. Demonstrative examples can be seen on *Figure 4.6*.

HFOs with increased power were detected within the ripple frequency range during 60/78 SPAs (77%), 5/9 sIIDs (56%), and 14/15 bIISs (93%) from the ResEpi group, while ripples were detected during 43/65 SPAs (66%) and 11/13 bIISs (85%) from the NoEpi group. No significant

DOI:10.15774/PPKE.ITK.2020.008

differences were found between the different patient groups or between population activities. The maxima of the peak drawn by the power-increase during the SPAs was 2.3 ± 1.5 dB in the ResEpi slices while 2.5 ± 1.2 dB in NoEpi slices (not significantly different). The average frequencies were 178.2 ± 39.3 Hz and 205.7 ± 40.8 Hz in ResEpi and NoEpi slices respectively (significantly different, $p < 0.01$, two-tailed Mann-Whitney U test). During sIIDs, the characteristic frequency of ripples was 149.8 ± 20.3 Hz with an average power of 4.7 ± 1.1 dB. The frequency of ripples during NoEpi SPAs were significantly different from those during sIIDs ($p < 0.05$, two-tailed Mann-Whitney U test). After the application of bicuculline, in the presence of bIISs, the power of ripples increased significantly in both groups ($p < 0.00001$, two-tailed Mann-Whitney U test). An average of 12.5 ± 5.0 dB and 16.1 ± 3.3 dB have been observed in ResEpi and Noepi slices, respectively. The average frequencies did not change considerably.

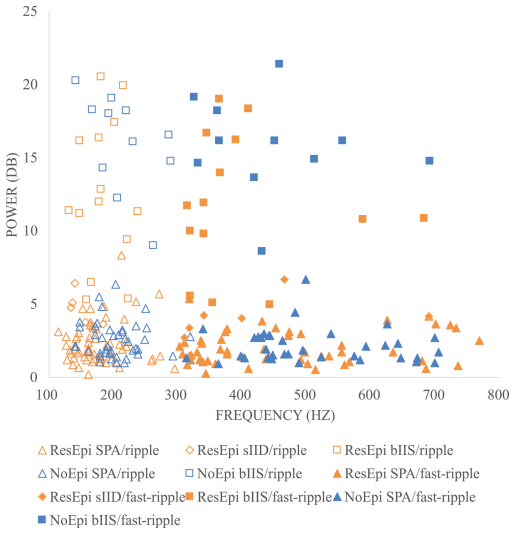

Figure 4.9. Summary of HFOs during the different kind of population activities.
Markers: orange: ResEpi, blue: NoEpi; triangle: SPA, rhombus: sIID, square: bIIS; empty: ripple, filled: fast-ripple.

Fast-ripples were detected during 53/78 SPAs (68%), 6/9 sIIDs (67%) and 14/15 bIIS (93%) in the ResEpi group and during 36/65 SPAs (55%) and 11/13 bIISs (85%) in the NoEpi group. No significant differences were found between the different patient groups, or between population activities. There were similarities in the variation of the power maxima before and after the application of bicuculline to the results observed with ripples. In the presence of SPAs, the average powers were 1.9 ± 1.1 dB (at 461.5 ± 138.0 Hz) and 2.1 ± 1.2 dB (at 507.9 ± 108.9 Hz) in ResEpi and NoEpi slices, respectively (not significantly different). During sIIDs, the power increased to an average of 4.2 ± 1.4 dB, while the average frequency was 419.5 ± 144.2 Hz (not significantly different). With the appearance of bIISs, the power of fast-ripples showed a 3-fold increase in the ResEpi group and a 4-fold increase in the NoEpi group (significantly different, $p < 0.00001$, two-tailed Mann-Whitney U test), without significant change in the average frequencies.

DOI:10.15774/PPKE.ITK.2020.008

Table 4.7. High-frequency oscillations during population activities. All data are provided in **median [1st and 3rd quartile]** and in mean ± standard deviation. HFOs in both ripple (130-250 Hz) and fast-ripple (300-700 Hz) frequency ranges have been investigated. Only oscillations superimposed on SPAs, sIIDs and bIISs were detected.

Patient group	Population activity	Number of PAs with increased ripple activity	Ripple frequency (Hz)	Ripple power (dB)	Number of PAs with increased fast-ripple activity	Fast-ripple frequency (Hz)	Fast-ripple power (dB)
ResEpi	SPA	60	**169.0 [150.7 195.3]** 178.2±39.3	**1.9 [1.3 2.8]** 2.3±1.5	53	**432.0 [338.0 552.7]** 461.5±138.0	**1.7 [1.2 2.6]** 1.9±1.1
	sIID	5	**139.6 [136.7 156.3]** 149.8±20.3	**4.8 [3.7 5.0]** 4.7±1.1	6	**368.7 [323.0 447.3]** 419.5±144.2	**4.1 [3.5 4.2]** 4.2±1.4
	bIIS	14	**178.3 [159.2 211.4]** 182.6±32.5	**11.7 [9.8 16.3]** 12.5±5.0	14	**358.4 [339.6 403.3]** 397.2±107.8	**11.3 [9.8 15.6]** 11.8±4.7
NoEpi	SPA	43	**200.0 [178.9 226.6]** 205.7±40.8	**2.1 [1.6 3.2]** 2.5±1.2	36	**475.6 [435.2 598.4]** 507.9±108.9	**1.8 [1.3 2.7]** 2.1±1.2
	bIIS	11	**187.8 [206.1 245.6]** 215.6±47.2	**16.5 [14.5 18.2]** 16.1±3.3	11	**429.7 [362.3 483.4]** 444.4±109.0	**16.1 [14.7 17.2]** 15.8±3.3
Significant differences			ResEpi sIID<NoEpi SPA ($p<0.05$) ResEpi sIID>ResEpi SPA($p<0.01$)	ResEpi SPA<ResEpi bIIS ($p<0.00001$) NoEpi SPA<NoEpi bIIS ($p<0.00001$)			ResEpi SPA<ResEpi bIIS ($p<0.00001$) NoEpi SPA<NoEpi bIIS ($p<0.00001$)

DOI:10.15774/PPKE.ITK.2020.008

4.2 Results related to the comparison of cell firing and population activities in the human neocortex

4.2.1 Firing characteristics of the detected cells

During control conditions, 193 cells have been separated in the ResEpi group (16 slices, 13 patients) by clustering method, while 182 cells were detected in the NoEpi group (14 slices, 11 patients). After the application of bicuculline, 191 cells from ResEpi slices (18 slices, 15 patients) and 167 cells from NoEpi slices (14 slices, 10 patients) were clustered (*Table 4.8*, *Figure 4.13*). An interesting result is that different neuron populations were active during different conditions. Usually, units detected on one channel of the recording in the physiological bath could not be seen on the same channel after using bicuculline and vice versa (*Figure 4.10*). While in physiological solution, cells tended to be more active in the supragranular and infragranular layers, in the slices with bicuculline, a closing up of the granular layer could be observed. In addition to that, the latter often showed a very characteristic, bursting-like firing pattern (*Figure 4.10*). Another observation was that in the presence of bicuculline cells prefered to fire during the population activities and often remained silent in between. In eight cases, this behaviour was so extreme that units could be detected only during sIID or seizure events.

In physiological conditions 76 principal cells (PCs), 38 interneurons (INs) and 79 unclassified cells (UCs) were detected in the ResEpi group, while 50 PCs, 39 INs and 93 UCs were found in the NoEpi groups, which shows an unambiguous dominance of principal cells in both patient groups (*Table 4.8*, *Figure 4.13*). This power relation considerably changed after the application of bicuculline: 28 PCs, 69 INs and 94 UCs were clustered in the ResEpi group, and 30 PCs, 56 INs and 81 UCs were clustered in the NoEpi group (*Table 4.8*, *Figure 4.13*). The differences between the control and the BIC groups were significant, in ResEpi and NoEpi, $p < 0.0001$ and $p < 0.05$, respectively, using a Chi-square test.

For a summary of the characteristic firing behaviour of the different neuron types detected, see *Table 4.8* and *Figure 4.13*. Some demonstrative example can also be seen on *Figure 4.10*. Briefly, the average firing frequency of cells was slightly higher in the ResEpi groups than the one in the NoEpi group, during both conditions. Usually, INs tended to fire more frequently than PCs in physiological conditions. None of these observations was significant.

DOI:10.15774/PPKE.ITK.2020.008

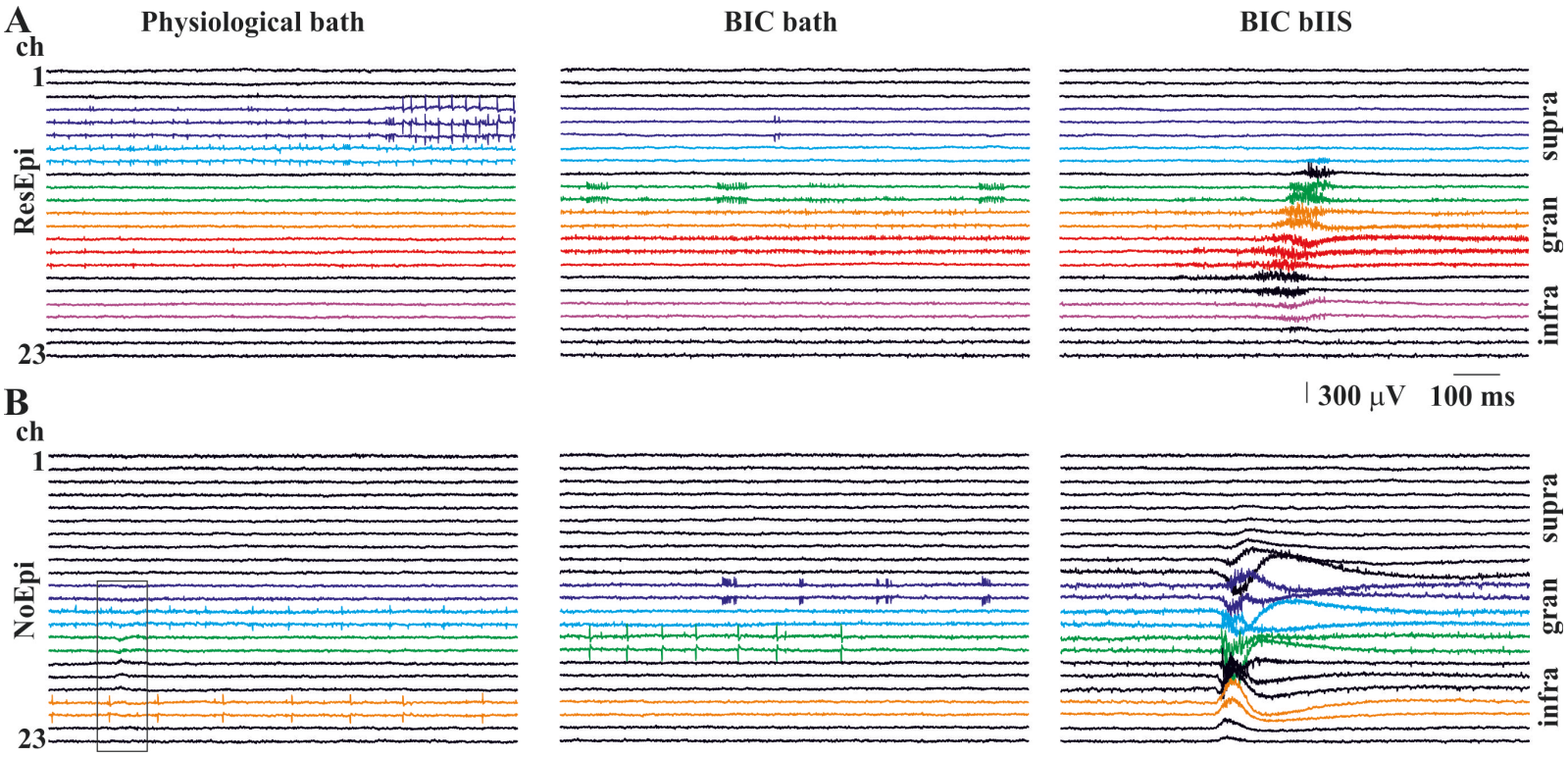

Figure 4.10. The behaviour of single units in physiological bath (left) and after the application of bicuculline, with (right) and without (middle) the presence of an sIID. Rectangles are indicating SPAs (note the difference in amplitude compared to sIIDs). Different colours of the channels are attempting to indicate the presence or absence of the same unit before and after the application of bicuculline bath. A: Cells on the purple and light blue channels are firing in control but remain silent in the presence of bicuculline, while the cell on the green channel does the opposite. B: Cells on the light blue and orange channels only fire during physiological bath, while cells on the purple and green channels being only active after using bicuculline. Note the characteristic bursting-like behaviour of the neuron on green (A) and purple (B) channels in bicuculline bath.

DOI:10.15774/PPKE.ITK.2020.008

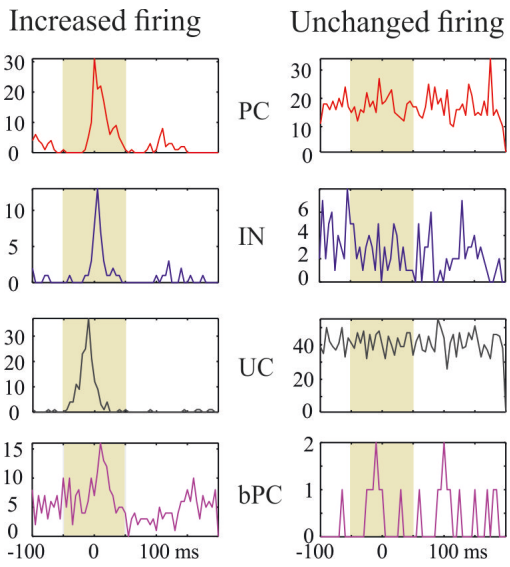

Figure 4.11. Examples for increased (left) and unchanged (right) firing of different cell types during PAs (PC: red, IN: blue, UC: black, bPC: purple). The ordinate indicates the number of APs, while the abscissa shows the time in ms. Timepoint zero is chosen to be at the peak of the PA; the coloured band is emphasising the width of the event.

Admittedly, investigating only the firing frequency can lead to controversial results considering such specific behaviour pattern. Hence, the interevent interval (IEI) and burstiness of cells were analysed as well, to have a more detailed picture of the nature of neurons. The burstiness of all neurons were higher, while the IEI was shorter in the BIC group than the ones in control. This was also the case with INs. All differences were significant ($p < 0.0001$), using a Chi-square test. PCs showed significantly higher burstiness ($p < 0.05$), in bicuculline bath, the IEI values were more confusing. Despite that, these results support our observations about the altered firing behaviour of cells.

Another interesting result was observed concerning the different cell types. During physiological conditions, PCs had significantly higher burstiness values than INs, with significantly shorter IEI, in both ResEpi (burstiness of PC > IN: $p < 0.05$, IEI of PC < IN: $p < 0.01$) and NoEpi (burstiness of PC > IN: $p < 0.001$, IEI of PC < IN: $p < 0.0001$) groups. After the application of bicuculline, the differences between the different cell types were blurred.

4.2.2 Cellular behaviour during SPAs

Different approaches were tested to investigate the involvement of different neuron population in network mechanisms.

An attempt was made to certify a preceding theory about the build-up period of single units at the initiation of synchronous events in rodent hippocampus [188]–[190]. In our case, with SPAs in the human neocortex, this kind of build-up discharge could be experienced only in 7/21 ResEpi and in 6/22 NoEpi tissue. Considering all detected SPA events of all recordings neuronal discharges preceding SPAs could be observed in $1.6 \pm 4.9\%$ of the events in ResEpi and only in $0.1 \pm 0.1\%$ of the events in NoEpi tissue.

The following approach was used to investigate which cells are increasing their firing rate

DOI:10.15774/PPKE.ITK.2020.008

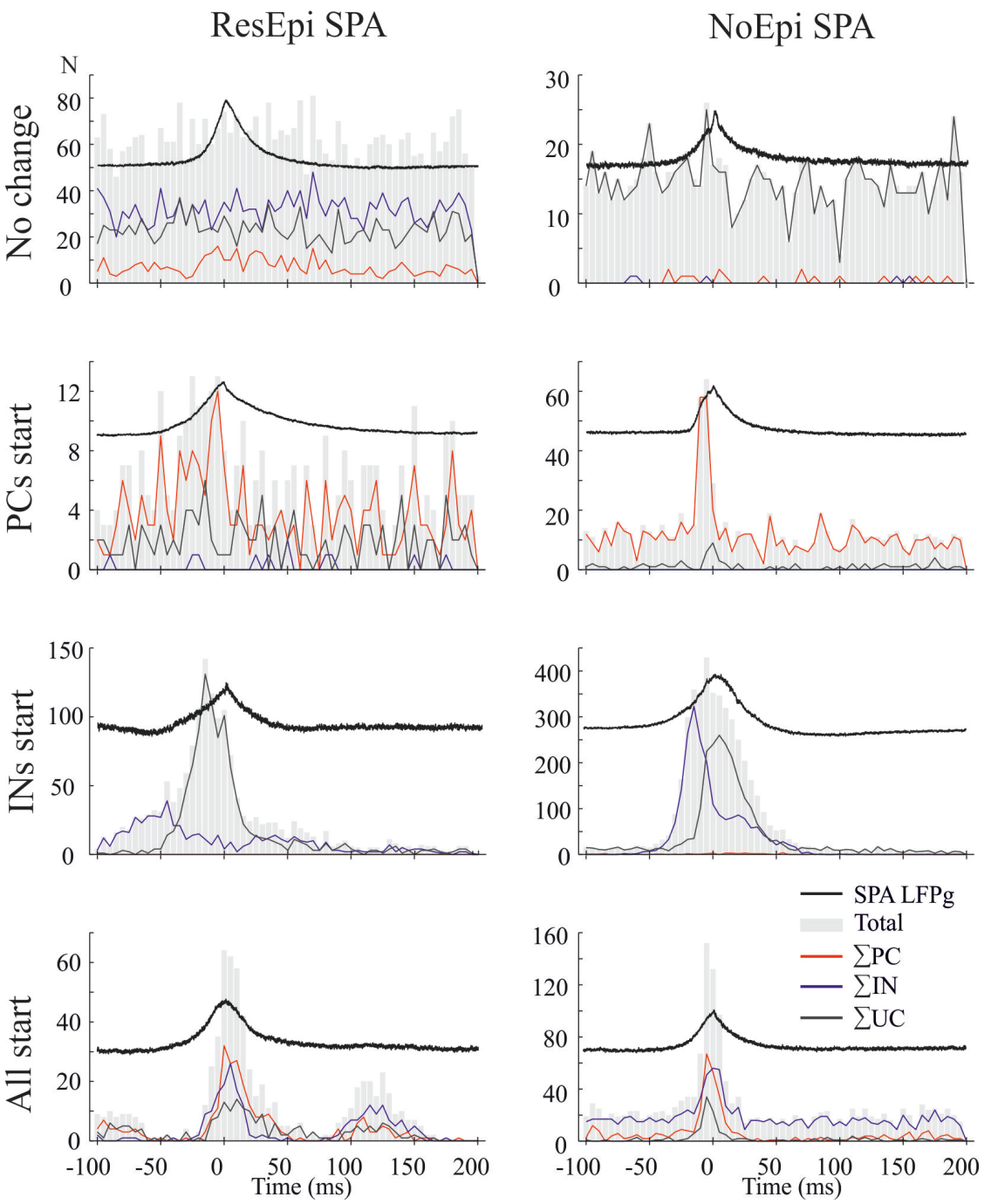

Figure 4.12. Firing behaviour of single units during SPAs in ResEpi (left) and NoEpi (right) slices. No change: none of the detected single cells contributes to the synchrony during the SPA. PCs start: PCs start to increase their firing first compared to other cell types during the SPA. INs start: INs start to increase their firing first before other cell types. All start: all the cell types start to fire at the same time during the SPA. The ordinate indicates the number of cell APs, while the abscissa shows the time in ms. Timepoint zero is chosen to be at the peak of the SPA. Red, blue and dark grey colours illustrate the different cell types; SPAs are drawn by black; light grey bars are showing the sum of APs of all cell types.

DOI:10.15774/PPKE.ITK.2020.008

Table 4.8. Firing characteristics of the detected cells. The firing frequency (Hz), interevent interval (ms) and burstiness (% of APs within burst) were calculated. All data are provided in a **median [1st and 3rd quartile]** and mean ± standard deviation.

		Number of clustered cells		Firing frequency (Hz)		Interevent interval median (ms)		Burstiness (% of APs within burst)	
		Control	BIC	Control	BIC	Control	BIC	Control	BIC
ResEpi	Total	193	191	**0.21 [0.07 0.70]** (1.01±2.78)	**0.17 [0.05 0.69]** (0.82±1.68)	**0.18 [0.05 0.84]** (3.86±16.18)	**0.03 [0.01 0.15]** (1.80±7.48)	**0.00 [0.00 0.07]** (0.06±0.12)	**0.15 [0.00 0.39]** (0.23±0.23)
	PC	76 (39.4%)	28 (14.7%)	**0.19 [0.06 0.67]** (1.11±2.85)	**0.19 [0.05 0.51]** (0.48±0.78)	**0.11 [0.04 0.58]** (4.91±21.46)	**0.02 [0.01 0.79]** (4.44±12.61)	**0.00 [0.00 0.17]** (0.08±0.14)	**0.14 [0.00 0.22]** (0.15±0.19)
	IN	38 (19.7%)	69 (36.1%)	**0.33 [0.07 1.27]** (0.91±1.23)	**0.22 [0.09 1.12]** (1.20±2.36)	**0.38 [0.17 1.23]** (4.83±15.62)	**0.02 [0.01 0.12]** (1.25±3.96)	**0.00 [0.00 0.00]** (0.03±0.07)	**0.15 [0.00 0.41]** (0.23±0.24)
	UC	79 (40.9%)	94 (49.2%)	**0.22 [0.08 0.58]** (0.96±3.23)	**0.13 [0.04 0.62]** (0.65±1.17)	**0.12 [0.04 0.97]** (2.40±9.03)	**0.03 [0.01 0.15]** (1.41±7.36)	**0.00 [0.00 0.07]** (0.05±0.11)	**0.18 [0.04 0.41]** (0.25±0.23)
NoEpi	Total	182	167	**0.20 [0.06 0.52]** (0.70±1.39)	**0.17 [0.05 0.65]** (0.64±1.38)	**0.23 [0.07 1.61]** (2.11±5.47)	**0.01 [0.01 0.06]** (1.82±10.91)	**0.00 [0.00 0.07]** (0.08±0.17)	**0.16 [0.01 0.41]** (0.25±0.26)
	PC	50 (27.5%)	30 (18.0%)	**0.12 [0.05 0.80]** (0.87±1.73)	**0.18 [0.04 0.87]** (0.77±1.59)	**0.09 [0.04 0.23]** (0.68±2.05)	**0.03 [0.01 0.18]** (2.78±8.31)	**0.05 [0.00 0.13]** (0.10±0.14)	**0.11 [0.00 0.28]** (0.15±0.17)
	IN	39 (21.4%)	56 (33.5%)	**0.22 [0.06 0.47]** (0.65±1.23)	**0.14 [0.05 0.34]** (0.58±1.07)	**1.43 [0.30 3.89]** (4.09±6.26)	**0.01 [0.00 0.04]** (0.41±1.54)	**0.00 [0.00 0.00]** (0.04±0.12)	**0.18 [0.01 0.54]** (0.30±0.31)
	UC	93 (51.1%)	81 (48.5%)	**0.21 [0.08 0.47]** (0.62±1.25)	**0.19 [0.05 0.68]** (0.63±1.50)	**0.26 [0.07 1.45]** (2.06±6.13)	**0.01 [0.01 0.04]** (2.43±14.78)	**0.00 [0.00 0.05]** (0.09±0.20)	**0.19 [0.03 0.34]** (0.24±0.24)
Significant differences between patient groups						ResEpi IN< NoEpi IN ($p<0.05$)	ResEpi Total>NoEpi Total ($p<0.001$) ResEpi IN>NoEpi IN ($p<0.0001$) ResEpi UC>NoEpi UC ($p<0.0001$)		

DOI:10.15774/PPKE.ITK.2020.008

Table 4.8 continued from previous page

	Number of clustered cells		Firing frequency (Hz)		Interevent interval median (ms)		Burstiness (% of APs within burst)	
	Control	BIC	Control	BIC	Control	BIC	Control	BIC
Significant differences between cell types					ResEpi PC<ResEpi IN (p<0.01) ResEpi PC<ResEpi UC (p<0.05) NoEpi PC<NoEpi UC<NoEpi IN (p<0.0001)	NoEpi PC>NoEpi IN (p<0.001) NoEpi PC>NoEpi UC (p<0.05)	ResEpi IN<ResEpi PC (p<0.05) NoEpi IN<NoEpi PC (p<0.001)	
Significant differences between control and BIC					ResEpi Total control>ResEpi Total BIC (p<0.0001) NoEpi Total control>NoEpi Total BIC (p<0.0001) ResEpi IN control>ResEpi IN BIC (p<0.0001) ResEpi UC control>ResEpi UC BIC (p<0.0001) NoEpi IN control>NoEpi IN BIC (p<0.0001) NoEpi UC control>NoEpi UC BIC (p<0.0001)		ResEpi Total control<ResEpi Total BIC (p<0.0001) NoEpi Total control<NoEpi Total BIC (p<0.0001) ResEpi PC control<ResEpi PC BIC (p<0.05) ResEpi IN control<ResEpi IN BIC (p<0.0001) ResEpi UC control<ResEpi UC BIC (p<0.0001) NoEpi IN control<NoEpi IN BIC (p<0.0001) NoEpi UC control<NoEpi UC BIC (p<0.0001)	

DOI:10.15774/PPKE.ITK.2020.008

during SPAs compared to the periods between the events (*Figure 4.11*). At least 150% of increment during the SPAs compared to the baseline (i.e. a normalised firing change of 0.66) was considered to be an increased firing. The normalised firing change of all neurons during SPAs was 0.55 ± 0.30 in ResEpi and 0.64 ± 0.31 in NoEpi tissue. Only 39% of neurons from the ResEpi group and 56% of neurons from the NoEpi group enhanced their firing in the presence of SPAs. There might be a slight difference between the two patient groups, it was not significant in none of the cases. No significant differences were found between ResEpi and NoEpi groups regarding the different cell types as well. Likewise, no significant difference occurred between INs, PCs or bursting PCs (bPCs). See *Table 4.9* for further details.

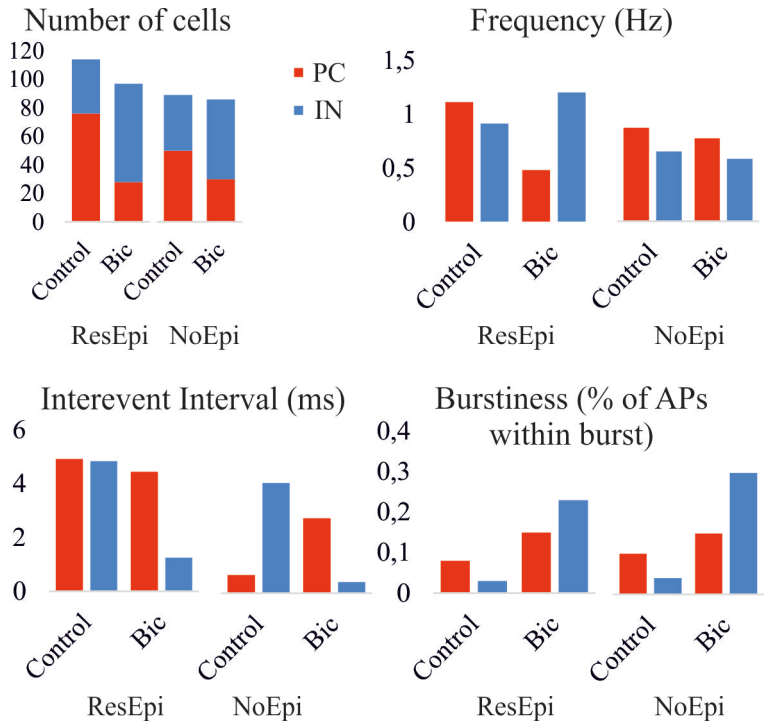

Figure 4.13. Summary of *Table 4.8*

After that, the involvement of excitatory and inhibitory cells in the initiation of SPAs has been investigated. A sum of all PCs, INs, bPCs, as well as the total number of neurons which fired during the SPA events was calculated for each recording (*Figure 4.12*). During 6/15 SPA from the ResEpi group and 5/14 SPA from the NoEpi tissue, no clear population firing enhancement was observed. In 2 cases from ResEpi slices and 3 cases from NoEpi slices, INs started to increase their firing first. PCs opened the sequence of firing in 4 and 3 cases in ResEpi and NoEpi slices, respectively. The remaining population activities were initiated by UCs, or all neuron types were activated at the same time.

Calculating the ratio of distinct neuron types compared to all neurons, which fired during SPAs, we experienced that 32.7 ± 36.7% of the detected APs originated from PCs, whereas 24.3

DOI:10.15774/PPKE.ITK.2020.008

± 30.8% came from INs in the ResEpi group. In the meantime, 31.7 ± 33.2% of the detected APs came from PCs and 15.4 ± 21.5% from INs during NoEpi SPAs. The involvement of bPCs to the overall firing was 3.9 ± 13.1% in ResEpi slices and 7.2 ± 14.7% in NoEpi slices (See also *Table 4.10*). No significant difference was found.

DOI:10.15774/PPKE.ITK.2020.008

Table 4.9. Normalised firing change of cells during PAs, which shows the firing frequency change of a cell during the population activity compared to the firing frequency during the baseline. In case of increased firing, the normalised firing change is at least 0.6 (i. e. 150% of the baseline firing).

	ResEpi			NoEpi		
	SPA	bIIS	Seizure	SPA	bIIS	Seizure
Total N of cells	136	138	72	124	129	38
N of cells with increased firing	53 (39%)	119 (86%)	71 (99%)	69 (56%)	123 (95%)	38 (100%)
Normalised firing change of all cells	**0.52 [0.43 0.71]** (0.55±0.30)	**1.0 [0.94 1.0]** (0.86±0.31)	**1.0 [1.0 1.0]** (0.97±0.12)	**0.64 [0.46 0.92]** (0.64±0.31)	**1.0 [1.0 1.0]** (0.95±0.17)	**1.0 [1.0 1.0]** (1.0±0.00)
N of PCs	44	19	21	34	28	2
N of PCs with increased firing	18 (41%)	17 (90%)	20 (95%)	17 (50%)	26 (93%)	2 (100%)
Normalised firing change of PCs	**0.52 [0.34 0.71]** (0.50±0.33)	**1.0 [0.91 1.0]** (0.89±0.25)	**1.0 [1.0 1.0]** (0.95±0.22)	**0.59 [0.44 0.78]** (0.60±0.30)	**1.0 [1.0 1.0]** (0.94±0.20)	**1.0 [1.0 1.0]** (1.0±0.00)
N of bursting PCs	3	4	0	5	3	0
N of bursting PC with increased firing	2 (67%)	3 (75%)	0	2 (40%)	3 (100%)	0
Normalised firing change of bursting PCs	**0.60 [0.57 0.62]** (0.59±0.03)	**1.0 [1.0 1.0]** (1.0±0.00)		**0.67 [0.40 0.73]** (0.55±0.36)	**1.0 [0.92 1.0]** (0.97±0.05)	
N of INs	35	49	21	28	33	23
N of INs with increased firing	11 (31%)	42 (86%)	21 (100%)	16 (57%)	33 (100%)	23 (100%)
Normalised firing change of INs	**0.50 [0.47 0.65]** (0.52±0.23)	**1.0 [0.97 1.0]** (0.88±0.27)	**1.0 [1.0 1.0]** (0.98±0.04)	**0.72 [0.37 0.94]** (0.62±0.34)	**1.0 [1.0 1.0]** (0.98±0.08)	**1.0 [1.0 1.0]** (1.0±0.00)
N of UCs	57	70	30	62	68	13
N of UCs with increased firing	24 (42%)	60 (86%)	30 (100%)	36 (58%)	64 (94%)	13 (100%)
N firing change of UCs	**0.56 [0.43 0.88]** (0.58±0.32)	**1.0 [0.94 1.0]** (0.83±0.35)	**1.0 [1.0 1.0]** (0.98±0.06)	**0.64 [0.50 0.93]** (0.66±0.30)	**1.0 [1.0 1.0]** (0.95±0.19)	**1.0 [1.0 1.0]** (1.0±0.00)
Significant differences between PA types	ResEpi SPA<ResEpi bIIS ($p<0.0001$) ResEpi SPA<ResEpi seizure ($p<0.0001$)			NoEpi SPA<NoEpi bIIS ($p<0.0001$) NoEpi SPA<NoEpi seizure ($p<0.0001$)		

DOI:10.15774/PPKE.ITK.2020.008

4.2.3 Cellular behaviour during BIPAs

Before bIISs, the appearance of the build-up period formed by single units occurred more often than before SPAs: in case of 7/17 ResEpi bIISs and 7/14 NoEpi bIISs. Neuronal discharges could be observed preceding 21.9 ± 40.6% and in 30.3 ± 41.2% of the population events in ResEpi and NoEpi slices, respectively. In contrast to that, no cell firing before the bicuculline induced seizures could be detected. Neuronal discharges initiated with the first LFPg component.

The normalised firing change during bIISs of all cells were 0.86 ± 0.31 in the ResEpi group and 0.95 ± 0.17 in the NoEpi group. Both values were significantly different compared to the ones calculated for SPAs, using Kruskal-Wallis ANOVA test ($p < 0.001$). 86% of ResEpi cells and 95% of NoEpi cells increased their firing in the presence if bIISs, which are also significantly different from the control (SPA) groups (chi-squared, $p < 0.001$). The differences were even higher, considering seizures. The normalised firing change was 0.97 ± 0.12 in ResEpi slices, while 99% of the cells increased their firing. In slices derived from NoEpi patients, the normalised firing change reached the value of 1.0 ± 0.0 and 100% of the cells increased their firing. Similarly to SPAs, there was no significant difference between neither patient groups, nor the distinct cell types (*Table 4.9*).

In contrast to earlier studies, the recent observations indicated the dominant role of inhibitory cells against bPCs in the initiation of epileptogenic discharges [184], [190]. INs started to enhance their firing before any other type of neurons during seven bIISs in the ResEpi group (*Figure 4.14*). PCs and UCs initiated the sequence of discharges during the remaining three and two bIISs, respectively. In the NoEpi group, INs started to fire first in 5 cases, PCs in 2 cases and UCs in 6 cases. The difference between patient groups was not significant (Fisher's exact test, $p > 0.6$). None of the detected bPCs began the discharging pattern superimposed on bIISs. In the presence of seizures, INs and UCs together started to fire first in 3 cases, PCs started in 2 cases, and UCs started in only one case in ResEpi slices. In the NoEpi group, INs initiated the discharging sequence during two seizures, while INs and UCs initiated together during one seizure. SPAs and BIPAs emerging on the same recording site were initiated by the same neuron type in 2/14 and 2/13 cases in the ResEpi and NoEpi groups, respectively. In every other slice, different cell types triggered SPAs than BIPAs.

DOI:10.15774/PPKE.ITK.2020.008

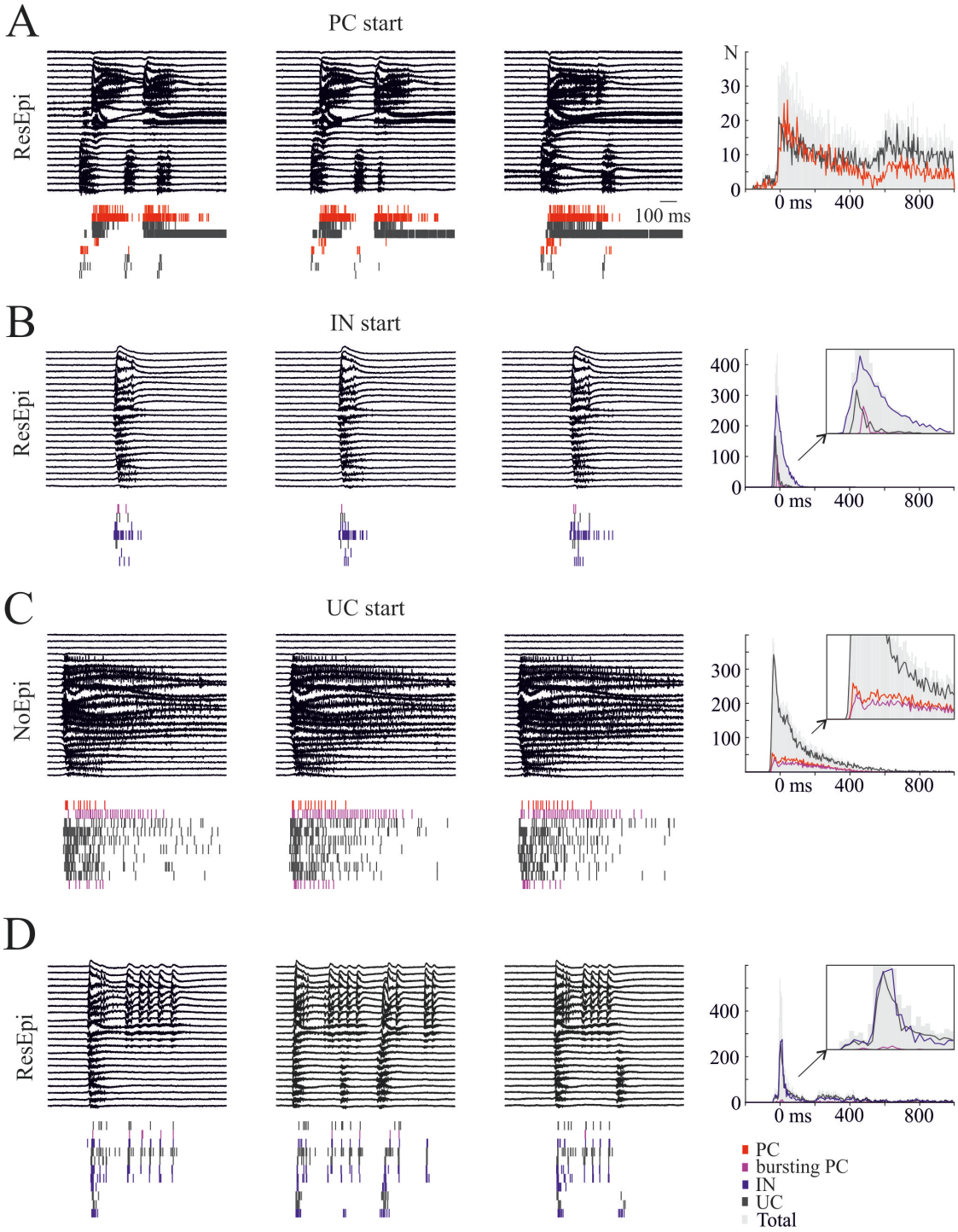

Figure 4.14. Firing increase of different cell types during BIPAs. Examples for different initiation patterns is shown: A: PCs start firing, and UCs follow; B: INs start firing, and other cell types follow; C: UCs start to fire while INs and PCs follow; D: UCs and INs start to fire together. Illustrations on the left show one event with the PETH of the underlying discharges. Graphs on the right contain the sum of all AP events in one recording, where the ordinate indicates the number of cell APs, while the abscissa shows the time in ms. Timepoint zero is chosen to be at the peak of the PAs. The different cell types are colour-coded: red = PC, purple = bPC, blue = IN, dark grey = UC. Grey bars show the summed APs of all cell types.

DOI:10.15774/PPKE.ITK.2020.008

Table 4.10. Contributions of the different kinds of neurons to PAs. The percentages of PC/IN/UC APs relative to the sum of all APs in the time window of the SPA events (-50 to +50 ms), or at the initial phase (-100 to +200 ms) of bIISs and seizures have been calculated. All data are provided in **median [1st and 3rd quartile]** and in mean ± standard deviation.

	ResEpi			NoEpi		
	SPA (n=15)	bIIS (n=15)	Seizure (n=6)	SPA (n=14)	bIIS (n=13)	Seizure (n=3)
Contribution of PC firing (%)	**13.9 [0.0 61.1]** (32.7±36.7)	**3.6 [0.0 14.4]** (16.5±29.0)	**4.4 [1.1 23.8]** (18.8±30.9)	**23.9 [1.1 50.7]** (31.7±33.2)	**12.6 [0.0 23.8]** (14.2±16.4)	**2.6 [0.0 8.3]** (3.6±4.3)
Contribution of bursting PC firing (%)	**0.0 [0.0 0.0]** (3.9±13.1)	**0.0 [0.0 1.0]** (1.7±3.7)		**0.0 [0.0 8.6]** (7.2±14.7)	**0.0 [0.0 0.0]** (1.4±3.9)	
Contribution of IN firing (%)	**16.8 [0.0 44.8]** (24.3±30.8)	**42.5 [9.1 69.2]** (43.4±34.3)	**32.8 [29.7 47.1]** (32.2±17.7)	**1.4 [0.0 25.7]** (15.4±21.5)	**40.7 [23.8 55.8]** (43.3±29.7)	**64.3 [31.1 84.2]** (59.9±26.8)
Contribution of UC firing (%)	**30.2 [6.0 76.6]** (43.0±37.8)	**43.1 [14.5 54.0]** (40.1±28.7)	**53.7 [29.1 68.3]** (49.0±20.4)	**55.4 [20.8 81.8]** (52.9±33.5)	**40.7 [35.7 56.8]** (42.6±28.2)	**33.0 [15.8 60.6]** (36.5±22.6)
Significant differences				NoEpi SPA IN<NoEpi IIS IN ($p<0.05$)		

DOI:10.15774/PPKE.ITK.2020.008

The contribution of different cell types to the epileptic population synchronies was the opposite compared to SPAs (*Table 4.10*). Only 16.5 ± 29.0% of the APs firing during ResEpi bIISs came from PCs, while 43.4 ± 34.3% of the APs were originated from INs. In case of NoEpi bIISs, PCs gave 12.2 ± 15.4%, and INs gave 46.4 ± 29.1% of the APs during the event. bPCs contributed to the total firing only in 1.7 ± 3.7% in ResEpi and 1.1 ± 3.6% in NoEpi bIIS.The difference might be obvious, significance only has been found between the INs of NoEpi SPAs and bIISs ($p < 0.05$). Similarly, PCs made the 18.8 ± 30.9% and 3.6 ± 4.3% of APs during ResEpi and NoEpi seizures, respectively. While 32.2 ± 17.7% of APs came from INs in the presence of ResEpi seizure and 59.9 ± 26.8% of the APs originated from INs during NoEpi seizures.

DOI:10.15774/PPKE.ITK.2020.008

5. Discussion

5.1 Spontaneous synchronies in the neocortical tissue

Two different types of synchronies were observed under physiological conditions in the human neocortical slices derived from epileptic patients. SPAs emerged in both epileptic and non-epileptic tissue, while sIIDs were only detected in epileptic slices. The recurrence frequency of sIIDs was a magnitude lower than those of the SPAs, but their duration was twice as much compared to SPAs. Moreover, there was a significant difference between the intensity in the recruitment of the neuron populations. Both LFPg and MUA amplitudes related to the peak of the sIID were more than three times larger than those of the SPA. In the meantime, the power of ripples and fast-ripples were two times higher in the case of sIIDs. Another noticeable dissimilarity is the location. While a considerable proportion of SPAs developed in the supragranular layers of the neocortex, sIIDs were restricted to the deeper structures.

The layer of the emergence, the occurrence rate and the network characteristics made the distinction of the two activities unambiguous. According to the data provided here, primarily the granular and infragranular layers of the neocortex generated sIIDs, exclusively in the slices derived from patients with epilepsy in their anamnesis. The prominent role of deeper cortical structures in the generation of paroxysmal depolarisation shift, and thus IISs were already demonstrated in animal models [1], [184] and in in vivo human studies [12]. The recurrence frequency of sIID is comparable to those observed on 4-aminopyridine induced epileptiform synchronies recorded from human neocortical slices [187] and on spiking activity obtained from the subiculum of patients with epilepsy [13]. While, the large LFPg transient, the enhanced firing and the initiative current sinks resemble the features of IISs observed on epileptic patients in vivo [12], [13] and the Mg^{2+}-free solution-induced hypersynchronous discharges recorded in vitro [191]. Furthermore, the HFOs with remarkably higher powers during sIIDs might indicate the presence of more excessive excitability. The conspicuous resemblance to in vivo IISs and pharmacologically induced epileptiform activities suggests the pathological nature of the sIID. This theory is supported by the fact that they were observed only on neocortical slices of patients

DOI:10.15774/PPKE.ITK.2020.008

with epilepsy.

The investigation of the epileptogenicity of network mechanisms maintaining spontaneous activity in vitro yet debated a question. Since in human studies, the data accessibility is very restricted, subjects are highly various regarding their age, condition, anamnesis and the obtained cortical region. Furthermore, healthy human samples are not available for obvious reasons. Thus, the use of animal tissue as control became widely used. However, the comparison of distinct species has its pitfalls as well. No spontaneous field potentials could be detected in vitro in healthy rodent [3], [14] or primate [15] neocortical slices. Though the observation of population activity arising in healthy rodents and primate hippocampal slices raised the possibility that synchronous bursts are not related to epilepsy [15], [17]. Moreover, populational spiking was evoked by activating a single PC in neocortical slices of tumour patients [16]. Pallud et al. (2014) detected interictal-like bursting activity in neocortical slices of tumour patients without the manifestation of preoperative seizures. Admitting, patients included in this study suffered from grade II-IV gliomas, which is known to be highly epileptogenic. Thus, whether SPAs occurring in the human neocortex have a pathogenic origin or not remains an open question.

The SPAs described here rather resembled population activities found in epileptic human neocortical [3], [5] and hippocampal [7], [8], [10] slices in vitro. Our data show that contrary to sIIDs, SPAs prefered to develop in the superficial layers of the neocortex, which is comparable to some earlier studies [3], [6]. Along with the remarkable difference in the recurrence frequency, all investigated network properties (the amplitude of LFPg and MUA, the CSD, the power of HFOs) showed significantly lower values in case of SPAs. This might suggest that a considerably lower amount of cells are participating in the synchronisation during the events. Last but not least, the $GABA_A$ receptor antagonist bicuculline is widely used to induce epileptogenic activity in humans and animals as well [2], [3], [14], [19], [90], [140], [162]–[166]. In contrary to that, the application of this convulsant results in the elimination of SPAs in all cases. This also suggests the essential role of GABAergic inhibition in the maintenance of the events. All in all, our data shows that SPAs can be detected in human neocortical slices derived from patients without any clinical or electrographic manifestations of seizures or epileptogenicity. In addition, the presence of sIIDs in the epileptic slices indicate the presence of epileptic hyperexcitability, as it presumably corresponds to an epileptiform synchronous event.

DOI:10.15774/PPKE.ITK.2020.008

5.2 The presence of hyperexcitability in the epileptic human neocortex

Spontaneous synchronous population activity has been observed on the LFPg recordings from postoperative neocortical slices derived from epileptic and non-epileptic patients [186]. The SPA emerged under physiological conditions, without any artificial induction [3]. It consists of rhythmically recurring extracellular LFP deflections superimposed by increased cellular firing and fast oscillations [3], [7]. The CSD profile of the events implies the recruitment of local forces.

It is an everlasting issue to explore the role of the excessive excitation in the epileptic neocortex in the generation of populational discharges. The investigation of spontaneously occurring SPAs revealed that the hyperexcitability is not only manifested at the cellular [14] but also at the network level. SPAs found in slices derived from epileptic and non-epileptic patients share the same main features. Still, the few aspects which differed in the two groups could point to that enhanced tension. SPAs emerged in a higher proportion of slices, with higher LFPg amplitude and significantly more multiple SPA developed in the epileptic compared to non-epileptic tissue. Moreover, the sIID, which indicates a more prominent level of synchronisation, appeared only in the epileptic samples.

High-frequency oscillations have been observed in both epileptic and healthy human neocortex [192]. Though, it has been suggested that the distribution of different subclasses of HFOs could highlight epileptic brain areas [159]. Fast oscillations reflect a short-term synchronisation of neuron populations [46]. An alteration in the organisation could contribute to the excitability of cortical networks. Increased ripple and fast ripple activity might facilitate the identification of the epileptogenic zone [193], [194]. A similar tendency could be noticed in this study. A higher proportion of SPAs were linked with HFOs in epileptic than in non-epileptic tissue. Furthermore, the power of both ripples and fast ripples were twice as large during sIIDs as in the presence of SPAs. These data also suggest the hypersynchronous nature of epileptic mechanisms.

The results reported here suggest, that the development of populational discharges might be related to the enhanced excitation and synchrony in the pathological human neocortex. Epileptic tissue shows a higher tendency to generate SPA compared to non-epileptic brain tissue which can be linked to a higher grade of excitability. A well-known phenomenon in epilepsy, the synaptic reorganisation and axonal sprouting can lead to a more complex organisation of cortical networks[61], [195]. Which might facilitate the appearance of more SPAs (larger amount of slices generating SPA, there are more multiple SPAs). The emergence of sIIDs shows an even higher level of excitation, regarding the significantly larger values of LFPg, MUA and HFO

DOI:10.15774/PPKE.ITK.2020.008

power.

5.3 Synchrony-generating hubs in the epileptic neocortex

After the application of the $GABA_A$ receptor antagonist, bicuculline-induced interictal-like or seizure-like activities emerged in all patient groups. The length, the field potential amplitude, and the cell-firing increase were comparable in the ResEpi and NoEpi slices. However, the epilepsy-related tissue tended to develop BIPAs more often, and with higher recurrence frequency. Furthermore, the epileptic slices showed much more variability in the recruitment of different cortical networks. In the non-epileptic group, only simple bIISs occurred, which spread through all the cortical layers. In contrast to that, ResEpi and TreatEpi slices generated distinct combinations of temporally and spatially simple and complex bIISs. That is, epileptic tissue was able to promote multiple spikes recurring together, which could be sustained by neuron populations of various locations. In addition, spatially more restricted bIISs were detected in ResEpi slices, i.e. supragranular and infragranular bIISs were observed beside the entire ones. These events could reappear jointly, rhythmically activating different cortical layers as temporally and spatially complex events (See *Figure 4.4*). These results show that epileptic neural circuits are more susceptible to initiate hypersynchronous events than non-epileptic networks. On top of that, in the ResEpi group, smaller neuron populations were able to maintain sIIDs, compared to NoEpi slices. The formation of highly connected hub cells was already hypothesised in the epileptic hippocampus [196], [197]. The structural reorganisation is the result of certain cell loss and axonal sprouting [61], [62], [195]–[197]. As a consequence, spatially more restricted and intensely excitable networks arise [196], [197]. As in the hippocampus, these 'pathologically interconnected neuron clusters' [198] might be the initiators of the crescent hypersynchronous events in the neocortex as well.

5.4 Altered cell-firing during bicuculline bath

The first obtrusive observation was that those neurons, which were firing in physiological ACSF, usually disappeared after the application of bicuculline. In the meantime, other cells became active, which were silent earlier. This finding was true not only on a single cell but on the network level. That is, while supragranular and infragranular neurons fired more prominently in control, the granular layer tended to close up in the activation after the application of bicuculline. Moreover, cells of the middle layers had a peculiar, bursting-like firing pattern. These data further confirm the observation according to which distinct neuron populations are involved in

DOI:10.15774/PPKE.ITK.2020.008

physiological and pathological mechanisms [197].

In physiological ACSF considerably higher proportion of PCs were detected than INs. This ratio turned after the application of bicuculline, i.e. significantly more INs became active compared to PCs. A possible explanation might lie in the various synaptic input of the distinct cell types. PCs of the CA1 in the rodent hippocampus was shown to have a relatively low proportion of inhibitory synapses (around 3%) [199]. While INs investigated so far received a higher ratio of inhibitory terminals: 29.4% of the inputs on calbindin-positive INs, 20.7% of the synapses terminating on calretinin-positive INs and 35.85% on cholecystokinin-containing INs were symmetric [200], [201]. Only the parvalbumin-containing INs had a ratio of synaptic inputs comparable to PCs (6.4% is GABAergic) [200]. When cells are released from their fast GABAergic hyperpolarizing input, what is happening after the application of bicuculline, they will be liberated from their usual inhibition. As INs receive a considerably higher proportion of symmetric synapses, the effect of this freedom might have a more excessive outcome, which leads to a large amount of spontaneously firing inhibitory cells. Admitting that the material provided here is derived from the rodent hippocampus, it might correlate with the behaviour of human neocortical PCs and INs.

It cannot be excluded, that the application of bicuculline, the excessive firing and bursting discharges distort the shape of APs. This might lead to the misinterpretation of the active neuron populations of the neocortex. Bicuculline is thought to reduce the afterhyperpolarisation phase, but it very likely does not affect the depolarisation and repolarisation phases [172]. During the analysis of the neurons reported here the length of the AP at the half-max amplitude was used to separate the different cell types, in contrast to the peak-to-through durations, which would be deformed by the drug. Thus, it is very likely that the identification of the neurons is not confused by the effects of the bicuculline.

5.5 What does happen to the synchrony when the GABAergic inhibition is eliminated?

The contribution of inhibitory and excitatory processes was investigated in the development of the putative physiological and pathological activities. A considerably higher level of synchrony was observed during bicuculline-induced bIISs and seizures compared to SPAs. Only half of the neurons enhanced their firing accompanying SPAs with a normalised firing increase of around 0.6. While 90% of the cells raised their firing in the presence of bIISs with an average normalised firing increase of 0.9. The highest level of synchrony was observed during seizures, which

DOI:10.15774/PPKE.ITK.2020.008

literally recruited all the cells with a normalised firing increase of 1.0.

It has been a longstanding question of debate whether interneurons or principal busters are responsible for the initiation of epileptiform discharges. Both excitatory bursting PCs [184] and inhibitory INs [6] were found to trigger IISs in neocortical slices. While heterogeneous firing pattern was observed during spiking in the neocortex and hippocampus of epileptic patients [202]. In a like manner, the onset of seizure activity was associated with both excitatory [9] and inhibitory [22] processes, according to the morphology of the hypersynchronous event. Our data show that different neuron populations are activated accompanying physiological or pathological synchronies. A considerably higher proportion of PCs contributed to the overall firing than INs during SPAs, and also they initiated more populational discharge. During BIPAs this ratio reversed: a noticeably higher percentage of INs accompanied the event, furthermore they tended to initiate the hypersynchronous discharges more frequently.

To clarify the mechanism contributing to the generation of seizures yet need further investigation. The relatively low number of samples does not allow to draw far-reaching conclusions. In addition, there are methodological boundaries which can complicate the study of these hypersynchronous epileptiform events. The highly complex electrical activity of the brain could alter the extracellular properties of APs [179]. This might confuse the outcome of cell clustering and thus makes the identification unreliable. Though, this complication was mostly valid in case of multielectrode arrays with large interelectrode distances. In this case, the array literally registers multiple single electrode recordings. Tetrodes with higher electrode density made the identification of single-cell firing more accurate. The electrode-configuration used in this study has a significantly smaller contact distance, which allows a relatively good separation of different neuron types. Though, it has to be noted that the identification of cells during seizure discharges remain less accurate despite the advanced recording tools. On the other hand, seizure activity very likely has a similar impact on the clustering of both PCs and INs. Which might imply that our assumption about the contribution of distinct cell types to the seizure initiation is supported by the results.

Overall, the data reported here suggest that the emergence of SPAs is based on the balance of excitatory and inhibitory networks. This is in accordance with earlier in vivo studies, which propose that the dynamic balance of excitation and inhibition in the neocortex is crucial for the maintenance of physiological conditions [20]. When bicuculline artificially disturbed this balance, it resulted in a hypersynchronous epileptiform activity, which recruited the vast majority of neuron populations. While PCs seem to have a leading role in the maintenance of SPAs, pathological synchronies seems to be driven by inhibitory neurons. But how could this be possible,

DOI:10.15774/PPKE.ITK.2020.008

when the GABAergic transmission is cut out?

5.6 The role of non-synaptic mechanisms in the maintenance of synchronisation

So the balance of inhibitory and excitatory networks are crucial in the maintenance of the convenient function of the cortex. Any change in the weight of inhibition and excitation leads to compensatory effects destined to sustain the excitability of the system [94], [131]. A good example is the formation of new excitatory circuits as a consequence of selective interneuron loss in the epileptic hilus [203]. There exist several non-synaptic mechanisms which contribute to the establishment of cortical activity on the network level: gap junctions, ephaptic effects and changes in the extracellular ion concentrations [204], as well as neuropeptides [111].

The data presented here show that BIPAs are often introduced by an intense IN discharge. Which raises the question, how the extensive synchronisation is possible when the synaptic transmission via postsynaptic $GABA_A$ receptors is arrested. The consequence has to be taken into account that non-synaptic cellular interactions might have an essential role in the formation of disinhibition-induced hypersynchronous discharges of the human neocortex. The proportion of gap junctions between GABAergic neurons are relatively high, and they connect mainly INs of the same type [32]. It was already shown that neural networks linked by electrical coupling regulate bicuculline-induced epileptiform activity in the guinea pig brain preparation [151]. Fast spiking parvalbumin-positive INs seem to have high affinity to form gap junctions in the rat neocortex [109], which cell type is considered to be the source of rhythmic population synchrony [205].

It was hypothesised that ephaptic transmission might have a role in the synchronisation of epileptic hippocampal circuits [206]. The lower density of neurons in the neocortex might not be suitable for the establishment of electrical field coupling. An increase of extracellular potassium level was observed during ictal [207] and interictal [151] epileptic discharges. The higher level of extracellular K^+ was shown to enhance membrane depolarisation and intrinsic burst firing [1]. Because of these effects, it was widely used to induce epileptiform activity in vitro. In the case of disinhibition-induced hypersynchronous events, it is rather the paroxysmal bursts which increase the extracellular K^+ concentrations. Since it was shown to elevate after the onset of epileptiform discharges [208]. Last but not least, neuropeptides released by INs might contribute to the altered activity of the cell population in the presence of bicuculline. Though, some neuropeptides such as neuropeptide Y, cholecystokinin or somatostatin is thought to reduce

DOI:10.15774/PPKE.ITK.2020.008

the release of neurotransmitters on the presynaptic terminals [111]. Neuropeptide Y was actually found to have an anticonvulsive effect, as it decreases the level of glutamate and GABA release [114].

After all, the results presented here suggest that electrical coupling via gap junctions might contribute to the synchronisation of neuron populations in the human neocortex after the blockade of $GABA_A$ receptors. The role of other non-synaptic mechanisms has not been approved. Although to confirm the recent findings, further investigation might be necessary.

5.7 Human disease vs animal models

The epileptiform events induced by bicuculline were hypersynchronous discharges accompanied by intense IN firing at the initial phase. This was in contradiction with the experience of the same bicuculline model in rodents. Earlier studies proposed that excessive synchronisation is the consequence of the loss in inhibitory control and cells were recruited into population activities via the recurrent excitatory pathways [209]. Bursting principal neurons were shown to trigger bicuculline-induced interictal-like in rodent neocortical [184] and hippocampal [189], [190] slices. In contrast to that, none of the intrinsically bursting PCs initiated the paroxysmal events in the disinhibited human neocortex. Quite the opposite, they rather followed the other neuron types. The information provided by previous studies is scarce regarding the mechanisms contributing to the generation of IISs in the epileptic human neocortex. It was shown that around half of the detected neurons are accompanying the spikes in both the neocortex [202], [210] and the hippocampus [211] with heterogeneous firing pattern [202]. Although the different cell types have not been separated, thus the contribution of excitatory and inhibitory networks to the populational events remained unclarified.

Bicuculline induced seizure-like activity detected here consisted of continuously bursting interictal-like spikes, lasting 15-28 s. It resembles seizures observed in vivo, which either being comprised of periodic spikes [21] or spike and wave complexes [212]. Seizures in animal models which were initiated by hypersynchronous spikes were also related to excitatory networks [213], [214]. Likewise, it was the case with preictal discharges in human brain preparations [9]. In contrast to that in our experiment, bicuculline-induced seizures (just as bIISs) were introduced by increased firing of INs. The underlying mechanism was seen at low voltage fast activity seizure in rodents [215] and patients with epilepsy [22], [216].

Inconsistencies found in the recent experiments, as well as in previous studies, might be a consequence of differences between the neural circuits of distinct species. The variability of research conditions and methods could affect the results in a different manner. The use of distinct

DOI:10.15774/PPKE.ITK.2020.008

cortical regions can influence the results as well. Differences between the species can be the explanation how could it be possible, that while bursting PCs are responsible for the initiation of bicuculline-induced interictal discharges in the guinea pig [184], INs were observed to trigger bIISs in human neocortical slices. Population discharges experienced in vitro on slice preparations will never be identical to in vivo mechanisms. Likewise, the manipulation of cortical circuits by pharmacons will not induce synchronies equal to spontaneously occurring epileptiform events. Hypersynchronous activities evoked by the elimination of GABAergic transmission differ from epileptic seizures, which are the results of the corruption in the dynamic balance of excitatory and inhibitory networks [216]. Finally, dissimilarities between the mechanisms underlying the distinct synchronies might be explained by the use of different cortical areas. In the three-layered hippocampal formation, excitatory networks were found to have a special role in the generation of hypersynchronous spikes [9] and seizures [213]. While BIPAs with similar morphology were related to increased IN firing in the six-layered neocortex. The data presented here suggest that epileptiform activity induced by reduction of GABAergic inhibition has substantial differences compared to the human disease. Moreover, the same disinhibition model has a distinct effect and recruit different circuits on human and rodent brain preparations.

DOI:10.15774/PPKE.ITK.2020.008

6. Summary

6.1 Conclusions

This research aimed to investigate the physiological and pathological nature of the distinct synchronies raising in postoperative human neocortical slices derived from epileptic and non-epileptic patients in vitro.

It has long been a matter of debate whether healthy human neocortical slices are able to generate physiological population activity. Since human brain slices are not available for obvious ethical reasons, researches reached for animal tissue as control. However, comparing different species definitely has its pitfalls. The results presented in this study propose that the spontaneous synchronous population activity is based on the dynamic balance of excitatory and inhibitory mechanisms. This balance is distracted in the epileptic tissue. Cortical structures were shown to suffer specific inhibitory cell-loss and the reorganisation of excitatory circuits. Changing the weight of excitatory and inhibitory networks leads to compensatory effects which were destined to maintain the excitability of the system. Advanced spontaneous population activities and interictal discharges might be the evidence for this enhanced tension in the epileptic human neocortex.

The effect of the reduced GABAergic transmission was investigated on the physiological network properties. The disinhibition of the neocortical circuits leads to a disturbance in the balance of excitation and inhibition. As a result, physiological population activities vanished, and in the meantime, hypersynchronous epileptiform events showed up. Bicuculline-induced interictal-like activities were uniform in the non-epileptic tissue: they were exclusively simple events invading all the cortical layers. In contrast to that, slices derived from epileptic patients generated heterogeneous events. These paroxysmal discharges either spread to the entire neocortex or restricted to smaller regions with a high temporal and spatial variability. The results propose that epileptic neocortical slices contain smaller neuron populations which are able to develop an epileptiform activity.

The data provided here propose that different neuron populations contribute to physiological

DOI:10.15774/PPKE.ITK.2020.008

and pathological events. While principal cells had a leading role in the initiation and formation of spontaneous population bursts, epileptiform discharges were dominated by interneurons. The extraordinary commitment of inhibitory cells in the disinhibition model proposes that other, non-synaptic mechanisms are also involved in the synchrony generation. Electrical coupling between specific interneurons might be a promising assumption, but further investigation is necessary for confirmation. The results presented here regarding hypersynchronous epileptiform discharges differ from those obtained in epileptic patients or animal models in earlier studies. This suggests that distinct neuron populations are involved in the disinhibited human neocortex compared to human epilepsies or animal models of epilepsy. Therefore, the limits of extrapolation should be considered from animals to human as well as from model to the disease before drawing far-reaching conclusions in the case of pharmacologically induced epileptiform activity.

6.2 Thesis statements

6.2.1 Thesis groups 1: The emergence of population synchronies in the human neocortex

Thesis Ia: I have revealed that postoperative human neocortical slices are able to generate distinct types of synchronous activities, in vitro.

I have observed four different types of synchronous events with different morphologies in the human neocortex, in vitro. Spontaneous synchronous population activities (SPAs) emerged in physiological solution regardless of the patient groups. In the meantime, spontaneous interictal-like discharges (sIIDs) developed in physiological solution as well, but only in slices derived from epileptic patients. In bicuculline bath, spontaneous activities disappeared, while bicuculline-induced interictal-like events (bIISs) or seizures arose. I have observed these synchronies in both epileptic and non-epileptic patient groups.

Thesis Ib: I have established that postoperative human neocortical tissue derived from epileptic patients manifest a higher level of excitability.

More epileptic slices generate synchronous population activities compared to non-epileptic tissue. Epileptic slices develop multiple synchronies more often, and these synchronies have a higher field potential amplitude. Hypersynschronous discharges resembling in vivo interictal spikes emerge only in tissue derived from patients with epilepsy in their anamnesis. The blockade of $GABA_A$ receptors results in a higher level of synchrony with more complex events in

DOI:10.15774/PPKE.ITK.2020.008

epileptic slices compared to non-epileptic slices. All these data propose the enhanced excitability of neural circuits in neocortical tissue derived from patients with epilepsy.

Thesis Ic: I have confirmed that smaller neuron populations (hubs) are able to generate hypersynchronous events in the epileptic neocortex.

In the disinhibition model, slices of epileptic patients developed spacially and temporally complex interictal-like events, unlike non-epileptic slices. Epileptic tissue was able to generate spacially more restricted bIISs as well. Only events spreading through all the layers of the neocortex emerged in the non-epileptic tissue. This suggests that smaller cellular networks (hubs) are able to maintain hypersynchronous discharges in the epileptic neocortex.

6.2.2 Thesis groups 2: Synchronisation on the cellular and network level in the disinhibition model

Thesis IIa: I have found that different neuron populations are activated in physiological conditions compared to the disinhibition model.

Those neurons, which are firing in the presence of physiological solution, usually remain silent after the application of bicuculline and vice versa. In the physiological solution, the prominent role of the supragranular layers is observable. During the condition of disinhibition, the close up of the granular layer is apparent. In the physiological solution, principal cells are significantly more active compared to interneurons. In the presence of bicuculline, INs take over the leadership.

Thesis IIb: I have proven that SPAs and BIPAs are maintained by different cellular networks.

Only one-half of the active cells are accompanying the SPA. In contrast to that, 90 % and almost 100 % of the detected cells are associated with the bIISs and seizures. SPAs are usually initiated by PCs, while BIPAs are initiated majorly by INs. Similarly, more PCs contribute to the development of SPAs, while more INs participate in the emergence of the BIPAs. Thus, it could be claimed that different neuron populations are involved in different synchronies.

Thesis IIc: I have uncovered that neocortical circuits are able to maintain synchronised discharges when the GABAergic transmission is reduced.

The disinhibition model shows a high level of synchrony, usually through an excess excitation. Our data showed the prominent role of INs in the initiation of BIPA. As the GABAergic trans-

DOI:10.15774/PPKE.ITK.2020.008

mission is eliminated, and INs have a leading role in the synchronisation, other mechanisms have to be responsible for the collective activation of neuron populations. Probably non-synaptic processes, such as gap-junctions become conspicuous with the blockade of GABAergic inhibition.

Thesis IId: I have shown that the population activities of the non-epileptic neocortex, the epileptic neocortex and those induced by disinhibition reflect different levels of synschronies.

The field potential amplitude, the level of multi-unit activity and the power of HFOs show a gradual growth from the SPAs towards the BIPAs. sIIDs recruit more neurons than SPAs, and BIPAs form an even higher level of synchrony. Furthermore, different neurons and different layers are activated during pathological and spontaneous populational discharges. After the application of the $GABA_A$ receptor antagonist bicuculline, the spontaneous activity disappears, while bicuculline-induced epileptiform events start to develop. All these results show that various neuron populations are responsible for distinct events. They all represent a different level of synchronisation in the following order: SPA < sIID < BIPA.

DOI:10.15774/PPKE.ITK.2020.008

Acknowledgements

First and foremost, I would like to express my deep gratitude to *Wittner Lucia* who was my tutor during the undergraduate and PhD years. She devoted so much time, attention and patience to teach me scientific research with unbroken enthusiasm and encouragement.

I am very grateful to *Ulbert István* for his support during my studies and for giving me the opportunity to work in his research group.

Many thanks to my former and current colleagues *Katharina Hofer, Kinga Tóth* and *Estilla Tóth* for their help, and contribution to the research, thanks to which this dissertation came into being. I would also like to thank the surgeons and clinicians, *Loránd Erőss, Dániel Fabó, László Entz, Attila Bagó* and *Gábor Nagy* without whom this project would not be possible.

I am very thankful to the Doctoral School, especially to *Prof. Péter Szolgay* for the opportunity to participate in the doctoral program and *Tivadarné Vida* for her kind help.

Last but certainly not least, I will be grateful forever to my family and friends, who stood by me and supported me in all possible ways.

Funding

This research has been partially supported by the European Union, co-financed by the European Social Fund (EFOP-3.6.3-VEKOP-16-2017-00002); by the Hungarian Brain Research Program, KTIA_13_NAP-A-IV/1-4,6, KTIA 13 NAP-A-I/1 and 2017-1.2.1-NKP-2017-00002 (to István Ulbert) and KTIA_NAP_13-1-2013-0001, KTIA-NAP17-3-2017-0001 (to Dániel Fabó); by the Hungarian National Research Fund OTKA K119443 (to Lucia Wittner) and PD121123 (to Kinga Tóth); by the HAS Postdoctoral grant (to Kinga Tóth);

DOI:10.15774/PPKE.ITK.2020.008

Publications

List of journal publications underlying the thesis

1. Kandracs A, Hofer KT, Toth K, Toth EZ, Entz L, Bago AG, Eross L, Jordan Z, Nagy G, Fabo D, Ulbert I, Wittner L. Presence of synchrony-generating hubs in the human epileptic neocortex. (2019) JOURNAL OF PHYSIOLOGY 597(23):5639-5670 doi: 10.1113/JP278499

2. Toth K, Hofer KT, Kandracs A, Entz L, Bago A, Eross L, Jordan Z, Nagy G, Solyom A, Fabo D, Ulbert I, Wittner L. Hyperexcitability of the network contributes to synchronization processes in the human epileptic neocortex. (2018) JOURNAL OF PHYSIOLOGY 596(2):317-342 doi: 10.1113/JP275413

List of journal publications not related to the subject of the thesis

1. Marton G, Toth EZ, Wittner L, Fiath R, Pinke D, Orban G, Meszena D, Pal I, Gyori EL, Bereczki Z, Kandracs A, Hofer KT, Pongracz A, Ulbert I, Toth K. The neural tissue around SU-8 implants: A quantitative in vivo biocompatibility study. (2020) MATERIALS SCIENCE & ENGINEERING C 110870 doi: 10.1016/j.msec.2020.110870

2. Hofer KT, Kandracs A, Ulbert I, Pal I, Szabo C, Heja L, Wittner L. The hippocampal CA3 region can generate two distinct types of sharp wave-ripple complexes, in vitro. (2014) HIPPOCAMPUS 25(2):169-186 doi: 10.1002/hipo.22361

DOI:10.15774/PPKE.ITK.2020.008

References

[1] M. de Curtis and G. Avanzini, "Interictal spikes in focal epileptogenesis", *Progress in Neurobiology*, vol. 63, pp. 541–567, 2001.

[2] D. A. McCormick, "Gaba as an inhibitory neurotransmitter in human cerebral cortex", *Journal of Neurophysiology*, vol. 62, pp. 1018–1027, 5 1989.

[3] R. Kohling, A. Lucke, H. Straub, E.-J. Speckmann, I. Tuxhorn, P. Wolf, H. Pannek, and F. Oppel, "Spontaneous sharp waves in human neocortical slices excised from epileptic patients", *Brain*, vol. 121, pp. 1073–1087, 1998.

[4] A. Gorji, J.-M. Hohling, M. Madeja, H. Straub, R. Kohling, I. Tuxhorn, A. Ebner, P. Wolf, H. Panneck, F. Behne, R. Lahl, and E.-J. Speckmann, "Effect of levetiracetam on epileptiform discharges in human neocortical slices", *Epilepsia*, vol. 43, pp. 1480–1487, 12 2002.

[5] A. K. Roopun, J. D. Simonotto, M. L. Pierce, A. Jenkins, C. Nicholson, I. S. Schofield, R. G. Whittakera, M. Kaiser, M. A. Whittington, R. D. Traube, and M. O. Cunninghama, "A nonsynaptic mechanism underlying interictal discharges in human epileptic neocortex", *Proceedings of the National Academy of Sciences of the United States of America*, vol. 107, pp. 338–343, 1 2010.

[6] J. Pallud, M. L. V. Quyen, F. Bielle, C. Pellegrino, P. Varlet, M. Labussiere, N. Cresto, M.-J. Dieme, M. Baulac, C. Duyckaerts, N. Kourdougli, G. Chazal, B. Devaux, C. Rivera, R. Miles, L. Capelle, and G. Huberfeld, "Cortical gabaergic excitation contributes to epileptic activities around human glioma", *Science Translational Medicine*, vol. 6, 244ra89, 244 2014.

[7] I. Cohen, V. Navarro, S. Clemenceau, M. Baulac, and R. Miles, "On the origin of interictal activity in human temporal lobe epilepsy in vitro", *Science*, vol. 298, pp. 1418–1421, 5597 2002.

[8] C. Wozny, A. Knopp, T.-N. Lehmann, U. Heinemann, and J. Behr, “The subiculum: A potential site of ictogenesis in human temporal lobe epilepsy”, *Epilepsia*, vol. 46, pp. 17–21, 5 2008.

[9] G. Huberfeld, L. M. de la Prida, J. Pallud, I. Cohen, M. L. V. Quyen, C. Adam, S. Clemenceau, M. Baulac, and R. Miles, “Glutamatergic pre-ictal discharges emerge at the transition to seizure in human epilepsy”, *Nature Neuroscience*, vol. 14, pp. 627–634, 2011.

[10] L. Wittner, G. Huberfeld, S. Clemenceau, L. Eross, E. Dezamis, L. Entz, I. Ulbert, M. Baulac, T. F. Freund, Z. Magloczky, and R. Miles, “The epileptic human hippocampal cornu ammonis 2 region generates spontaneous interictal-like activity in vitro”, *Brain*, vol. 132, pp. 3032–3046, 2009.

[11] G. Huberfeld, L. Wittner, S. Clemenceau, M. Baulac, K. Kaila, R. Miles, and C. Rivera, “Perturbed chloride homeostasis and gabaergic signaling in human temporal lobe epilepsy”, *The Journal of Neuroscience*, vol. 27, pp. 9866–9873, 37 2007.

[12] I. Ulbert, G. Heit, J. Madsen, G. Karmos, and E. Halgren, “Laminar analysis of human neocortical interictal spike generation and propagation: Current source density and multiunit analysis in vivo”, *Epilepsia*, vol. 45, no. 4, pp. 48–56, 2004.

[13] D. Fabo, Z. Magloczky, L. Wittner, A. Pek, L. Eross, S. Czirjak, J. Vajda, A. Solyom, G. Rasonyi, A. Szucs, A. Kelemen, V. Juhos, L. Grand, B. Dombovari, P. Halasz, T. F. Freund, E. Halgren, G. Karmos, and I. Ulbert, “Properties of in vivo interictal spike generation in the human subiculum”, *Brain*, vol. 131, pp. 485–499, 2008.

[14] M. Avoli, J. Louvel, R. Pumain, and R. Kohling, “Cellular and molecular mechanisms of epilepsy in the human brain”, *Progress in Neurobiology*, vol. 77, pp. 166–200, 2005.

[15] P. A. Schwartzkroin and M. M. Haglund, “Spontaneous rhythmic synchronous activity in epileptic human and normal monkey temporal lobe”, *Epilepsia*, vol. 27, pp. 523–533, 1986.

[16] G. Molnar, S. Olah, G. Komlosi, M. Fule, J. Szabadics, C. Varga, P. Barzo, and G. Tamas, “Complex events initiated by individual spikes in the human cerebral cortex”, *PLoS BIOLOGY*, vol. 6, 9 2008. DOI: 10.1371/journal.pbio.0060222.

[17] G. Buzsaki, “Hippocampal sharp wave-ripple: A cognitive biomarker for episodic memory and planning”, *Hippocampus*, vol. 25, pp. 1073–1188, 2015.

[18] D. Mattia, A. Olivier, and M. Avoli, “Seizure-like discharges recorded in human dysplastic neocortex maintained in vitro”, *Neurology*, vol. 45, pp. 1391–1395, 7 1995.

[19] G. G. Hwa, M. Avoli, A. Oliver, and J.-G. Villemure, “Bicuculline-induced epileptogenesis in the human neocortex maintained in vitro”, *Experimental Brain Research*, vol. 83, pp. 329–339, 1991.

[20] N. Dehghani, A. Peyrache, B. Telenczuk, M. L. V. Quyen, E. Halgren, S. S. Cash, N. G. Hatsopoulos, and A. Destexhe, “Dynamic balance of excitation and inhibition in human and monkey neocortex”, *Scientific Reports volume*, vol. 6, p. 23 176, 2016.

[21] P. Perucca, F. Dubeau, and J. Gotman, “Intracranial electroencephalographic seizure-onset patterns: Effect of underlying pathology”, *Brain*, vol. 137, pp. 183–196, 2014.

[22] B. Elahian, N. E. Lado, E. Mankin, S. Vangala, A. Misra, K. Moxon, I. Fried, A. Sharan, M. Yeasin, R. Staba, A. Bragin, M. Avoli, M. R. Sperling, J. E. Jr, and S. A. Weiss, “Low-voltage fast seizures in humans begin with increased interneuron firing”, *Annals of Neurology*, vol. 84, pp. 588–600, 4 2018.

[23] G. J. Tortora and B. Derrickson, *Principles of anatomy and physiology*, 15th edition. Hoboken, New Jersey: Wiley, 2017.

[24] R. B. Wells, “Cortical neurons and circuits: A tutorial introduction”, 2005.

[25] J. Szentagothai and M. Rethelyi, *Funkcionalis anatomia III.* Medicina Konyvkiado Zrt., 2006.

[26] R. S. Swenson. (2006). “Review of clinical and functional neuroscience”, [Online]. Available: `https://www.dartmouth.edu/~rswenson/NeuroSci/index.html`.

[27] X. Jiang, G. Wang, A. J. Lee1, R. L. Stornetta1, and J. J. Zhu, “The organization of two new cortical interneuronal circuits”, *Nature Neuroscience*, vol. 16, pp. 210–218, 2013.

[28] M. F. Bear, B. W. Connors, and M. A. Paradiso, *Neuroscience: exploring the brain*, 4th edition. Lippincott Williams Wilkins, 2015.

[29] M. A. Arbib, Ed., *The Handbook of Brain Theory and Neural Networks*, 2nd edition. The MIT Press, 2003.

[30] G. M. Shepherd, Ed., *The synaptic organization of the brain*, 5th edition. Oxford University Press, 2003.

[31] T. F. Freund and G. Buzsaki, “Interneurons of the hippocampus”, *Hippocampus*, vol. 6, pp. 347–470, 4 1998.

[32] R. Tremblay, S. Lee, and B. Rudy, “GABAergic interneurons in the neocortex: From cellular properties to circuits”, *Neuron*, vol. 91, pp. 260–292, 2 2016.

[33] M. A. Arbib, P. Erdi, and J. Szentagothai, *Neural organization*. The MIT Press, 1998.

[34] P. Somogyi, “The study of golgi stained cells and of experimental degeneration under the electron microscope: A direct method for the identification in the visual cortex of three successive links in a neuron chain”, *Neuroscience*, vol. 3, pp. 167–180, 2 1978.

[35] J. C. Eccles, *The Physiology Of Synapses*. Springer, 1964.

[36] C. Pesold, W. S. Liu, A. Guidotti, E. Costa, and H. J. Caruncho, “Cortical bitufted, horizontal, and Martinotti cells preferentially express and secrete reelin into perineuronal nets, nonsynaptically modulating gene expression”, *Proceedings of the National Academy of Sciences of the United States of America*, vol. 96, pp. 3217–3222, 6 1999.

[37] L. Overstreet-Wadiche1 and C. J. McBain, “Neurogliaform cells in cortical circuits”, *Nature Reviews Neuroscience*, vol. 16, pp. 458–468, 2015.

[38] J. E. Jr. and T. A. Pedley, *Epilepsy, A comprehensive textbook*, 2nd edition. Wolters Kluwer Lippincott Williams Wilkins, 2007.

[39] WHO, I. L. A. Epilepsy, and I. B. for Epilepsy, *Atlas: epilepsy care in the world*. WHO, 2005.

[40] W. Feindel, R. Leblanc, and A. N. de Almeida, “Epilepsy surgery: Historical highlights 1909-2009”, *Epilepsia*, vol. 50, pp. 131–151, 2009.

[41] R. S. Fisher, W. van Emde Boas, W. Blume, C. Elger, P. Genton, P. Lee, and J. E. Jr., “Epileptic seizures and epilepsy: Definitions proposed by the International League Against Epilepsy (ILAE) and the International Bureau for Epilepsy (IBE)”, *Epilepsia*, vol. 46, pp. 470–472, 2005.

[42] R. S. Fisher, C. Acevedo, A. Arzimanoglou, A. Bogacz, J. H. Cross, C. E. Elger, J. E. Jr, L. Forsgren, J. A. French, M. Glynn, D. C. Hesdorffer, B. Lee, G. W. Mathern, S. L. Moshe, E. Perucca, I. E. Scheffer, T. Tomson, M. Watanabe, and S. Wiebe, “ILAE Official report: A practical clinical definition of epilepsy”, *Epilepsia*, vol. 50, pp. 475–482, 2014.

[43] R. S. Fisher, J. H. Cross, J. A. French, N. Higurashi, E. Hirsch, F. E. Jansen, L. Lagae, S. L. Moshe, J. Peltola, E. R. Perez, I. E. Scheffer, and S. M. Zuberi, “Operational classification of seizure types by the International League Against Epilepsy: Position paper of the ILAE commission for classification and terminology”, *Epilepsia*, vol. 58, pp. 522–530, 4 2017.

[44] E. Kiriakopoulos and P. O. Shafer. (2017). “Types of seizures”, [Online]. Available: `https://www.epilepsy.com/learn/types-seizures` (visited on 09/04/2019).

[45] I. E. Scheffer, S. Berkovic, G. Capovilla, M. B. Connolly, J. French, L. Guilhoto, E. Hirsch, S. Jain, G. W. Mathern, S. L. Moshe, D. R. Nordli, E. Perucca, T. Tomson, S. Wiebe, Y. Zhang, and S. M. Zuberi, "ILAE classification of the epilepsies: Position paper of the ILAE commission for classification and terminology", *Epilepsia*, vol. 58, pp. 512–521, 4 2017.

[46] P. A. Schwartzkroin, Ed., *Encyclopedia of Basic Epilepsy Research*, 1st Edition. Academic Press, 2009.

[47] Z. Yasiry and S. D. Shorvon, "How phenobarbital revolutionized epilepsy therapy: The story of phenobarbital therapy in epilepsy in the last 100 years", *Epilepsia*, vol. 53, pp. 26–39, 2012.

[48] M. P. Jacobs, G. G. Leblanca, A. Brooks-Kayal, F. E. Jensen, D. H. Lowenstein, J. L. Noebels, D. D. Spencer, and J. W. Swann, "Curing epilepsy: Progress and future directions", *Epilepsy and Behavior*, vol. 14, pp. 438–445, 3 2009.

[49] E. H. Reynolds, "Spatiotemporal dynamics of neocortical excitation and inhibition during human sleep", *The ILAE/IBE/WHO Epilepsy Global Campaign History*, vol. 43, pp. 9–11, 2012.

[50] D. J. Thurman, E. Beghi, C. E. Begley, A. T. Berg, J. R. Buchhalter, D. Ding, D. C. Hesdorffer, W. A. Hauser, L. Kazis, R. Kobau, B. Kroner, D. Labiner, K. Liow, G. Logroscino, M. T. Medina, C. R. Newton, K. Parko, A. Paschal, P. Preux, J. W. Sander, A. Selassie, W. Theodore, T. Tomson, and S. Wiebe, "Standards for epidemiologic studies and surveillance of epilepsy", *Epilepsia*, vol. 52, pp. 2–26, 2011.

[51] D. Hirtz, D. J. Thurman, K. A. Gwinn-Hardy, M. Mohamed, A. R. Chaudhuri, and R. Zalutsky, "How common are the 'common' neurologic disorders?", *Neurology*, vol. 68, pp. 326–337, 5 2007.

[52] A. Gaitatzis and J. W. Sander, "The mortality of epilepsy revisited", *Epileptic Disorders*, vol. 6, pp. 3–13, 2004.

[53] E. Olafsson, P. Ludvigsson, G. Gudmundsson, D. Hesdorffer, O. Kjartansson, and W. A. Hauser, "Incidence of unprovoked seizures and epilepsy in iceland and assessment of the epilepsy syndrome classification: A prospective study", *The Lancet Neurology*, vol. 4, pp. 627–634, 10 2005.

[54] M. F. Shamji, E. C. Fric-Shamji, and B. G. Benoit, "Brain tumors and epilepsy: Pathophysiology of peritumoral changes", *Neurosurgical Review*, vol. 32, pp. 275–285, 3 2009.

[55] M. S. M. van Breemen, E. B. Wilms, and C. J. Vecht, “Epilepsy in patients with brain tumours: Epidemiology, mechanisms, and management”, *The Lancet Neurology*, vol. 6, pp. 421–430, 5 2007.

[56] E. K. Avila and J. Graber, “Seizures and epilepsy in cancer patients”, *Current Neurology and Neuroscience Reports*, vol. 10, pp. 60–67, 1 2010.

[57] E. Aronica, B. Yankaya, G. H. Jansen, S. Leenstra, C. W. M. van Veelen, J. A. Gorter, and D. Troost, “Ionotropic and metabotropic glutamate receptor protein expression in glioneuronal tumours from patients with intractable epilepsy”, *Neuropathology and Applied Neurobiology*, vol. 27, pp. 223–237, 3 2001.

[58] D. E. Bateman, J. Hardy, J. R. McDermott, D. S. Parker, and J. A. Edwardson, “Amino acid neurotransmitter levels in gliomas and their relationship to the incidence of epilepsy”, *Neurological Research*, vol. 10, pp. 112–114, 2 1988.

[59] N. V. Klinger, A. K. Shah, and S. Mittal, “Management of brain tumor-related epilepsy”, *Neurology India*, vol. 65, pp. 60–70, 7 2017.

[60] K. Sendrowski and W. Sobaniec, “Hippocampus, hippocampal sclerosis and epilepsy”, *Pharmacological Reports*, vol. 65, pp. 555–565, 3 2013.

[61] M. Thom, “Review: Hippocampal sclerosis in epilepsy: A neuropathology review”, *Neuropathology and Applied Neurobiology*, vol. 40, pp. 520–543, 5 2014.

[62] P. Halasz, Ed., *Hippocampus mint neuropszichiatriai betegsegek kozos nevezoje*. Melinda, 2005.

[63] S. D. Shorvon, D. R. Fish, F. Andermann, G. M. Bydder, and H. Stefan, Eds., *Magnetic Resonance Scanning and Epilepsy*. Springer US, 1994.

[64] J. Janszky, “Az epilepszia diagnozisa”, *Ideggyogyaszati Szemle*, vol. 57, pp. 5–6, 1994.

[65] S. D. Shorvon, “Mri of cortical dysgenesis”, *Epilepsia*, vol. 30, pp. 13–18, s10 1997.

[66] T. Kral1, H. Clusmann, I. Blumcke, R. Fimmers, B. Ostertun, M. Kurthen, and J. Schramm, “Outcome of epilepsy surgery in focal cortical dysplasia”, *Journal of Neurology, Neurosurgery and Psychiatry*, vol. 74, pp. 183–188, 2 2003.

[67] D. C. Taylor, M. A. Falconer, C. J. Bruton, and J. A. N. Corsellis, “Focal dysplasia of the cerebral cortex in epilepsy”, *Journal of Neurology, Neurosurgery and Psychiatry*, vol. 34, pp. 369–387, 4 1971.

DOI:10.15774/PPKE.ITK.2020.008

[68] I. Blumcke, M. Thom, E. Aronica, D. D. Armstrong, H. V. Vinters, A. Palmini, T. S. Jacques, G. Avanzini, A. J. Barkovich, G. Battaglia, A. Becker, C. Cepeda, F. Cendes, N. Colombo, P. Crino, J. H. Cross, O. Delalande, F. Dubeau, J. Duncan, R. Guerrini, P. Kahane, G. Mathern, I. Najm, C. Ozkara, C. Raybaud, A. Represa, S. N. Roper, N. Salamon, A. Schulze-Bonhage, L. Tassi, A. Vezzani, and R. Spreafico, "The clinicopathologic spectrum of focal cortical dysplasias: A consensus classification proposed by an ad hoc Task Force of the ILAE Diagnostic Methods Commission", *Epilepsia*, vol. 52, pp. 158–174, 1 2010.

[69] J. Kabat and P. Krol, "Focal cortical dysplasia - review", *Polish Journal of Radiology*, vol. 77, pp. 35–43, 2 2012.

[70] I. Awad and P. Jabbour, "Cerebral cavernous malformations and epilepsy", *Neurosurgical Focus*, vol. 21, pp. 1–9, 1 2006.

[71] A. Williamson, P. R. Patrylo, S. Lee, and D. D. Spencer, "Physiology of human cortical neurons adjacent to cavernous malformations and tumors", *Epilepsia*, vol. 44, pp. 1413–1419, 11 2003.

[72] J. F. Kerrigan, Y.-t. Ng, S. Chung, and H. L. Rekate, "The hypothalamic hamartoma: A model of subcortical epileptogenesis and encephalopathy", *Seminars in Pediatric Neurology*, vol. 12, pp. 119–131, 2 2005.

[73] E. Labos, "Az elektrofiziologia fejlodesenek allomasai", *Fizikai Szemle*, vol. 6, p. 195, 1996.

[74] G. Czeh and Z. Puskar, *Cellularis neurobiologia.* Nordex Nonprofit Kft, 2001.

[75] J. M. Bower and D. Beeman, Eds., *The book of GENESIS: Exploring Realistic Neural Models with the GEneral Neural SImulation System*, Internet Edition. 2003. [Online]. Available: `http://www.genesis-sim.org/GENESIS`.

[76] F. Bezanilla, "The action potential: From voltage-gated conductances to molecular structures", *Biological Research*, vol. 39, pp. 425–435, 3 2006.

[77] L. R. Squire, D. Berg, F. E. Bloom, S. D. Lac, A. Ghosh, and N. C. Spitzer, Eds., *Fundamental Neuroscience*, 4th edition. Elsevier, 2012.

[78] A. L. Hodgkin and A. F. Huxley, "A quantitative description of membrane current and its application to conduction and excitation in nerve", *The Journal of Physiology*, vol. 117, pp. 500–544, 4 1952.

[79] G. J. Siegel, R. W. Albers, S. T. Brady, and D. L. Price, Eds., *Basic Neurochemistry*, 7th edition. Elsevier Academic Press, 2006.

[80] K. Gyires and Z. Furst, Eds., *A farmakologia alapjai*. Medicina Konyvkiado Zrt, 2011.

[81] N. G. Bowery, B. Bettler, W. Froestl, J. P. Gallagher, F. Marshall, M. Raiteri, T. I. Bonner, and S. J. Enna, "International union of pharmacology. xxxiii. mammalian gamma-aminobutyric acidb receptors: Structure and function", *Pharmacological Reviews*, vol. 54, pp. 247–264, 2 2002.

[82] T. J. Jentsch, V. Stein, F. Weinreich, and A. A. Zdebik, "Molecular structure and physiological function of chloride channels", *Physiological Reviews*, vol. 82, pp. 503–568, 2002.

[83] G. M. Shepherd, Ed., *Neurobiology*, 3th edition. Oxford University Press, 1994.

[84] J. R. Cooper, F. E. Bloom, and R. H. Roth, Eds., *The biochemical basis of neuropharmacology*, 8th Edition. 2003.

[85] E. B. Bromfield, J. E. Cavazos, and J. I. Sirven, Eds. (2006). "An introduction to epilepsy", [Online]. Available: `https://www.ncbi.nlm.nih.gov/books/NBK2510/`.

[86] N. Nayeem, T. P. Green, I. L. Martin, and E. A. Barnard, "Quaternary structure of the native gabaa receptor determined by electron microscopic image analysis", *Journal of Neurochemistry*, vol. 62, pp. 815–818, 1994.

[87] R. R. Matsumoto, "Gaba receptors: Are cellular differences reflected in function?", *Brain Research Reviews*, vol. 14, pp. 203–225, 1989.

[88] R. E. Study and J. L. Barker, "Diazepam and (–)-pentobarbital: Fluctuation analysis reveals different mechanisms for potentiation of gamma-aminobutyric acid responses in cultured central neurons", *Proceedings of the National Academy of Sciences of the United States of America*, vol. 78, pp. 7180–7184, 11 1981.

[89] M. Inoue, Y. Oomura, T. Yakushiji, and N. Akaike, "Intracellular calcium ions decrease the affinity of the gaba receptor", *Nature*, vol. 324, pp. 156–158, 1986.

[90] Y. Ben-Ari, J.-L. Gaiarsa, R. Tyzio, and R. Khazipov, "Gaba: A pioneer transmitter that excites immature neurons and generates primitive oscillations", *Physiological Reviews*, vol. 87, pp. 1215–1284, 4 2007.

[91] A. T. Gulledge and G. J. Stuart, "Excitatory actions of gaba in the cortex", *Neuron*, vol. 37, pp. 299–309, 2003.

[92] J. Szabadics, C. Varga, G. Molnar, S. Olah, P. Barzo, and G. Tamas, "Excitatory effect of gabaergic axo-axonic cells in cortical microcircuits", *Science*, vol. 311, pp. 233–235, 5758 2006.

[93] A. Woodruff, Q. Xu, S. A. Anderson, and R. Yuste, "Depolarizing effect of neocortical chandelier neurons", *Frontiers in Neural Circuits*, vol. 3, 2009. DOI: 10.3389/neuro.04.015.2009.

[94] J. S. Isaacson and M. Scanziani, "How inhibition shapes cortical activity", *Neuron*, vol. 72, pp. 231–243, 2 2011.

[95] C. Luscher, L. Y. Jan, M. Stoffel, R. C. Malenka, and R. A. Nicoll, "G protein-coupled inwardly rectifying k+ channels (girks) mediate postsynaptic but not presynaptic transmitter actions in hippocampal neurons", *Neuron*, vol. 19, pp. 687–695, 1997.

[96] E. Perez-Garci, M. Gassmann, B. Bettler, and M. E. Larkum, "The gabab1b isoform mediates long-lasting inhibition of dendritic ca2+ spikes in layer 5 somatosensory pyramidal neurons", *Neuron*, vol. 50, pp. 603–616, 2006.

[97] D. Zhang, Z.-H. Pan, M. Awobuluyi, and S. A. Lipton, "Structure and function of gabac receptors: A comparison of native versus recombinant receptors", *TRENDS in Pharmacological Sciences*, vol. 22, pp. 121–132, 3 2001.

[98] L. R. Squire, Ed., *Encyclopedia of neuroscience*. Elsevier, 2009.

[99] (). "The handbook of receptor classification and signal transduction", [Online]. Available: https://www.sigmaaldrich.com/technical-documents/articles/biology/rbi-handbook.html.

[100] D. M. Treiman, "Gabaergic mechanisms in epilepsy", *Epilepsia*, vol. 42, pp. 8–12, 2001.

[101] R. W. Olsen and M. Avoli, "Gaba and epileptogenesis", *Epilepsia*, vol. 38, pp. 399–407, 4 1997.

[102] J. W. McDonald, E. A. Garofalo, T. Hood, J. C. Sackellares, S. Gilman, P. E. McKeever, J. C. Troncoso, and M. V. Johnston, "Altered excitatory and inhrbitory ammo acid receptor binding in hippocampus of patients with temporal lobe epilepsy", *Annals of Neurology*, vol. 29, pp. 529–541, 1991.

[103] G. Huberfeld, T. Blauwblomme, and R. Miles, "Hippocampus and epilepsy: Findings from human tissues", *Revue Neurologique*, vol. 171, pp. 236–251, 3 2015.

[104] D. C. Spray and R. Dermeitzel, Eds., *Gap junctions in the nervous system*. Singer, 1996.

[105] M. Beierlein, J. R. Gibson, and B. W. Connors, "A network of electrically coupled interneurons drives synchronized inhibition in neocortex", *Nature Neuroscience*, vol. 3, pp. 904–910, 9 2000.

DOI:10.15774/PPKE.ITK.2020.008

[106] C. E. Landisman, M. A. Long, M. Beierlein, M. R. Deans, D. L. Paul, and B. W. Connors, "Electrical synapses in the thalamic reticular nucleus", *The Journal of Neuroscience*, vol. 22, pp. 1002–1009, 3 2002.

[107] M. Galarreta and S. Hestrin, "Electrical synapses between gaba-releasing interneurons", *Nature Reviews Neuroscience*, vol. 2, pp. 425–433, 2001.

[108] Y. Wang, A. Barakat, and H. Zhou, "Electrotonic coupling between pyramidal neurons in the neocortex", *PLoS One*, vol. 5, e10253, 4 2010.

[109] M. Galarreta and S. Hestrin, "A network of fast-spiking cells in the neocortex connected by electrical synapses", *Nature*, vol. 402, pp. 72–75, 6757 1999.

[110] P. L. Carlen, F. Skinner, L. Zhang, C. Naus, M. Kushnir, and J. L. P. Velazquez, "The role of gap junctions in seizures", *Brain Research Reviews*, vol. 32, pp. 235–241, 1 2000.

[111] A. N. van den Pol, "Neuropeptide transmission in brain circuits", *Neuron*, vol. 76, pp. 98–115, 1 2012.

[112] H. Demeulemeester, F. Vandesande, G. A. Orban, C. Brandon, and J. J. Vanderhaeghen, "Heterogeneity of gabaergic cells in cat visual cortex", *The Journal of Neuroscience*, vol. 8, pp. 988–1000, 3 1988.

[113] S. H. Hendry, E. G. Jones, J. DeFelipe, D. Schmechel, C. Brando, and P. C. Emson, "Neuropeptide-containing neurons of the cerebral cortex are also gabaergic", *Proceedings of the National Academy of Sciences of the United States of America*, vol. 81, pp. 6526–6530, 1984.

[114] A. Bacci, J. R. Huguenard, and D. A. Prince, "Differential modulation of synaptic transmission by neuropeptide y in rat neocortical neurons", *Proceedings of the National Academy of Sciences of the United States of America*, vol. 99, pp. 17 125–17 130, 26 2002.

[115] D. A. McCormick, B. W. Connors, J. W. Lighthall, and D. A. Prince, "Comparative electrophysiology of pyramidal and sparsely spiny stellate neurons of the neocortex", *Journal of Neurophysiology*, vol. 54, pp. 782–806, 4 1985.

[116] J. R. Hotson and D. A. Prince, "A calcium-activated hyperpolarization follows repetitive firing in hippocampal neurons", *Journal of Neurophysiology*, vol. 43, pp. 409–419, 2 1980.

[117] B. W. Connors and M. J. Gutnick, "Intrinsic firing patterns of diverse neocortical neurons", *Trends in Neurosciences*, vol. 13, pp. 99–104, 3 1990.

DOI:10.15774/PPKE.ITK.2020.008

[118] R. K. S. Wong and D. A. Prince, “Participation of calcium spikes during intrinsic burst firing in hippocampal neurons”, *Brain*, vol. 159, pp. 385–390, 2 1978.

[119] S. Inawashiro, S. Miyake, and M. Ito, “Spiking neuron models for regular-spiking, intrinsically bursting, and fast-spiking neurons”, *6th International Conference on Neural Information Processing*, vol. 1, pp. 32–36, 1999.

[120] L. G. Nowak, M. V. Sanchez-Vives, and D. A. McCormick, “Influence of low and high frequency inputs on spike timing in visual cortical neurons”, *Cerebral Cortex*, vol. 7, pp. 487–501, 6 1997.

[121] R. R. Llinas, “The intrinsic electrophysiological properties of mammalian neurons: Insights into central nervous system function”, *Science*, vol. 242, pp. 1654–1664, 4886 1988.

[122] R. Llinas and M. Sugimori, “Electrophysiological properties of in vitro purkinje cell dendrites in mammalian cerebellar slices”, *The Journal of Physiology*, vol. 305, pp. 197–213, 1980.

[123] G. Buzsaki, *Rhythms of the Brain*. Oxford University Press, 2006.

[124] L. L. Glickfeld, B. V. Atallah, and M. Scanziani, “Complementary modulation of somatic inhibition by opioids and cannabinoids”, *The Journal of Neuroscience*, vol. 28, pp. 1824–1832, 8 2008.

[125] C. Holmgren, T. Harkany, B. Svennenfors, and Y. Zilberter, “Pyramidal cell communication within local networks in layer 2/3 of rat neocortex”, *The Journal of Physiology*, vol. 551, pp. 139–153, 1 2003.

[126] A. M. Packer and R. Yuste, “Dense, unspecific connectivity of neocortical parvalbumin-positive interneurons: A canonical microcircuit for inhibition?”, *The Journal of Neuroscience*, vol. 31, pp. 13 260–13 271, 37 2011.

[127] Y. Yoshimura and E. M. Callaway, “Fine-scale specificity of cortical networks depends on inhibitory cell type and connectivity”, *Nature Neuroscience*, vol. 8, pp. 1552–1559, 2005.

[128] E. Fino and R. Yuste, “Dense inhibitory connectivity in neocortex”, *Neuron*, vol. 69, pp. 1188–1203, 6 2011.

[129] G. Buzsaki, “Feed-forward inhibition in the hippocampal formation”, *Progress in Neurobiology*, vol. 22, pp. 131–153, 1984.

DOI:10.15774/PPKE.ITK.2020.008

[130] L. L. G. Christoph Kapfer and, B. V. Atallah, and M. Scanziani, “Supralinear increase of recurrent inhibition during sparse activity in the somatosensory cortex”, *Nature Neuroscience volume*, vol. 10, pp. 743–753, 2007.

[131] G. Turrigiano, “Too many cooks? intrinsic and synaptic homeostatic mechanisms in cortical circuit refinement”, *Annual Review of Neuroscience*, vol. 34, pp. 89–103, 2011.

[132] M. Galarreta and S. Hestrin, “Electrical and chemical synapses among parvalbumin fast-spiking gabaergic interneurons in adult mouse neocortex”, *The Proceedings of the National Academy of Sciences*, vol. 99, pp. 12 438–12 443, 19 2002.

[133] G. Tamas, P. Somogyi, and E. H. Buhl, “Differentially interconnected networks of gabaergic interneurons in the visual cortex of the cat”, *The Journal of Neuroscience*, vol. 18, pp. 4255–4270, 11 1998.

[134] P. Mann-Metzer and Y. Yarom, “Electrotonic coupling interacts with intrinsic properties to generate synchronized activity in cerebellar networks of inhibitory interneurons”, *The Journal of Neuroscience*, vol. 19, pp. 3298–3306, 9 1999.

[135] M. V. Sanchez-Vives, M. Massimini, and M. Mattia, “Shaping the default activity pattern of the cortical network”, *Neuron*, vol. 94, pp. 993–1001, 5 2017.

[136] C. Wilson, “Up and down states”, *Scholarpedia journal*, vol. 3, p. 1410, 6 2080.

[137] M. Steriade, A. Nunez, and F. Amzica, “A novel slow (< 1 hz) oscillation of neocortical neurons in vivo: Depolarizing and hyperpolarizing components”, *Journal of Neuroscience*, vol. 13, pp. 3252–3265, 8 1993.

[138] M. V. Sanchez-Vives, M. Mattia, A. Compte, M. Perez-Zabalza, M. Winograd, V. F. Descalzo, and R. Ramon, “Inhibitory modulation of cortical up states”, *Journal of Neurophysiology*, vol. 104, pp. 1314–1324, 3 2010.

[139] D. A. Prince and R. K. S. Wong, “Human epileptic neurons studied in vitro”, *Brain Research*, vol. 210, pp. 323–333, 1-2 1981.

[140] R. Kohling, J.-M. Hohling, H. Straub, D. Kuhlmann, U. Kuhnt, I. Tuxhorn, A. Ebner, P. Wolf, H.-W. Pannek, A. Gorji, and E.-J. Speckmann, “Optical monitoring of neuronal activity during spontaneous sharp waves in chronically epileptic human neocortical tissue”, *Journal of Neurophysiology*, vol. 84, pp. 2161–2165, 4 2000.

[141] B. W. Strowbridge, L. M. Masukawa, and D. D. Spencer, “Hyperexcitability associated with localizable lesions in epileptic patients”, *Brain Research*, vol. 587, pp. 158–163, 1 1992.

[142] H. Kubista, S. Boehm, and M. Hotka, “The paroxysmal depolarization shift: Reconsidering its role in epilepsy, epileptogenesis and beyond”, *International Journal of Molecular Sciences*, vol. 20, p. 577, 3 2019.

[143] J. Gotman, “Relationships between interictal spiking and seizures: Human and experimental evidence”, *Canadian Journal of Neurological Sciences*, vol. 18, pp. 573–576, 4 1991.

[144] P. A. Schwartzkroin, D. A. Turner, W. D. Knowles, and A. K. Wyler, “Studies of human and monkey epileptic neocortex in the in vitro slice preparation”, *Annals of Neurology*, vol. 13, pp. 249–257, 1983.

[145] D. Johnston, J. J. Hablitz, and W. A. Wilson, “Voltage clamp discloses slow inward current in hippocampal burst-firing neurones”, *Nature*, vol. 286, pp. 391–393, 1980.

[146] M. S. Jensen, R. Azouz, and Y. Yaari, “Variant firing patterns in rat hippocampal pyramidal cells modulated by extracellular potassium”, *Journal of Neurophysiology*, vol. 71, pp. 831–839, 3 1994.

[147] B. W. Connors, M. J. Gutnick, and D. A. Prince, “Electrophysiological properties of neocortical neurons in vitro”, *Journal of Neurophysiology*, vol. 48, pp. 1302–1320, 6 1982.

[148] W. H. Hoffman and L. B. Haberly, “Bursting-induced epileptiform epsps in slices of piriform cortex are generated by deep cells”, *Journal of Neuroscience*, vol. 11, pp. 2021–2031, 7 1991.

[149] G.-F. Tseng and L. B. Haberly, “Deep neurons in piriform cortex. ii. membrane properties that underlie unusual synaptic responses”, *Journal of Neurophysiology*, vol. 62, pp. 386–400, 2 1989.

[150] R. S. Jones and U. Heinemann, “Synaptic and intrinsic responses of medical entorhinal cortical cells in normal and magnesium-free medium in vitro”, *Journal of Neurophysiology*, vol. 59, pp. 1476–1496, 5 1988.

[151] M. de Curtis, A. Manfridi, and G. Biella, “Activity-dependent ph shifts and periodic recurrence of spontaneous interictal spikes in a model of focal epileptogenesis”, *Journal of Neuroscience*, vol. 18, pp. 7543–7551, 18 1998.

[152] J. P. Dreier, S. Major, H.-W. Pannek, J. Woitzik, M. Scheel, D. Wiesenthal, P. Martus, M. K. L. Winkler, J. A. Hartings, M. Fabricius, E.-J. Speckmann, and A. Gorji, “Spreading convulsions, spreading depolarization and epileptogenesis in human cerebral cortex”, *Brain*, vol. 135, pp. 259–275, 1 2012.

[153] Y. Ben-Ari, E. Cherubini, R. Corradetti, and J.-L. Gaiarsa, “Giant synaptic potentials in immature rat ca3 hippocampal neurones”, *Journal of Physiology*, vol. 416, pp. 303–325, 1989.

[154] K. J. Staley and F. E. Dudek, “Interictal spikes and epileptogenesis”, *Epilepsy Currents*, vol. 6, pp. 199–202, 6 2006.

[155] J. L. Hellier, P. R. Patrylo, P. Dou, M. Nett, G. M. Rose, and F. E. Dudek, “Assessment of inhibition and epileptiform activity in the septal dentate gyrus of freely behaving rats during the first week after kainate treatment”, *Journal of Neuroscience*, vol. 19, pp. 10 053–10 064, 22 1999.

[156] I. I. Goncharova, R. Alkawadri, N. Gaspard, R. B. Duckrow, D. D. Spencer, L. J. Hirsch, S. S. Spencer, and H. P. Zaveri, “The relationship between seizures, interictal spikes and antiepileptic drugs”, *Clinical Neurophysiology*, vol. 127, pp. 3180–3186, 9 2016.

[157] M. de Curtisa, L. Librizzi, and G. Biella, “Discharge threshold is enhanced for several seconds after a single interictal spike in a model of focal epileptogenesis”, *European Journal of Neuroscience*, vol. 14, pp. 174–178, 2001.

[158] W. Yan, J. D. Mitzelfelt, J. C. Principe, and J. C. Sanchez, “The effects of interictal spikes on single neuron firing patterns in the hippocampus during the development of temporal lobe epilepsy”, *2008 30th Annual International Conference of the IEEE Engineering in Medicine and Biology Society, Vancouver, BC*, pp. 4134–4137, 2008.

[159] A. Bragin, J. Engel, C. L. Wilson, I. Fried, and G. Buzsaki, “High-frequency oscillations in human brain”, *Hippocampus*, vol. 9, pp. 137–142, 1999.

[160] J. G. R. Jefferys, L. M. de la Prida, F. Wendling, A. Bragin, M. Avoli, I. Timofeev, and F. H. L. da Silva, “Mechanisms of physiological and epileptic HFO generation”, *Progress in Neurobiology*, vol. 98, pp. 250–264, 2012.

[161] T. Fukuda and T. Kosaka, “Gap junctions linking the dendritic network of GABAergic interneurons in the hippocampus”, *Journal of Neuroscience*, vol. 20, pp. 1519–1528, 4 2000.

[162] A. M. Campbell and O. Holmes, “Bicuculline epileptogenesis in the rat”, *Brain Research*, vol. 323, pp. 239–246, 2 1984.

[163] Y. Ben-Ari, E. Tremblay, D. Riche, G. Ghilini, and R. Naquet, “Electrographic, clinical and pathological alterations following systemic administration of kainic acid, bicuculline or pentetrazole: Metabolic mapping using the deoxyglucose method with special reference to the pathology of epilepsy”, *Neuroscience*, vol. 6, pp. 1361–1391, 7 1981.

[164] R. Kohling, M. Qu, K. Zilles, and E.-J. Speckmann, “Current-source-density profiles associated with sharp waves in human epileptic neocortical tissue”, *Neuroscience*, vol. 94, pp. 1039–1050, 1999.

[165] A. Gulyas-Kovacs, J. Doczi, I. Tarnawa, L. Detari, I. Banczerowski-Pelyhe, and I. Vilagi, “Comparison of spontaneous and evoked epileptiform activity in three in vitro epilepsy models”, *Brain Research*, vol. 945, pp. 174–180, 2002.

[166] S. Borbely, K. Halasy, Z. Somogyvari, L. Detari, and I. Vilagi, “Laminar analysis of initiation and spread of epileptiform discharges in three in vitro models”, *Brain Research Bulletin*, vol. 69, pp. 161–167, 2006.

[167] P. R. Andrews and G. A. R. Johnston, “Gaba agonists and antagonists”, *Biochemical Pharmacology*, vol. 28, pp. 2697–2702, 18 1979.

[168] G. A. R. Johnston, “Advantages of an antagonist: Bicuculline and other gaba antagonists”, *British Journal of Pharmacology*, vol. 169, pp. 328–336, 2013.

[169] V. Seutin and S. W. Johnson, “Recent advances in the pharmacology of quaternary salts of bicuculline”, *Trends in Pharmacological Sciences*, vol. 20, pp. 268–270, 7 1999.

[170] S. Ueno, J. Bracamontes, C. Zorumski, D. S. Weiss, and J. H. Steinbach, “Bicuculline and gabazine are allosteric inhibitors of channel opening of the gabaa receptor”, *Journal of Neuroscience*, vol. 17, pp. 625–634, 2 1997.

[171] R. L. Macdonald, C. J. Rogers, and R. E. Twyman, “Kinetic properties of the gabaa receptor main conductance state of mouse spinal cord neurones in culture”, *Journal of Physiology*, vol. 410, pp. 479–499, 1 1989.

[172] V. Seutin, J. Scuvee-Moreau, and A. Dresse, “Evidence for a non-gabaergic action of quaternary salts of bicuculline on dopaminergic neurones”, *Neuropharmacology*, vol. 36, pp. 1653–1657, 1997.

[173] I. Ulbert, E. Halgren, G. Heit, and G. Karmos, “Multiple microelectrode-recording system for human intracortical applications”, *Journal of Neuroscience Methods*, vol. 106, pp. 69–79, 2001.

[174] I. Ulbert, Z. Magloczky, L. Eross, S. Czirjak, J. Vajda, L. Bognar, S. Toth, Z. Szabo, P. Halasz, D. Fabo, E. Halgren, T. F. Freund, and G. Karmos, “In vivo laminar electrophysiology co-registered with histology in the hippocampus of patients with temporal lobe epilepsy”, *Experimental Neurology*, vol. 187, pp. 310–318, 2004.

[175] J. K. Mai, G. Paxinos, and T. Voss, *Atlas of the Human Brain, The Science of Microfabrication*, 3rd Edition. Elsevier, 2007.

DOI:10.15774/PPKE.ITK.2020.008

[176] L. Hazan, M. Zugaro, and G. Buzsaki, “Klusters, Neuroscope, NDManager: A free software suite for neurophysiological data processing and visualization”, *Journal of Neuroscience Methods*, vol. 155, pp. 207–216, 2006.

[177] D. Lehmann and W. Skrandies, “Reference-free identification of components of checkerboard-evoked multichannel potential fields”, *Electroencephalography and Clinical Neurophysiology*, vol. 48, pp. 609–621, 1980.

[178] W. Skrandies, “Global field power and topographic similarity”, *Brain Topography*, vol. 3, pp. 137–141, 1990.

[179] E. M. Merricks, E. H. Smith, G. M. McKhann, R. R. Goodman, L. M. Bateman, R. G. Emerson, C. A. Schevon, and A. J. Trevelyan, “Single unit action potentials in humans and the effect of seizure activity”, *Brain*, vol. 138, pp. 2891–2906, 2015.

[180] M. A. Wilson and B. L. McNaughton, “Dynamics of the hippocampal ensemble code for space”, *Science*, vol. 261, pp. 1055–1058, 1993.

[181] J. Csicsvari, H. Hirase, A. Czurko, A. Mamiya, and G. Buzsaki, “Oscillatory coupling of hippocampal pyramidal cells and interneurons in the behaving rat”, *Journal of Neuroscience*, vol. 19, pp. 274–287, 1999b.

[182] P. Bartho, H. Hirase, L. Monconduit, M. Zugaro, K. D. Harris, and G. Buzsaki, “Characterization of neocortical principal cells and interneurons by network interactions and extracellular features”, *Journal of Neurophysiology*, vol. 92, pp. 600–608, 2004.

[183] A. Peyrache, N. Dehghani, E. N. Eskandar, J. R. Madsen, W. S. Anderson, J. A. Donoghue, L. R. Hochberg, E. Halgren, S. S. Cash, and A. Destexhe, “Spatiotemporal dynamics of neocortical excitation and inhibition during human sleep”, *Proceedings of the National Academy of Sciences of the United States of America*, vol. 109, pp. 1731–1736, 2012.

[184] B. W. Connors, “Initiation of synchronized neuronal bursting in neocortex”, *Nature*, vol. 310, pp. 685–687, 5979 1984.

[185] R. J. Staba, C. L. Wilson, A. Bragin, I. Fried, and J. Engel, “Sleep states differentiate single neuron activity recorded from human epileptic hippocampus, entorhinal cortex, and subiculum”, *Journal of Neuroscience*, vol. 22, pp. 5694–5704, 2002.

[186] B. P. Kerekes, K. Toth, A. Kaszas, B. Chiovini, Z. Szadai, G. Szalay, D. Palfi, A. Baga, K. Spitzer, B. Razsa, I. Ulbert, and L. Wittner, “Combined two-photon imaging, electrophysiological, and anatomical investigation of the human neocortex in vitro”, *Neurophotonics*, vol. 1, p. 011 013, 1 2014.

DOI:10.15774/PPKE.ITK.2020.008

[187] M. Avoli, D. Mattia, A. Siniscalchi, P. Perreault, and F. Tomaiuolo, “Pharmacology and electrophysiology of a synchronous gaba-mediated potential in the human neocortex”, *Neuroscience*, vol. 62, pp. 655–666, 1994.

[188] L. M. de la Prida, R. Benavides-Piccione, R. Sola, and M. A. Pozo, “Electrophysiological properties of interneurons from intraoperative spiking areas of epileptic human temporal neocortex”, *Neuroreport*, vol. 13, pp. 1421–1425, 11 2002.

[189] I. Cohen, G. Huberfeld, and R. Miles, “Emergence of disinhibition-induced synchrony in the ca3 region of the guinea pig hippocampus in vitro”, *The Journal of Physiology*, vol. 570, pp. 583–594, 3 2006.

[190] L. Wittner and R. Miles, “Factors defining a pacemaker region for synchrony in the hippocampus”, *The Journal of Physiology*, vol. 584, pp. 867–883, 3 2007.

[191] M. Avoli, J. Louvel, C. Drapeau, R. Pumain, and I. Kurcewicz, “Gabaa-mediated inhibition and in vitro epileptogenesis in the human neocortex”, *Journal of Neurophysiology*, vol. 73, pp. 468–484, 2 1995.

[192] J. A. Blanco, M. Stead, A. Krieger, J. Viventi, W. R. Marsh, K. H. Lee, G. A. Worrell, and B. Litt, “Unsupervised classification of high-frequency oscillations in human neocortical epilepsy and control patients”, *Journal of Neurophysiology*, vol. 104, pp. 2900–2912, 5 2010.

[193] G. A. Worrell, A. B. Gardner, S. M. Stead, S. Hu, S. Goerss, G. J. Cascino, F. B. Meyer, R. Marsh, and B. Litt, “High-frequency oscillations in human temporal lobe: Simultaneous microwire and clinical macroelectrode recordings”, *Brain*, vol. 131, 2008.

[194] J. Jacobs, R. Staba, E. Asano, H. Otsubo, J. Y. Wu, M. Zijlmans, I. Mohamed, P. Kahane, F. Dubeau, V. Navarro, and J. Gotman, “High-frequency oscillations (hfos) in clinical epilepsy”, *Progress in Neurobiology*, vol. 98, pp. 302–315, 2012.

[195] P. Marco and J. DeFelipe, “Altered synaptic circuitry in the human temporal neocortex removed from epileptic patients”, *Experimental Brain Research*, vol. 114, pp. 1–10, 1997.

[196] S. F. Muldoon, I. Soltesza, and R. Cossart, “Spatially clustered neuronal assemblies comprise the microstructure of synchrony in chronically epileptic networks”, *Proceedings of the National Academy of Sciences of the United States of America*, vol. 110, pp. 3567–3572, 9 2013.

DOI:10.15774/PPKE.ITK.2020.008

[197] A. Bui, H. K. Kim, M. Maroso, and I. Soltesz, “Microcircuits in epilepsy: Heterogeneity and hub cells in network synchronization”, *Cold Spring Harbor Perspectives in Medicine*, vol. 5, a022855, 11 2015.

[198] A. Bragin, C. L. Wilson, and J. J Engel, “Chronic epileptogenesis requires development of a network of pathologically interconnected neuron clusters: A hypothesis”, *Epilepsia*, vol. 41, S144–52, 6 2000.

[199] M. Megias, Z. Emri, T. F. Freund, and A. I. Gulyas, “Total number and distribution of inhibitory and excitatory synapses on hippocampal ca1 pyramidal cells”, *Neuroscience*, vol. 102, pp. 527–540, 3 2001.

[200] A. I. Gulyas, M. Megias, Z. Emri, and T. F. Freund, “Total number and ratio of excitatory and inhibitory synapses converging onto single interneurons of different types in the ca1 area of the rat hippocampus”, *The Journal of Neuroscience*, vol. 19, pp. 10 082–10 097, 22 1999.

[201] F. Matyas, T. F. Freund, and A. I. Gulyas, “Convergence of excitatory and inhibitory inputs onto cck-containing basket cells in the ca1 area of the rat hippocampus”, *European Journal of Neuroscience*, vol. 19, pp. 1243–1256, 5 2004.

[202] C. J. Keller, W. Truccolo, J. T. Gale, E. Eskandar, T. Thesen, C. Carlson, O. Devinsky, R. Kuzniecky, W. K. Doyle, J. R. Madsen, D. L. Schomer, A. D. Mehta, E. N. Brown, L. R. Hochberg, I. Ulbert, E. Halgren, and S. S. Cash, “Heterogeneous neuronal firing patterns during interictal epileptiform discharges in the human cortex”, *Brain*, vol. 133, pp. 1668–1681, 6 2010.

[203] F. E. Dudek and T. P. Sutula, “Epileptogenesis in the dentate gyrus: A critical perspective”, *Progress in Brain Research*, vol. 163, pp. 755–773, 2007.

[204] J. G. Jefferys, “Nonsynaptic modulation of neuronal activity in the brain: Electric currents and extracellular ions”, *Physiological Reviews*, vol. 75, pp. 689–723, 4 1995.

[205] T. F. Freund and I. Katona, “Perisomatic inhibition”, *Neuron*, vol. 56, pp. 33–42, 1 2007.

[206] F. E. Dudek, S. W. Snow, and C. P. Taylor, “Role of electrical interactions in synchronization of epileptiform bursts”, *Advances in neurology*, vol. 44, pp. 593–617, 1986.

[207] J. William J Moody, K. J. Futamachi, and D. A. Prince, “Extracellular potassium activity during epileptogenesis”, *Experimental Neurology*, vol. 42, 2 1974.

[208] U. Heinemann, H. D. Lux, and M. J. Gutnick, “Extracellular free calcium and potassium during paroxysmal activity in the cerebral cortex of the cat”, *Experimental Brain Research*, vol. 27, pp. 237–43, 1977.

[209] R. Miles and R. K. Wong, “Inhibitory control of local excitatory circuits in the guinea-pig hippocampus. j”, *The Journal of Physiology*, vol. 388, pp. 611–629, 1 1987.

[210] B. Ishijima, T. Hori, N. Yoshimasu, T. Fukushima, and K. Hirakawa, “Neuronal activities in human epileptic foci and surrounding areas”, *Neuron*, vol. 39, pp. 643–650, 6 1975.

[211] C. Alvarado-Rojas, K. Lehongre, J. Bagdasaryan, A. Bragin, R. Staba, J. Engel, V. Navarro, and M. L. V. Quyen, “Single-unit activities during epileptic discharges in the human hippocampal formation”, *Frontiers in Computational Neuroscience*, vol. 7, 140 2013. DOI: doi:10.3389/fncom.2013.00140.

[212] W. Truccolo, O. J. Ahmed, M. T. Harrison, E. N. Eskandar, G. R. Cosgrove, J. R. Madsen, A. S. Blum, S. Potter, L. R. Hochberg, and S. S. Cash, “Neuronal ensemble synchrony during human focal seizures”, *The Journal of Neuroscience*, vol. 34, pp. 9927–9944, 30 2014.

[213] P. Salami, M. Levesque, J. Gotman, and M. Avoli, “Distinct eeg seizure patterns reflect different seizure generation mechanisms”, *Journal of Neurophysiology*, vol. 113, pp. 2840–2844, 7 2015.

[214] R. Kohling, M. D’Antuono, R. Benini, P. de Guzman, and M. Avoli, “Hypersynchronous ictal onset in the perirhinal cortex results from dynamic weakening in inhibition”, *Neurobiology of Disease*, vol. 87, pp. 1–10, 2016.

[215] V. Gnatkovsky, L. Librizzi, F. Trombin, and M. de Curtis, “Fast activity at seizure onset is mediated by inhibitory circuits in the entorhinal cortex in vitro”, *Annals of Neurology*, vol. 64, pp. 674–686, 6 2008.

[216] N. Dehghani, A. Peyrache, B. Telenczuk, M. L. V. Quyen, E. Halgren, S. S. Cash, N. G. Hatsopoulos, and A. Destexhe, “Dynamic balance of excitation and inhibition in human and monkey neocortex”, *Scientific Reports*, vol. 6, 23176 2016. DOI: doi:10.1038/srep23176.